UiT The Arctic University of Norway

The Faculty of Science and Technology

Department of technology and safety

Vessel operations in relation to new types of offshore aquaculture facilities, and weather windows in exposed areas

Elise Kristiansen

Master's thesis in Technology and Safety in the High North TEK-3901, June 2022

UiT The Arctic University of Norway

Acknowledgement

This is my MSc. thesis in order to obtain a Master of Science degree in Technology and Safety in the High North at The Arctic University of Norway, UiT. The thesis has been carried out during the period from January to June 2022.

I would like to express my appreciation and sincere gratitude to Associated Professor Karl Gunnar Aarsæther for all his supervision and guidance throughout my study. I am thankful for his encouragement and admire his expertise.

I would also like to extend my gratitude to Magne-Petter Sollid, and the rest of the Nautical team at UiT for five unforgettable years. I am grateful for the experience, knowledge and trust I have been given.

Finally, I want to express my deep gratitude to my parents Heidi and Charles, and my brother Ådne for their endless support throughout all my life. And for my fellow students at office 1.041 I am thankful for the time we spent together writing our theses.

Elise Kristiansen   Tromsø 31.05.2022

Abstract

The marine aquaculture industry is expanding the production into new sea areas. The technology is advancing, and offshore aquaculture facilities are being developed. The offshore developments can offer significant benefits that applies to the economy, optimization of operations and production, as well as minimizing the impact on the coastal areas.

Structural and operation procedures need to be adapted as a result of transitioning from traditional production sites. Offshore aquaculture facilities are large rigid structures which leads to new challenges due to environmental parameters and dimensions. The field is rather unexplored compared to offshore wind or oil and gas industry.

A dynamic analysis is conducted to study the response of the conceptual aquaculture facility ØyMerd. A 3D model of the structure is modeled, in order to further calculate the hydrostatic and hydrodynamic properties. The mesh of the structure is imported into a boundary element method code which provide option for hydrostatic computation, and solves the hydrostatic equilibrium for the given mass and center of gravity. Further, the hydrostatic data, mass distribution matrix, and hydrostatic restoring matrix is given as input for HAMS solver. ØyMerd is then modeled in the dynamic analysis software with the hydrodynamic data obtained from the potential theory software HAMS. The simulations in OrcaFlex contains a model of ØyMerd moored and service vessel, in order to analyze vessel operations in relation to the structure and wave parameters. Significant wave heigh and wave period data is analyzed for a potential production location. A weather window analysis is performed in order to identify the accessibility of the structure in relation to vessel operations.

Vessel operations in relation to new types of offshore aquaculture facilities are facing new challenges which effects the safety and accessibility. It is important to avoid operations when the sea condition is close to either the aquaculture facility or the vessel natural frequency. Even though a structure like ØyMerd is stable in waves, sea conditions can lead to great response. For future work, wave disturbance and shielding effect benefits could be addressed.

Table of Contents

List of Tables

List of Figures

Nomenclature

3DOF	Three degrees of freedom
6DOF	Six degrees of freedom
AROME	Applications of Research to Operations at Mesoscale
B	Centre of buoyancy
BEM	Boundary Element Method
BM	Metacentric Radius
DNV	Det Norske Veritas
FEM	Finite element method
G	Centre of gravity
GM	The metacentric height
GZ	Restoring level
HAMS	Hydrodynamic Analysis of Marine Structures
HARMONIE	HIRLAM–ALADIN Research on Mesoscale Operational NWP in Euromed
JONSWAP	Joint North Sea Wave
K	Keel
M	Metacentre
NORA3	The 3 km Norwegian reanalysis
NYTEK-regulations	The Norwegian Regulations on technical requirements for Marine fish farms

Symbols

Symbol	Description	Symbol	Description
$\vec{D}$	Acceleration vector	S_B	Immersed body boundary
$\vec{D}$	Velocity vector	t	time
C_D	Drag coefficient	T_C	Contingency time
C_M	Mass coefficient	T_p	Wave period
C_a	Drag coefficient	T_{POP}	Planned operation period
F_B	Buoyancy force	T_R	Operation reference period
F_D	Drag force	U	Velocity
F_I	Inertia force	V_n	Normal velocity
F_w	Hydrodynamic force	η_1	Surge
K_{hs}	Hydrostatic stiffness	η_2	Sway
OP_{WF}	Operation criterion	η_3	Heave
V_r	Fluid velocity	η_4	Roll
k_x	Radii of gyration x-direction	η_5	Pitch
k_y	Radii of gyration y-direction	η_6	Yaw
k_z	Radii of gyration z-direction	λ	Wavelength
ζ_A	Wave amplitude	ϕ	Velocity potential
$\ddot{\eta}$	Acceleration	k	Wave number
$\dot{\eta}$	Velocity	v	Wave number in deep water
ϕ_d	Diffracted wave potential	ζ	Wave elevation
ϕ_i	Incident wave potential	η	Motion
ϕ_r	Radiated wave potential	ω	Wave frequency
Δ	Mass displacement		
∇	Volume displacement		
ρ	Fluid mass density		
A	Projected area		
B	Damping		
C	Restoring		
C_g	Damping of the flexible structure		
D	Diameter		
E	Energy		
g	Acceleration of gravity		
H	Wave height		
h	Water depth		
H_s	Significant wave height		
I	Inertia		
K_g	Force of stiffness		
M	Added mass		
m	mass		
M(p,a)	Inertia load		
M_g	Mass and added mass		
OP_{LIM}	Design criterion		
R	Horizontal distance		
R^{ext}	Externally applied loads		
R^{int}	Internally applied loads		
R_l	Longitudinal metacentric radius		
R_t	Transversal metacentric radius		

1 Introduction

The world population is increasing, and the need of resources are following the growth in humankind. The food being produces in the future needs to be nutritious and sustainable. For the marine sector, this leads to an increasing in the demand of seafood. This demand is expected to continue, and because of experience and knowledge the Norwegian seafood industry is suited to keep up with the demand. The Norwegian government has for years been involved in the management of marine resources along the coast and in the oceans along the country. This has led to maintenance and conservations of several species in the Norwegian marine life. Although knowledges are gained by prioritize the marina, it is expected that the potential in the ocean is still to be more extensive than current technology and knowledge are covering (Olafsen et al., 2012, pp. 4–5).

The economic potential for the sea-based industries is projected to grow. The ocean is expected to hold opportunities for resources to provide food and energy for the world. Therefore, to realizing the full potential of the ocean it is of interest to ensure marine technology innovation, and offshore technology improvement (OECD, 2016). Contributors to the ocean economy is already established industries like shipping, fisheries, offshore oil and gas, ports and tourism, but also emerging ocean-based industries like, aquaculture, deep water oil and gas, offshore wind energy and other ocean renewables energy. The future economy is depending on the different industries and the further developments (Edvardsen & Almås, 2017).

Technology companies are investing in fields like offshore wind and sea food industry to expand production into new sea areas. Ocean wind is relatively new industry and comprehensive technology developments are aiming to be producing energy as cheaply as possible per kilowatt produced. For offshore wind to be able to replace and compete with other energy sources like fossil fuel, the investment and technology developments is crucial. Globally it is believed that offshore wind is potentially a sustainable energy source in the future. Funds are substituted to be able to conduct research and developments of offshore wind farms (Holte et al., 2016). Within aquaculture the technology is advancing and there is great competitiveness within equipment suppliers. Closed facilities both on land and at sea are developing, and an increase in exposed aquaculture facilities structure developments are shaping (Gentry et al., 2017).

Due to beneficial wind conditions, wind turbines are customarily built on the coastline, and fish is traditionally produced in costal places in open fish farms. Today, new offshore locations are considered as a result of technology and offshore building is making sea areas more accessible. The change in the wind and aquaculture facility industry is a result of less areas by the coast is being considers as available, both because of regulations and decreasing in available areas. An increasing proportion of the sea areas in Norway is used for various commercial and conservation purposes. It is assumed that the access to suitable land will be an additional factor for stopping the further growth in the industries (Fiskeri-og kystdepartementet, 2005). Traditional farming of salmon has also developed to take up more space as shown in Figure 1.
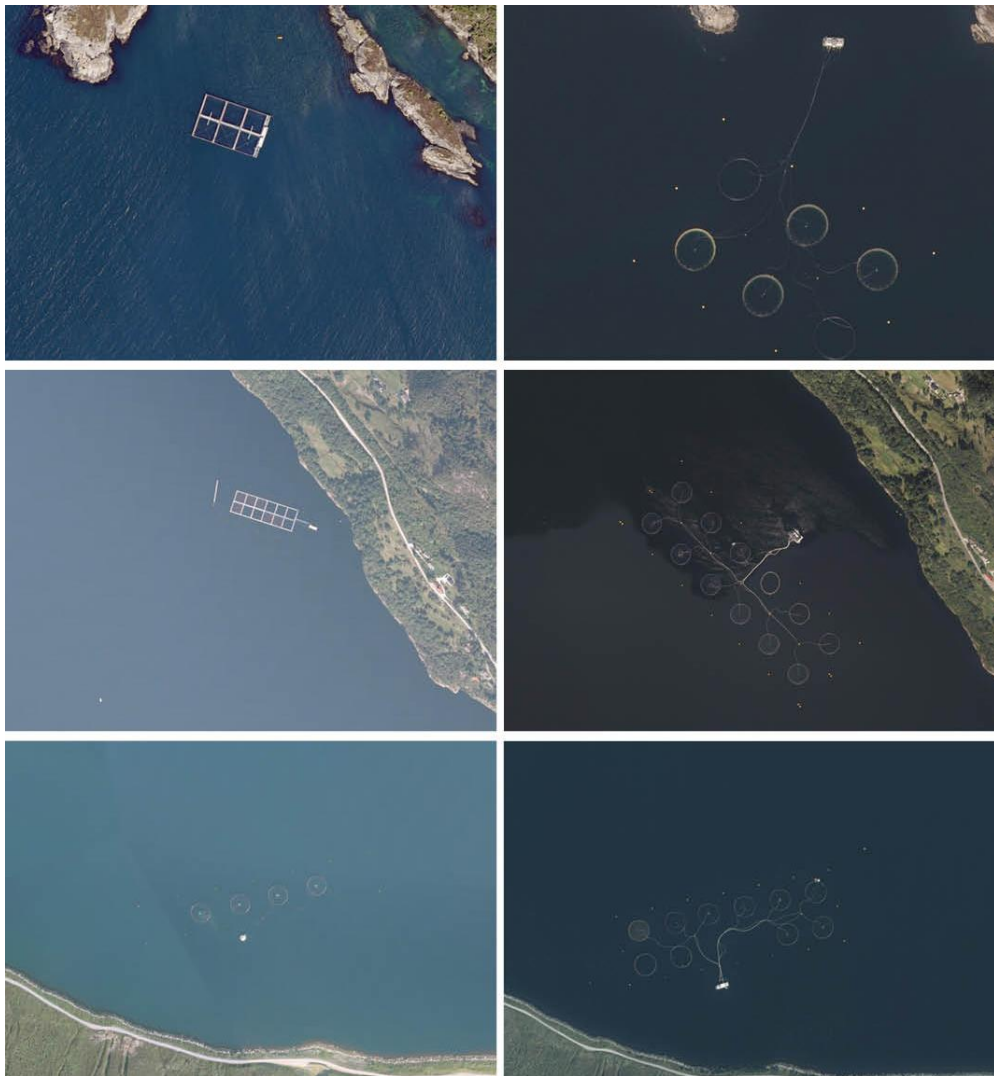
Figure 1 - How the configuration of the cages at three localities in Western Norway has changed from 2005 (left) to 2020 (right), Havforskningsinstituttet (Lund Pettersen, 2022).

Traditional farming of salmon starts with salmon fry developing in land-based storage until it is smolted, and then transported into open cages in the sea. Fresh seawater flows continuously through the cage and the fish grows to a weight of 4-5 kilograms. The traditional farming is most dominant in today's farming in Norway. New types of offshore aquaculture facilities are large and partly rigid structures. These types of offshore projects are complexed due to environmental parameters and dimensioning. This leads to high technological investments. The structures are being developed and tested to withstand exposed locations (Leira, 2017). Considerable experience has been gathered in offshore oil and gas industry, and exposed offshore areas are forcing developments in structure design and operation regarding the new offshore aquaculture facilities. Even though there is experience developed from the oil and gas industry, not all technology is suitable to be implemented in the offshore wind and aquaculture sites.

Structural and operation procedures need to be adapted to the weather parameters which is challenges offshore aquaculture facilities are facing in relation to open sea areas. Locations around the high north are particularly exposed to occasional extreme environmental factors like polar low pressured weather systems (Noer et al., 2011). Sudden changes in weather conditions in terms of wind, waves and low temperatures are factors that make maintaining more challenging, costly and time consuming. Also, operation aspects to consider is for example connected to vessel operations like loading and unloading of fish, transfer of bulk cargo and personnel transfer. Another challenge in areas with potential for offshore aquaculture facility are often connected to remote land areas. Many coastal locations are less accessible because of lack of infrastructure like undeveloped roads and ports. In connection to an offshore site, it is beneficial with a land base connection where vessels can operate from, storage and roads for vehicle transportation. The advantages of activities connected to offshore aquaculture facilities is increasing employment, especially new jobs outside the bigger cities.

1.1 Research question

New type of offshore aquaculture facilities is depending on ships for operations like fish transportation, feed supply, maintenance and personnel transfer. Rigid constructions are beneficial when operating with vessels because it can cause a shielding effect and are easier to maneuver into when docking. Calmer water due to breaking incoming waves, and a rigid platform could also be favorable when transferring crew or equipment.

Dynamics is interesting regarding ship operations in relation to aquaculture facilities in exposed locations. New offshore aquaculture facilities are rigid structures designed for offshore environmental conditions. By moving the productions sites from traditional location, the technology is transitioning to the new challenges expected. The industry is forced to adapt the new developments of offshore aquaculture facilities to new weather parameters, as well as remote places with lack of infrastructure. The rigid constructions are also consisting of flexible net systems for fish keeping. A large volume structures will cause wave disturbance when interacting with incoming waves, traditional aquaculture facilities are not. The changes are leading to synergies effects for other traditional aspects of the industry like vessel operations. ØyMerd which is presented in chapter 1.3 is a new type of floating structure. It is an example of a construction designed for an offshore aquaculture facility. These new types of structures are unique both because of the dimensions and operation areas. The aquaculture industry has not a lot of experience with structures like rigid constructions like ØyMerd. Traditional cages for salmon productions are flexible open structures. ØyMerd is not comparable with the traditional fish farms, nor a conventional vessel. The closest structure that is comparable might be a jackup-rigg.

To be able to maintain an offshore construction, the structure needs to be accessible for the vessel during the operation time. Often certain operations are depending on a weather window where the conditions are making the offshore facility safe to approach. Limiting environmental factor could be wave height and wave period for crane operations or personnel transfer. This relates to the new challenges which occurs when transition an industry into new offshore locations.

Vessel operations in relation to new types of offshore aquaculture facilities, and weather window in exposed areas:

I.   How to study the dynamics of an offshore aquaculture facility in a dynamic analysis software.
II.   What type of vessel operations in relation to an offshore aquaculture facility are expected, and how are the dynamic in relation to new types of offshore aquaculture facilities?
III. Elaboration of environmental conditions effects for vessel operations and weather windows in exposed environment.

1.2 Objective

Purpose of the thesis is to investigate the modeling of a new type of offshore aquaculture facility, which is a large rigid structure, and the dynamic during vessel operations in exposed locations. This is realized by using hydrostatic and hydrodynamic calculations and a dynamic analysis software. The analysis is carried out in OrcaFlex by importing hydrodynamic data for the structure ØyMerd, and modeling vessel operation in relation to the structure. The study is based on a mesh of the structure, hydrostatic computation and wave diffraction and radiation calculation for floating structures based on boundary integral equation in the potential flow theory. OrcaFlex is then used in order to simulate vessel operations and create some models to study marine operations and installations. The results will be discussed in order to utilize them for future study on offshore aquaculture facilities in exposed environment.

1.3 ØyMerd

Salmon fish farmers Gratanglaks and Kleiva Fishfarm are developing a new type of aquaculture facility. ØyMerd is a rigid structure with a technology that aims to increase salmon production in open weather-exposed waters. ØyMerd is a proposed aquaculture facility that has been planned. Each side is 120 meters long, with a total height of 10 meters and a draft of 7.5 meters. An operations facility will be in the very center of the floating platform. It has three cages for salmon production, as well as technical equipment and storage beneath the deck (Gratanglaks, 2022).

Figure 2 - ØyMerd illustration. Foto: Astafjord Ocean Salmon (Nedrejord, 2021).

2 Theory

Environmental conditions, which a floating offshore aquaculture facility structure is subjected, determine the way it behaves over time. The dynamic can be analysed with equations of motion and theoretical models for hydrodynamic forces. By simulation, using a dynamic analysis software, a numerical model of a real-world scenario is set up. Environmental conditions are specified, and the model theory of a software calculates the motion and the system dynamic response. The accuracy of the model depends on the accuracy of the hydrostatic and hydrodynamic calculations. It also relays on the accuracy of the dynamic analysis software when simulating the dynamics of a system subjected environmental conditions. In this chapter the theory regarding environmental parameters, hydrostatic, hydrodynamic, vessel operations and modelling is presented.

2.1 Waves

The modelling of a wave can be divided into a regular or irregular wave. A linear wave is described mathematically with a sine or cosine function, and are assumed to propagate with the same configurations:

$$\zeta = \zeta_A \cos{(kx - \omega t)} \tag{1}$$
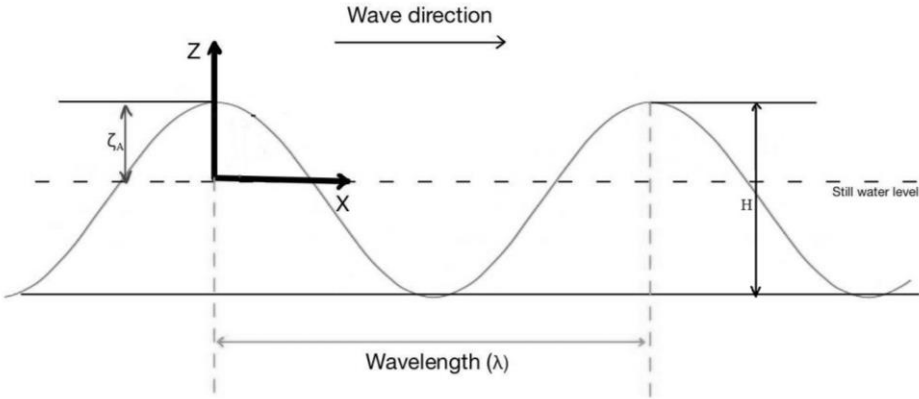
Figure 3 – Linear wave

If the sea surface is studied, we notice that the waves are not simply described by linear wave theory and a single wave component. The sea surface is composed of random waves with various lengths and periods as shown in Figure 4. The way we can modulate the sea surface is by a probability distribution of the different wave frequencies and wave components. If all the different waves are combined, we get the irregular sea state (Faltinsen, 1990, pp. 23–24).
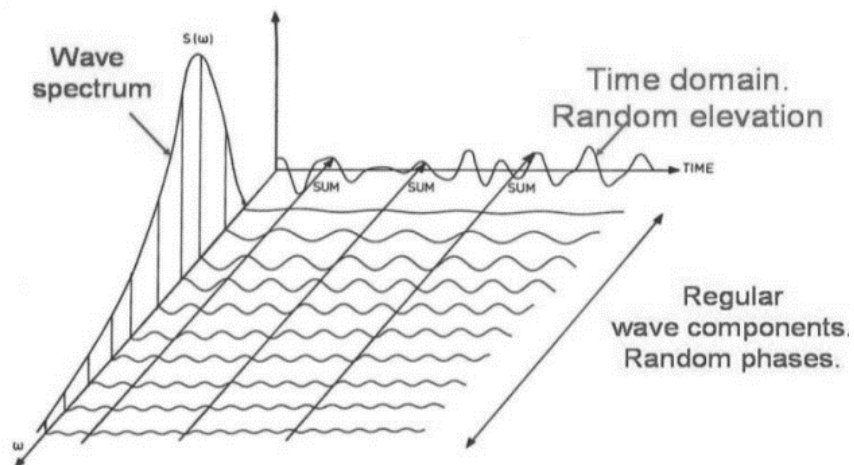
Figure 4 – Irregular sea state, illustration from the book "Sea Loads on Ships and Offshore Structures" (Faltinsen, 1990, p. 24)

To describe an irregular sea state, there have been developed different wave spectrums. The wave spectrums are empirical descriptions of standard wave spectrums. The most common spectrum used is JONSWAP (Joint North Sea Wave Project) and Pierson-Moskovitz. JONSWAP describes wind generated waves, and Pierson-Moskovitz describes a sea state where swells are common.

From the wave spectrums we can describe the sea state with one or to simple parameters like significant wave height and peak period. The significant wave heights are the average of the 1/3 highest waves shown in Figure 5.
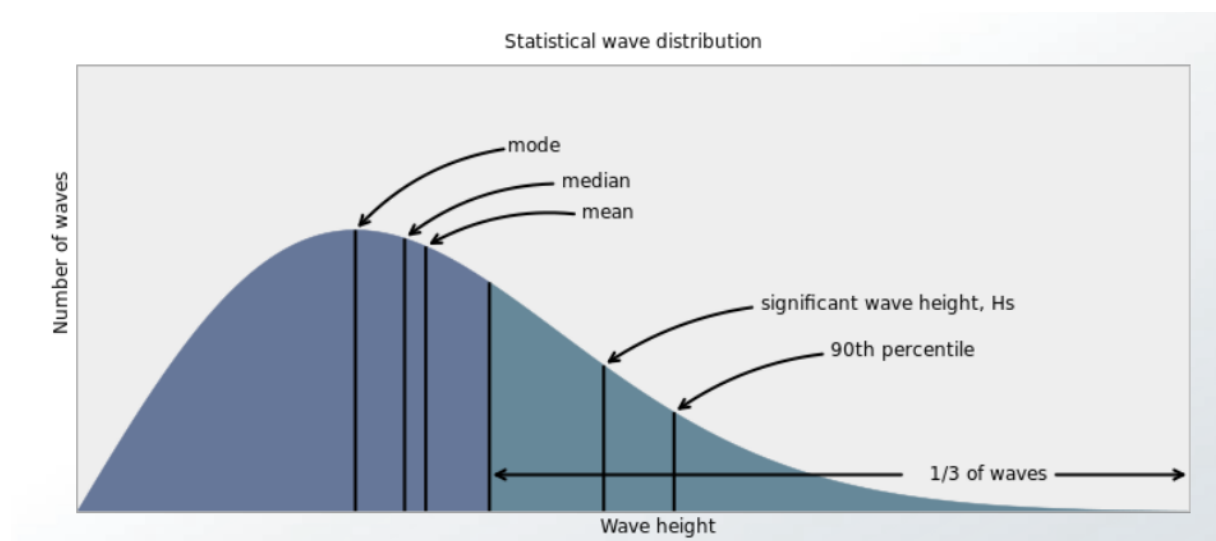
Figure 5 - Significant wave height Hs (Lecture note, MFA-2011, UiT)

The different waves are simply a visualization of different energies. The energy in the wave can be described as:

$$E = \frac{1}{2}\rho g \zeta_A^2 \lambda \tag{2}$$

The wave period with the most energy is the peak spectral period Tp (s), JONSWAP spectrum and Pierson-Moskowitz spectrum ($H_{1/3}$- significant wave height and T_2 – mean wave period) is shown in Figure 6. The dotted line shows the JONSWAP spectrum, and the solid line shows the modified Pierson-Moskowitz spectrum (Faltinsen, 1990, p. 26).
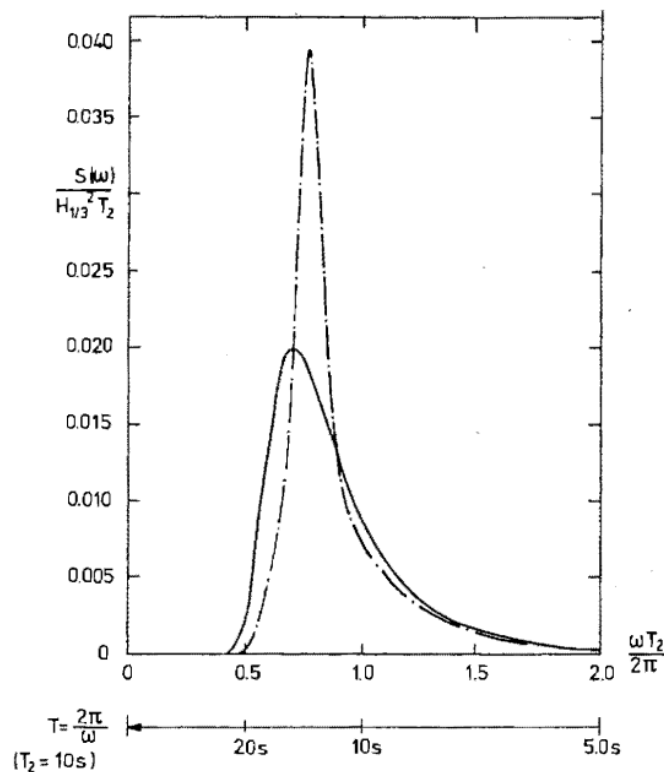
Figure 6 - Wave spectra, illustration from "Sea Loads on Ships and Offshore Structures" (Faltinsen, 1990, p. 26)

2.2 Rigid structure dynamics

The equation of motion is a mathematical description of the relation between an external loading and the structural response based on its inertia, damping and restoring force. When a structure is assumed to not deform when a force is applied, it is assumed to be rigid. A floating rigid body can translate and rotate in six degrees of freedom (6DOF). The time domain equation of motion for a floating body are described as:

$$F(t) = M\ddot{\eta} + B\dot{\eta} + C\eta \tag{3}$$

Where, the η vector represent the six degrees of freedom accelerations, velocity and a force proportional with the motion. The M, B and C are the mass, damping and restoring forces. The equation describes the system of a floating body in motion, with the damping and restoring forces. The motion of a floating body is often a combination of the different degrees of freedom shown in Figure 7, which means the description of the motions could be complex. Six degrees of freedom analysis are described by a 6x6 matrices.

6DOF: η1 – surge η2 – sway η3 – heave η4 – roll η5 – pitch η6 – yaw
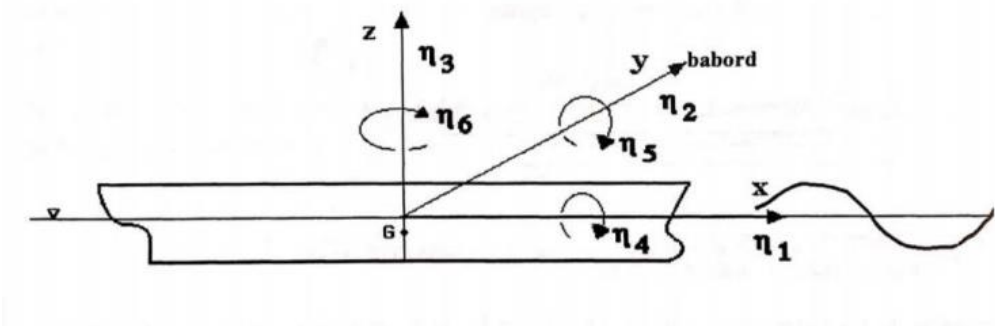
Figure 7 - Vessel axis system 6DOF (Lecture notes, MFA-2011 UiT)

The total load a floating body is subjected to is the sum of different types of loading applied. A moored rigid structure experiences a combination of loads caused by environmental conditions and restoring loads. External loads could be wave, current, restoring loads from hydrostatic restoring loads, mooring restoring loads and aerodynamic loads. These loads are not dependent on the time, but the velocity, acceleration and position of the body (Jaime Matthijs, 2020). Hydrodynamic loads are presented in chapter 2.3.

$$F_{external} = F_{wave} + F_{current} + F_{static} + F_{moorings} + F_{wind} \qquad (4)$$

2.2.1 Flexible body dynamics

Flexible objects could be net, moorings and hoses. When flexible object is analysed, it is harder to linearised the system in order to describe the behaviour. A common method to describe the flexibility of a structure is to divide det system into finite number of elements. The mass of the structure is distributed into this mass points and are connected by segments of springs as shown in Figure 8. The forces apply thru the springs, and the mass for each element is in the nodes.

The FEM-method, finite number of elements, could be a method to discretize flexible structure. The elements represent appropriate mass, stiffness and damping. The method uses shape functions to approximate the amount of stress and strained that is included in the dynamics. The governing equation for the elements, assuming the element mass and damping following from the discretisation and uses the same functions as the stiffness matrix can be written as followed (Lin & Trethewey, 1990):

$$\vec{R}^{ext} = M_g \ddot{\vec{D}} + C_g \dot{\vec{D}} + \vec{R}^{int} \tag{5}$$

Where R^{ext} are the externally applied loads, M_g is the mass an added mass, C_g is the damping of the flexible structure and R^{int} are the internally applied loads. $\ddot{\vec{D}}$ and $\dot{\vec{D}}$ are the acceleration and velocity vectors of the system. The internal forces for a linear elastic material can be written as a force of the stiffness of the element and the system displacement vector:

$$\vec{R}^{int} = K_g \vec{D} \tag{6}$$
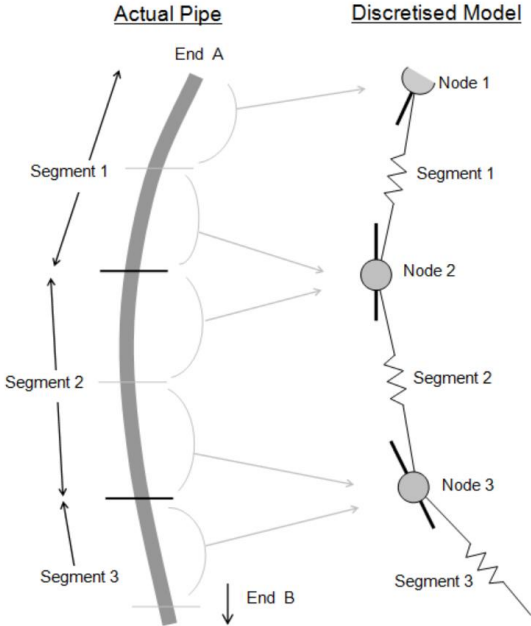
Figure 8 - Finite element model for a line (Orcina, 2022a).

2.3 Hydrodynamics

The motion of the fluids, and the forces applied to a floating body by the relative motion of the fluid, is described by hydrodynamics. An offshore aquaculture facility could be floating partly submerge in water. The forces applied causes motion of the structure and additionally movements of the fluid. This are explained in this chapter by describing the one of the hydrodynamic component waves.

Equation of motion with a linear assumption on hydrodynamic forces such as mass, added mass, damping and restoring forces:

$$F(t) = (M + A)\ddot{\eta} + B\dot{\eta} + C\eta \tag{7}$$

2.3.1 Wave loads

When describing the wave loads, first a description of regular wave behaviour is provided based on assumption made in potential flow theory. It is necessary to define the governing equation, boundary condition and initial conditions. The fluid is assumed to be inviscid, free of separation or lifting effects, irrotational and incompressible. The flow can be described by the velocity potential. The derivation is based on the assumptions which are given as a requirement for the flow.

Boundary conditions subjected respectively when solving the velocity potential (Faltinsen, 1990, pp. 13–17) (Faltinsen, 1990, pp. 13-17):

1. Bottom Boundary Condition describing no flow through the seabed and can be expressed as: $\left(\frac{\partial \phi}{\partial z}\right)_{z=-h} = 0$

2. Dynamic Free Surface Boundary Condition states that the pressure at the surface is equal to the atmospheric pressure: $g\zeta + \left(\frac{\partial \phi}{\partial t}\right)_{z=0} = 0$

3. Kinematic Free Surface Boundary Condition witch states that a particle on the surface, stays on the free surface: $\left(\frac{\partial \zeta}{\partial t}\right) = \left(\frac{\partial \phi}{\partial z}\right)_{z=0}$

Velocity potential solution for finite water depth (Faltinsen, 1990, p. 16):

$$\phi = \frac{g\zeta_A}{\omega} \frac{\cosh k(h+z)}{\cosh kh} \cos(kx - \omega t)$$ (8)

The velocity potential can be decomposed into the incident wave potential, the diffraction potential and radiated wave potential. Mathematically the velocity potentials satisfy the Laplace equation:

$$\nabla^2 \emptyset = 0$$ (9)

By inserting the velocity potential solution into the free surface kinematic boundary condition, it results in the dispersion relation. The dispersion relation gives an expression containing the relationship between the wavelength and wave frequency. From the velocity potential it is possible to obtain the wave surface elevation, vertical and horizontal velocity and acceleration.

$$\omega^2 = kg \tanh kh$$ (10)

In potential flow theory viscous force is neglected. The forces sustained by the structure is Foude-Krylov force and diffraction force. Also, when the floating body is forces in to oscillating in still water with natural frequency, waves will radiate from the structure. This are the loads in the motion equation damping, added mass and restoring force.

To understand linear response, we study excitation loads and diffraction applied on a structure when the structure is fixed and are experiencing an incoming wave with one frequency. Also, we study the structure oscillating in no waves but with the same frequency as the previous incoming waves. By combining the two scenarios added mass, damping and restoring forces and moments loads are known, as well as the response of the structure (Faltinsen, 1990, p. 39).

Excitation loads

Added mass
Damping and Restoring
forces and moments
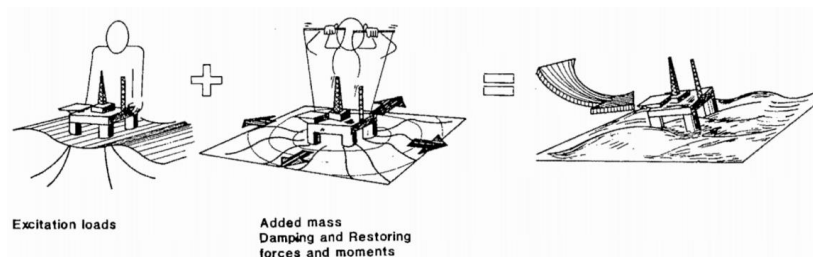
Figure 9 - Superposition of wave excitation, added mass, damping and restoring load, illustration from "Sea Loads on Ships and Offshore Structures" (Faltinsen, 1990, p. 40)

Excitation loads can be solved by sum of the Froude-Krilov force and diffraction problem. The diffraction problem is calculated by finding the incident wave velocity potential and the diffraction velocity potential.

$$F_{exc} = - \int P n_k ds - \sum a_j A_{kj} ds \tag{11}$$

The radiation problem can be solved when the body is oscillating with a frequency and amplitude. The added mass, damping and restoring is in phase with the acceleration and velocity.

$$F_k = -A_{kj}\ddot{\eta}_J - B_{kj}\dot{\eta}_j - C_{kj}\eta_j \tag{12}$$

A moored floating structure are exposed to large first order wave forces. These are linearised motions proportional to the wave height. Also, a moored floating structure like ØyMerd is exposed to second order mean and low frequency wave force and moments. The force is proportional to the square of the wave height. The wave effect from a second order wave force may be significant because a low frequency wave is closer to the natural frequency of systems (Løken et al., 1999). In designing of mooring systems mean and slowly varying wave loads are of importance. Second order wave forces result, in addition to linear wave consideration, mean forces and forces oscillating with different frequency or sum frequency (Faltinsen, 1990).

2.3.1.1 HAMS wave-structure interactions

The first order wave forces can be calculated in HAMS which is a potential theory software. HAMS is a software developed for analysing wave-structure interactions. The software is a frequency-domain pre-processor of computing wave excitation force, added mass, and wave radiation damping. The motion response of a marine structure can be predicted due to time domain solver via Fourier cosine and sine transformation.

The theoretical background of the hydrodynamic analysis of marine structure software (HAMS) is based on the assumptions in chapter 2.3 Hydrodynamics. As mentioned in the chapter the velocity potential $\phi(x,y,z)$ can be decomposed into three parts, incident wave potential $\phi_i(x,y,z)$, the diffracted wave potential $\phi_d(x,y,z)$, and the radiated wave potential $\phi_r(x,y,z)$:

$$\boldsymbol{\phi} = \boldsymbol{\phi_i} + \boldsymbol{\phi_d} + \boldsymbol{\phi_r} \tag{13}$$

The velocity potential needs to satisfy the Laplace equation in the entire fluid domain, as well as the free surface, on the body surface, at the sea bottom and in the far field (Liu, 2019):

$$\left.\frac{\partial \phi}{\partial z}\right|_{z=0} = v\phi$$

$$\left.\frac{\partial \phi}{\partial n}\right|_{S_B} = V_n$$

$$\left.\frac{\partial \phi}{\partial z}\right|_{z=-h} = 0 \tag{14}$$

$$\lim_{R \to \infty} \left[\sqrt{vR}\left(\frac{\partial \phi}{\partial R} - iv\phi\right)\right] = 0$$

Where the $v = \frac{\omega^2}{g}$ is the wave number in deep water, g is the acceleration of gravity, the normal velocity at a point on the immersed body boundary S_B is indicated by the V_n. R denotes the horizontal distance from the body, and h is the water depth in case of finite depth water. The last boundary condition in equation 12 shows the velocity potential gradually decomposes with the horizontal distance and disappear in the far field (Liu, 2019).

Deep water: $H > \frac{\lambda}{2}$ (15)

After solving the wave potentials HAMS calculates the wave forces by integrating the dynamic pressure over the wetted body. The values for the excitation and radiation force of the floating body for each case of wave frequency and wave direction. The HAMS solution contains both the magnitude of the force and the phase shift in relation to the waves. The radiating force contains a component for added mass and damping which are in phase with acceleration and velocity, respectively as shown in equation (12) (Liu, 2021). This gives a hydrodynamic database that can be imported into dynamic analysis software like OrcaFlex.

2.3.2 Damping and viscous loads

The floating body response in waves are limited by the damping. The damping force drain energy from the motion of a body. If an object floating in still water is forced into heave motion, it will eventually (due to damping) return to equilibrium stability. For a semi submerged body, the contributors to damping is viscous loads, wave drift damping, and wind and current impact. Wave drift damping is relevant for a body making constant speed in the

direction of a wave. Wind and current damping is relevant where environmental factors is included in the scenario (Faltinsen, 1990).

Viscous loads on a floating structure are friction and viscous effects because of pressure when making way thru water or being impact of waves and current. When we study an object, the friction component indicated the viscous force acting along the surface. This leads to a force acting the opposite direction of the streaming water. Due to the pressure difference between the bottom and top of the submerge body, a wake is created behind the object. The size of the wake indicates the pressure difference (Journée & Massie, 2005). Drag force:

$$F_D = \frac{1}{2}\rho C_D A U^2 \tag{16}$$
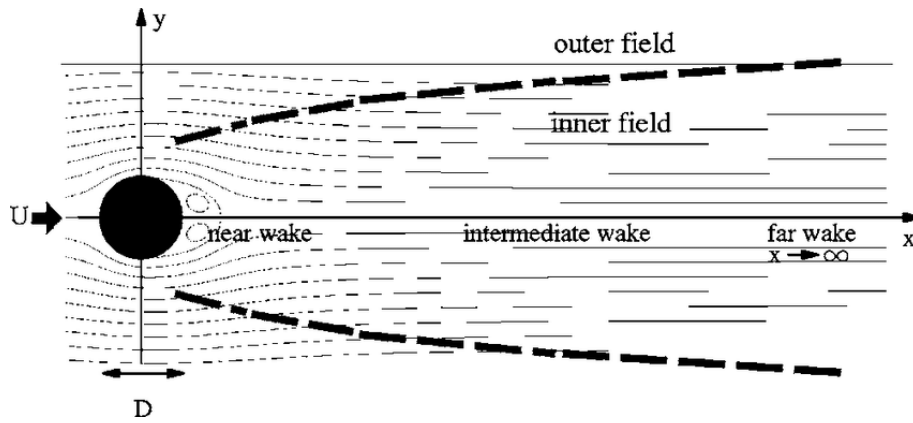
Figure 10 - Wake behind a round object (Tordella et al., 2006).

We get Morison equation by combine the drag force and inertia force. Morison equation is used to describe the mass dominate forces for small volume structures. The forces applied is the inertia force and drag force, where the inertia force is the integrated pressure around the submerged structure:

$$dF = \rho \frac{\pi D^2}{4} C_M a_x dz + \frac{1}{2}\rho C_D D u |u| dz \tag{17}$$

Where

$$u = \frac{\partial \phi}{\partial x}$$

$$a_x = \dot{u} = \frac{\partial^2 \phi}{\partial x \partial t}$$

The mass coefficient $C_M = 2$ for great $\frac{\lambda}{D}$ values.
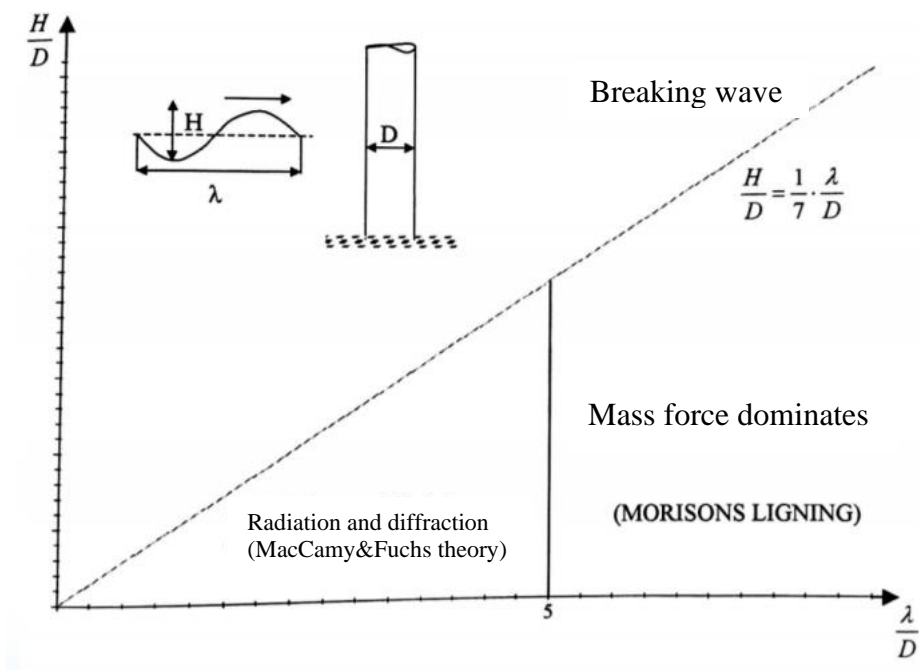
Figure 11 - Great volume and small volume fixed structures. Expected forces: Radiation and diffraction, and mass forces (Lecture note MFA-2011, UiT).
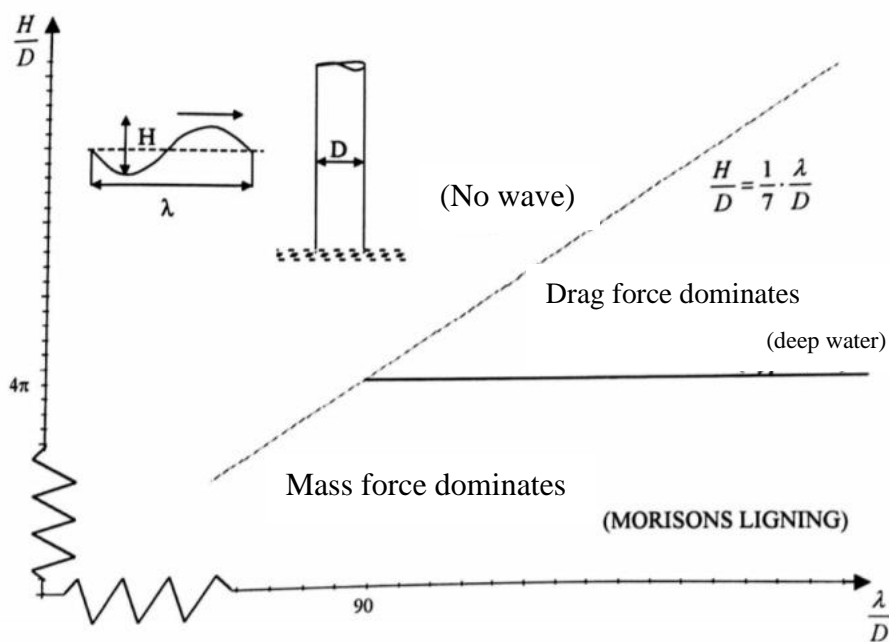
Figure 12 - Small volume fixed structures. Expected forces: Drag and mass forces (Lecture note MFA-2011, UiT).

Small volume structures such as moorings and traditional aquaculture facilities are dominated by viscous forces. Wave forces are dominant for ships making way thru waves. The nets in a fish farm can be modelled using equation (16) with the correct area and drag coefficient. The drag force on net panels depends on the geometrical parameters such as diameter and mesh size.

2.4 3D Mesh modelling

Meshes are essential component in 3D modelling. The mesh consist of single points
(vertexes) with x,y and z coordinates, edges connecting the vertexes, and faces. These three
components are used to create 3D illustrations of an object which is used in many fields to
computer graphics for visualization of complex data sets or entertainment purposes
(Havemann & W.Fellner, 2022).

Fine meshed objects, with a higher number of cells, would significantly prolong the required
computational time when for example using a diffraction analyse program (Martic et al.,
2017). However, for some calculations or analysis of a 3D model the object needs to be
meshed into fine elements. An example is when analysing propeller in water stream. Very
fine meshing is needed in regions of the propeller mesh to capture the flow correctly (Pawar
& Brizzolara, 2019). To determine if a mesh is propriate for use in any analyses, a mesh
sensitivity analysis can be performed. The mesh can be divided into fine, medium and coarse
mesh size or other parameters, to compare results of the calculations for suitability (Martic et
al., 2017).

2.5 Hydrostatic computation

Archimedes discovered the basic load buoyancy force acting on floating bodies. This physical
law carries the name Archimedes law and described that the force are equal to the gravitation
force working on the free floating body (Barrass & Derrett, 2011, p. 24).

$$F_B = \rho g \nabla = F_g \tag{18}$$

Where the ρ is the density of the fluid and ∇ is the displacement volume of the fluid witch the
body is floating in.
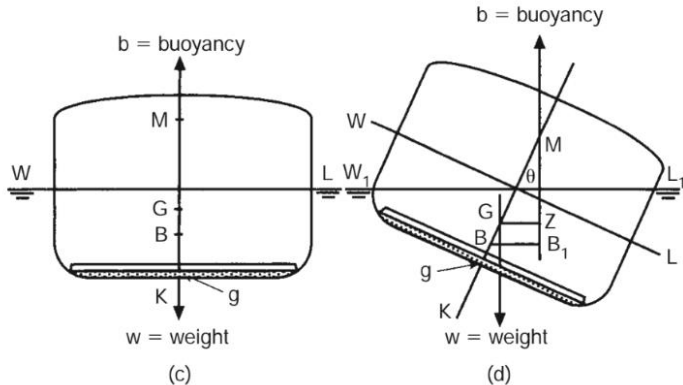
Figure 13 - Transverse stability (Barrass & Derrett, 2011, p. 52)

The transverse stability of a floating body is illustrated in Figure 13. G refers to the center of gravity, B refers to the center of buoyancy, K refers to the keel depth and the M refers to the metacenter. The stability of the body is given by the value GM, which is referred to as the metacentric height and is the vertical distance between G and M. If GM is positive the system is stable, and if zero the system is meta-stable. The stability is physical described as the buoyancy point counteracts the gravity force and forces the body to return to equilibrium position (Barrass & Derrett, 2011, p. 32).

$$GM = KB + BM - KG \tag{19}$$

$$BM = \frac{I}{\nabla} \tag{20}$$

A ship is in stable equilibrium if it returns to the initial position when inclined. The level of rightening level is referred to as GZ as shown in Figure 13. At a small angle of heel less than 15°:

$$GZ = GM \times sin\theta \tag{21}$$

Meshmagick[1] is a command line utility and python module for hydrodynamic calculation of floating body mesh (mesh modelling is presented in chapter 2.4). Meshmagick provides hydrostatic computations and can solve the hydrostatic equilibrium for a given mass or centre of gravity for a mesh. From the hydrostatic calculations, hydrostatic stiffness matrix, metacentric height and floating plane are properties that can be obtained.

From the python software Meshmagick, developed at LHEFA lab, the hydrostatic data is expressed as followed (2022):

Hydrostatic stiffness matrix.

$$K_{hs} = \begin{bmatrix} 0 & 0 & 0 & 0 & 0 & 0 \\ 0 & 0 & 0 & 0 & 0 & 0 \\ 0 & 0 & K_{33} & K_{34} & K_{35} & 0 \\ 0 & 0 & K_{43} & K_{44} & K_{45} & 0 \\ 0 & 0 & K_{53} & K_{54} & K_{55} & 0 \\ 0 & 0 & 0 & 0 & 0 & 0 \end{bmatrix} \tag{22}$$

---

[1] https://lheea.github.io/meshmagick/

The matrix is symmetric, so the hydrostatic coefficients is:

$$K_{33} = \rho g S_f \tag{23}$$

$$K_{34} = K_{43} = \rho g \iint_{S_f} y \, dS$$

$$K_{35} = K_{53} = -\rho g \iint_{S_f} x \, dS$$

$$K_{45} = K_{54} = -\rho g \iint_{S_f} xy \, dS$$

$$R_t = \frac{1}{\nabla} \iint_{S_f} y^2 \, dS$$

$$R_l = \frac{1}{\nabla} \iint_{S_f} x^2 \, dS$$

$$a = z_g - z_b$$

$$GM_t = R_t - a$$

$$GM_l = R_l - a$$

$$K_{44} = \rho g \nabla GM_t$$

$$K_{55} = \rho g \nabla GM_l$$

$$x_f = -\frac{K_{35}}{K_{33}}$$

$$x_f = -\frac{K_{34}}{K_{33}}$$

Where ∇ is the volume displacement of the body, R_t and R_l are the transversal and longitudinal metacentric radius, GM_t and GM_l is the transversal and longitudinal metacentric heights, and x_f and y_f are the horizontal position of the center of the floating plane Oxy.

2.6 OrcaFlex

Dynamic analyses were performed in OrcaFlex, a dynamic analysis software developed by Orcina. Hydrodynamic data can be imported from diffraction analysis programs like HAMS, but the scenarios can be modelled directly in OrcaFlex. The software contains different offshore technologies and objects to model marine operations. The purpose of OrcaFlex is to study how ships, structures, lines and buoys are behaving.

2.6.1 General data

OrcaFlex uses a global coordinate system for the model, and a local coordinate system for each object present in the model. Rotation is defined as positive when rotating clockwise when looking in the direction of the axis of rotation. When a rotation of an object is performed during time-domain analysis rotations of the object is performed first around z-axis, then y-axis and at the end around the x-axis. The results and data of a simulation is given relative to the global axis (Browne, 2013).

The static analysis calculates the equilibrium of the model, which is used for the dynamic analysis in OrcaFlex. The calculation includes the hydrostatic and inertial loads of the object, loads from mooring systems, and mean wave drift loads. The static is either calculated as the whole system static or separate buoy and line statics. A complexed model with several objects and buoys is calculated in a single iterative process for each component before analysing the system dynamics (Olsen, 2015).

OrcaFlex bases the dynamic analysis on ether a frequency or time domain approach. The frequency domain analysis is linear and solves the dynamic response of a system at either wave frequency or low frequency as determined by the user. The time domain approach is fully nonlinear and re-compute the system geometry at every time step.

Time domain solution

The time domain dynamic analysis is divided into the build-up and the main simulation. The waves and model motion are increasing from static to full developed dynamic in the build-up stage. The second part of the dynamic analysis is where the dynamic equation of motion is solved. Explicit and implicit integration are used by OrcaFlex to solve the dynamic equation of motion (Orcina, 2022c):

$$M(p,a) + C(p,v) + K(p) = F(p,c,t) \tag{24}$$

Where,

M(p,a) is the system inertia load

C(p,v) is the system damping load

K(p) is the system stiffness load

F(p,v,t) is the external load

p,v and a are the position, velocity and acceleration vectors respectively

t is the simulation time

Time domain analysis evaluate at each time step mass, damping and loading etc. The time varying geometry to the system is considering. OrcaFlex uses either explicit Euler integration or implicit integration using the Generalised-α scheme. By using the implicit integration scheme, the initial position and orientation of all objects in the model, included all node in all lines, are obtain from the static analysis. The system equation of motion is solved at the end of the time step. When applying the implicit integration method in dynamic analysis, the iterations are performed for each time step as the position, velocity and acceleration are unknown at the end. Therefore, the implicit integration is more time-consuming for each time step. However, for longer time steps the implicit integration is more stable and run faster than the explicit integration. The explicit Euler integration calculates the equation of motion in the beginning of the time step (Chung & Hulbert, 1993).

2.6.2 Vessel object

Vessel object is used to model ships, windmill or other floating structures. It is translation in surge, sway, heave, and rotating in roll pitch and yaw. The hydrodynamic properties can be prescribed by importing hydrodynamic data or edit the properties in OrcaFlex vessel type data.

For the vessel calculation static position and dynamic motion are determined when setting up a model. Included in static analysis the degrees of freedom which is going to be included in the calculations are specified. The available choices are none, 3DOF and 6DOF. For the time domain dynamics OrcaFlex provides vessel motion into two forms, primary and superimposed motion. Primary motion determines the primary position of the vessel: None, prescribed, calculated (3DOF), calculated (6DOF), time history or externally calculated. Superimposed motion is applied to describe an offset from the position given by the primary motion.

Table 1 - Low and wave frequencies load effects OrcaFlex

Included effects	Frequencies
Applied loads	Low and wave
Wave load (1st order)	Wave
Wave drift load (2nd order)	Low
Wave drift damping	Low
Sum frequency load (2nd order)	Not available in frequency domain
Added mass and damping	Low and wave
Maneuvering load	Not available in frequency domain
Other damping	Low, wave or both
Current load	Low
Wind load	Low

For all type of analysis, it can be chosen to include effect of different loads. These effects are presented in Table 1. The included effects are only appearing if the included on static analysis is other than none or the primary motion is in either calculated forms 3DOF or 6DOF. Some of the included effects depends on how the primary motion is treated as. Some included effect depends on low frequency primary motion, and others depends on wave frequency primary motion or both.

2.6.3 Line objects

In OrcaFlex flexible objects can be modulated by using line objects. The flexible line elements can be used as mooring lines, hoses, nets or other similar structures. The lines are represented by a lumped mass model which is shown in Figure 8. The line are series of nodes of mass joined together by a massless spring. The properties of the line can be defined, like its length, line type, stiffness etc. The mass, weight, buoyancy and drag properties are hold by the nodes, while the axial and torsional properties are represented in the segments.

Wave excitation forces

An extended form of the Morison equation is used to account the movement of the body. By

the strip theory the hydrodynamic forces are calculated per unit length of the line object. The hydrodynamic force of the line object is the sum of the inertial force and drag force.

$$F_w = F_I + F_D \tag{25}$$

The inertial force consists of the Froud-Krylov component and the added mass component.

$$F_I = \Delta a_E + C_m \Delta a_E \tag{26}$$

Where the Δ is the displacement mass of the fluid displaced by the object, a_E is the fluid acceleration relative to the earth and C_m is the added mass coefficient.

The drag force is calculated by using the cross flow principle.

$$F_D = \frac{1}{2} \rho V_r |V_r| C_a A \tag{27}$$

Where V_r are the fluid velocity relative to the body, C_a are the drag coefficient and A is the drag area.

2.7 Weather window

Weather window analysis are performed in order to quantify the level of access to marine structures, which are deployed for operations and maintenance activities. When a structure is deployed offshore it is not as accessible as similar devices in coastal areas. Environmental factors offshore make operating and maintain structures more difficult, costly and time consuming. Some of these operations require a certain period accessibility. This will require a weather window consisting of a wave height low enough for the device to be accessed to undertake the requirements of the operation.

The accessibility by vessel to a structure is decreasing when the structure is offshore. An example is the wind farm at Horns Rev in the North Sea. The accessibility is decreasing from onshore to remote offshore, which affects the availability of the large wind farm. The availability is defined as the amount of time the windfarm can produce energy. The accessibility is dependent on the wave and wind conditions. To increase the accessibility offshore helicopters can be used to transfer crew or equipment's. However, the use of helicopters offshore is also limited by environmental parameters (van Bussel, 2002).
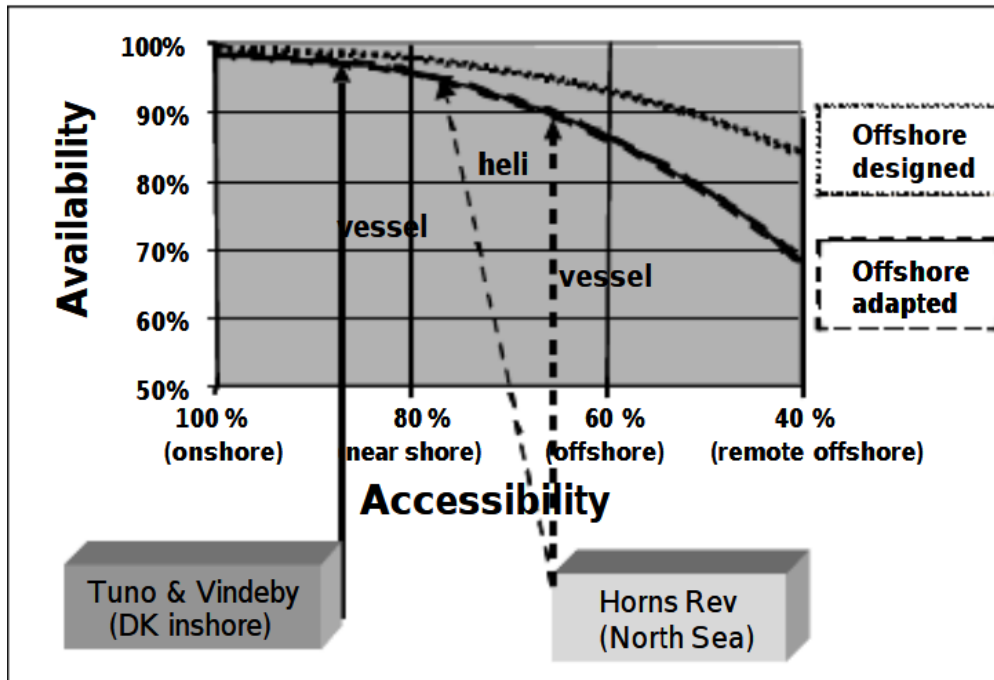
Figure 14 - Availability of an offshore wind farm as a function of the accessibility of the site (van Bussel, 2002).

2.7.1 Operation and design criteria

Weather window is defined as the period which is sufficient in length to safely carry out a marine operation. Environmental conditions during a weather window shall remain below the operational criteria (OP_{WF}) for the whole length of period. The OP_{WF} is determine during the planning process and controlled by the weather forecast. Design criteria (OP_{LIM}) is the weather condition used for calculation of design load effects and weather forces. The relation between the OP_{WF} and OP_{LIM} is the α - factor (DNV, 2011).

$$OP_{WF} = α \times OP_{LIM} \qquad (28)$$

Further,

Operation Reference Period, T_R – Duration of a marine operation

Planned Operation Period, T_{POP} – Planned schedule for the operation

Contingency time, T_C – General uncertainty in T_{POP} and required additional time for operation. The T_C should not be less than 6 hours.

$$T_R = T_{POP} + T_C \qquad (29)$$
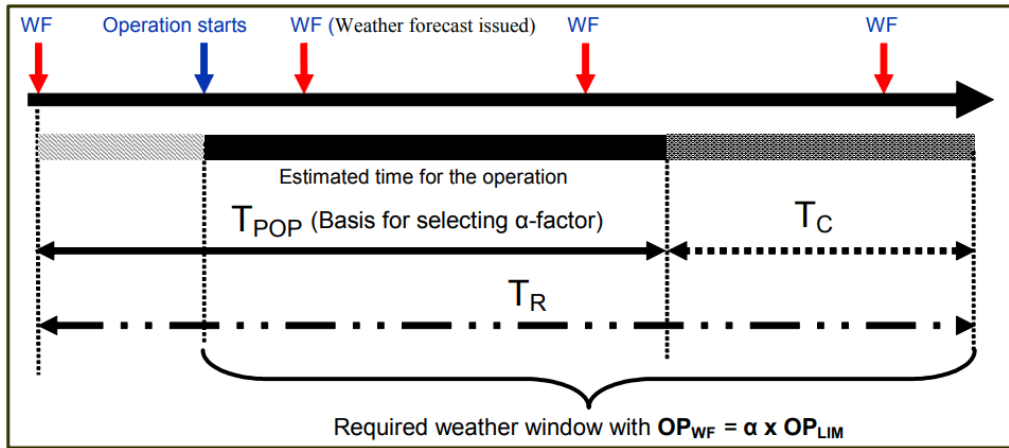
Figure 15 - Weather window components (Lecture notes, MFA-2011 UiT)

From the DNV-OS-H101; α - factors should be selected from the relevant table 4-1 through 4-5. Table 4-2 through 4-5 are specified for weather forecast level defined in chapter 2.7.1.1, only table 4-1 and 4-3 are presented in this chapter:

Table 4-1 α-factor for waves, base case

Operational Period [h]	Design Wave Height [m]						
	$H_s = 1$	$1 < H_s < 2$	$H_s = 2= 2$	$2 < H_s < 4$	$H_s = 4$	$4 < H_s < 6$	$H_s \geq 6$
$T_{POP} \leq 12$	0.65	Linear Interpolation	0.76	Linear Interpolation	0.79	Linear Interpolation	0.80
$T_{POP} \leq 24$	0.63		0.73		0.76		0.78
$T_{POP} \leq 36$	0.62		0.71		0.73		0.76
$T_{POP} \leq 48$	0.60		0.68		0.71		0.74
$T_{POP} \leq 72$	0.55		0.63		0.68		0.72

Figure 16 - α - factors for waves, base case (DNV, 2011, p. 32)

Table 4-3 α-factor for waves, Level A with meteorologist at site

Operational Period [h]	Design Wave Height [m]						
	$H_s = 1$	$1 < H_s < 2$	$H_s = 2$	$2 < H_s < 4$	$H_s = 4$	$4 < H_s < 6$	$H_s \geq 6$
$T_{POP} \leq 12$	0.72	Linear Interpolation	0.84	Linear Interpolation	0.87	Linear Interpolation	0.88
$T_{POP} \leq 24$	0.69		0.80		0.84		0.86
$T_{POP} \leq 36$	0.68		0.78		0.80		0.84
$T_{POP} \leq 48$	0.66		0.75		0.78		0.81
$T_{POP} \leq 72$	0.61		0.69		0.75		0.79

Figure 17 - α - factors for waves, Level A with meteorologist at site (DNV, 2011, p. 32)

Figure 18 shows the plot of the α - factors based on the table in Figure 17.
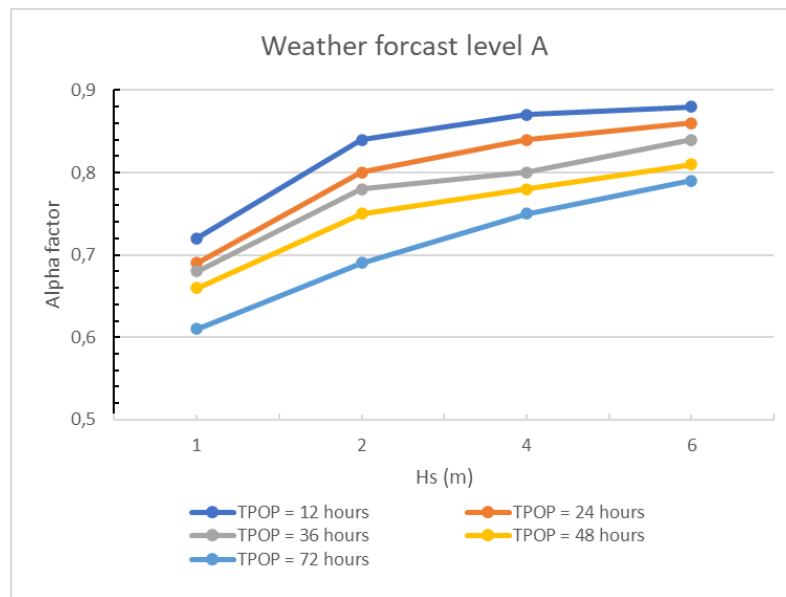
Figure 18 - Weather forecast level A α - factors

2.7.1.1 Weather forecast levels

The DNV-OS-101 (standard) define three weather forecast levels. The levels apply to marine operations:

Level A – Major marine Operations sensitive to weather (example offshore installation operations, multi barge towing and offshore float over).

Level B – Marine operations of significant importance regarding value and consequences and sensitive to environmental conditions (example offshore lifting, subsea installation and barge towing).

Level C – Conventional marine operations less sensitive to weather conditions (example onshore/inshore lifting, loads transfer and tows in shelter water).

2.7.2 Vessel type Hs and Tp limits

The conventional and most common method is use of vessels for different offshore operations. The operation limits for the vessels depends on vessel type, vessel operation, operation time and the safety aspect of the activity. Crew transfer and heavy lift operations are

examples where the safety margin is important. For personnel transfer catamarans[2] is often used because the vessel type can provide safe transfer in heavier seas due to its stability.

Table 2 - Operation limits for vessel type

	Vessel type	OP_{WF} [Hs]	Wave period limit [Tp]
Crew transport	Catamaran	2,0 m	12 s
Maintenance	Jack-Up Barge	1,0 m	16 s
Crane operations	Workboat	2,0 m	16 s

* Access limits (O'Connor et al., 2012)
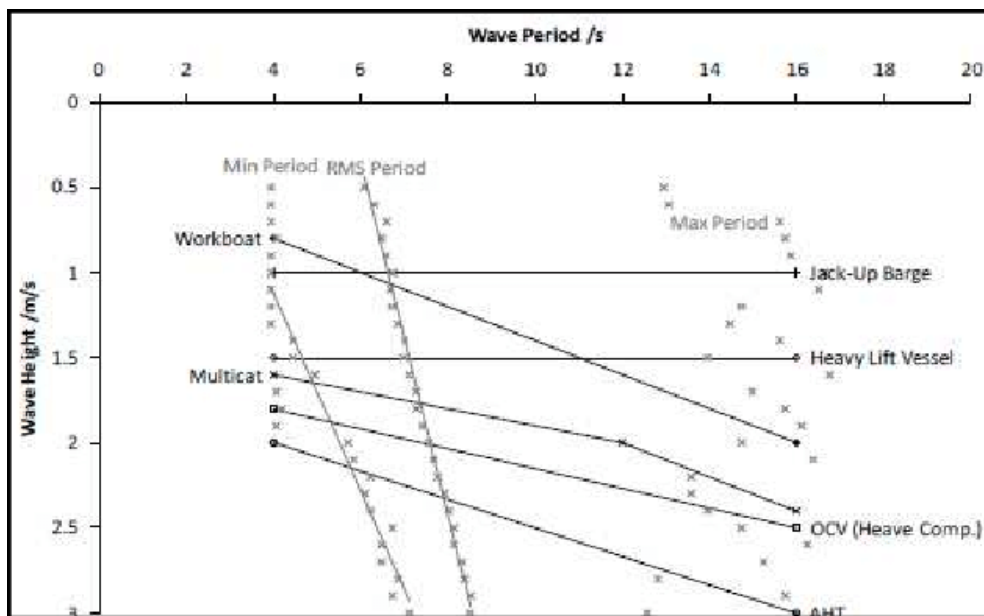
Figure 19 - Access limits in terms of significant wave height (Hs) and peak period (Tp) for a range of different vessel types (O'Connor et al., 2012)

2.7.3 Resource data

Wave data can be provided from a shared public service for environmental data, for example the Norwegian meteorological institute. Wave data is available from their thredds-server[3] based on a 3 kilometres Norwegian Reanalysis (NORA3) model.

NORA3 is a 15-yr mesoscale-permitting atmospheric hindcast of the North Sea, the Norwegian Sea and the Barents Sea. When using NORA3 a HARMONIE-Arome model with 3 km resolution covering a large domain is modelled. The wave model is further driven from the WAM 3-km model based on wind and air pressure from the Arome-model (Haakenstad et al., 2021). The dataset is provides modelldata and not observations, therefor the accuracy of

---

[2] https://www.windcatworkboats.com/fleet/

[3] https://thredds.met.no/thredds/catalog.html

the data is limited. The data can deviate in certain locations, expecially in areas with complicated bottom topography, but also along the coast of Norway due to the varying terrain.

Figure 20 shows a map of the location of observation stations and domain of NORA3. The maritime stations are indicated with blue dots, reference stations by red open circles, costal stations by green dots, mountain stations by yellow dots and light blue are Arctic stations.
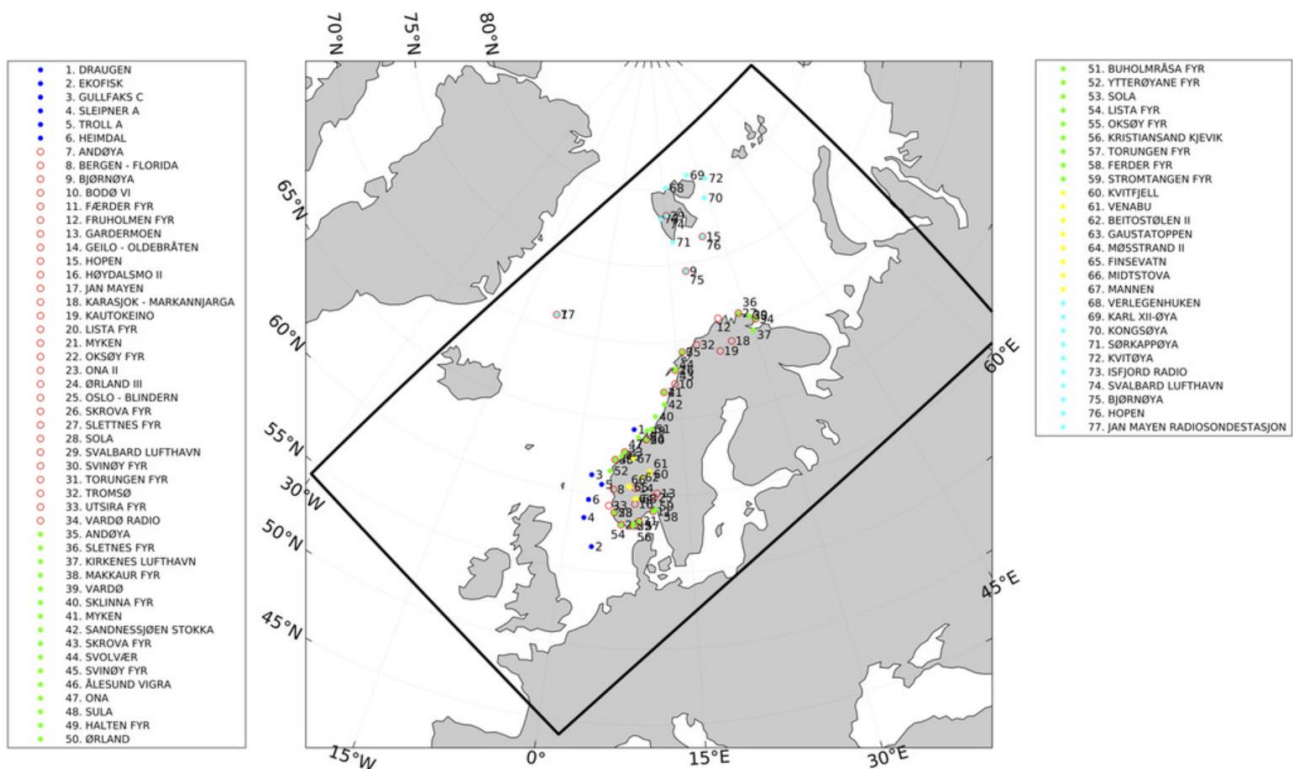
Figure 20 - Map showing the NORA3 domain and locations of observation stations (Haakenstad et al., 2021)

2.8 Vessel operation

The technology within the aquaculture facility industry is developing. The well boat industry in relation to the aquaculture industry is also adapting developments in terms of vessel size. The well boat shipping company Frøygruppen AS have during 2021 built the world's biggest well boat "Gåsø Høvdingen". The new vessel is 83,2 meter long and 30,9 meter wide, and was built because of a demand from their customers (Berge, 2022).

The vessels have several roles in the value chain for the salmon production. The first well boat involvement during the production is when transferring smolt from the smolt plant to the

ocean production site. During the production in the ocean, the well boats are used for different de-lice methods. When the salmon is between 5-6 kilos, the well boats are transporting them from the cage to the slaughterhouse (Cermaq, 2022). The smolt plants, salmon production sites and slaughterhouse are geographically dispersed. Well boats are the only appropriate method used in Norway to transport live salmon. Vessels are also used for personnel transfer and maintenance, this includes several crane operations (Lekang, 2013).

Several parameters determine the vessel operation time. Conventional aquaculture facilities with conventional de-lice methods (hydro/thermal) have an operation time in optimal conditions estimated to 3-4 hours ± 1 hours well boat docking and undocking the sea cage farm. However, method, well boat type, number of salmons, location, environment parameter etc impacts the time use. The biggest challenge, and the most limiting factor, is to maintain the welfare of the fish. The aquaculture management regulations §§26 and 28 are provisions for how suppliers and recipients must handle, care and release fish in aquaculture facilities. The fish needs to be in such condition and aquaculture facility needs to be in good living environment, that release does not lead to unnecessary stress and strain. Explicit regarding pumping of fish, for example from well boats, the pump distance have to be as short as possible, and the pumping height, pressure and drop height are regulated in such way that injuries are avoided (Akvakulturdriftsforskriften, 2008). Regulations and requirements for technical standards for floating aquaculture facilities are found in The Norwegian Regulations on technical requirements for Marine fish farms (NYTEK-forskriften, 2011). There are no specified national regulations for the vessel operations in relation to conventional aquaculture facility, nor new type of offshore facilities. The limitations and parameters are documented in internal procedures for the vessels and salmon companies.

2.8.1 De-lice methods

Hydrolicer is a non-medicinal, mechanical de-lice system. A vertical water turbulence causes the lice to unattached because it loses its vacuum against the salmon skin. It is then flushed off and the salmon is gently de-lice (Smir, 2022).

Thermal de-lice are based on leading the salmon thru heated sea water. A system that exists in today's market is Thermolicer. Thermolicer uses a flow system where the fish is pumped, filtered and led thru a pipe with heated sea water. The lice do not tolerate suddenly temperature changes. The fish is exposed to lukewarm water in a short period of time which shocks the lice and makes it unattached (ScaleAQ, 2022).

Freshwater de-lice is a de-lice method where salmon is kept in fresh water during a longer period. The lice which are found on the salmon is a saltwater species. When the lice are exposed to fresh water it will eventually die. When de-lice with freshwater method well boats are used to pump the fish into freshwater tanks. This is a time consuming process, which takes 4-8 hours to achieve a successful result (Buran Holan et al., 2017). Estimations of vessel operation time during different de-lice methods is shown in Table 3.

Table 3 - Estimations of vessel operation time during de-lice

	Operation time	Vessel docking and undocking
Thermal	6 hours	1 hour
Hydro	10 hours	1 hour
Fresh water	12 hours	1 hour

*(Personal communication with representative from SALMAR[4], 09.05.2022)

---

[4] https://www.salmar.no/

3 Method

Several steps have been developed in order to model and simulate the structure ØyMerd in a dynamic analysis software. The dynamic analysis of the structure in OrcaFlex requires some input data in terms of a 3D model, mass distribution and hydrostatic data. This input data has been performed from a graphic mesh modulation, as well as a hydrostatics and hydrodynamic analysis programs:

- Blender[5]: Open-source 3D computer graphics software.
- Meshmagick: A command line utility as well as a python module which provides hydrostatic computations (Meshmagick User's Guide, 2022).
- HAMS: Software developed for analysing wave-structure interactions (Liu, 2019).
- BEMRosetta: Boundary element methods, an open-source hydrodynamic coefficients converter (Zabala et al., 2021).
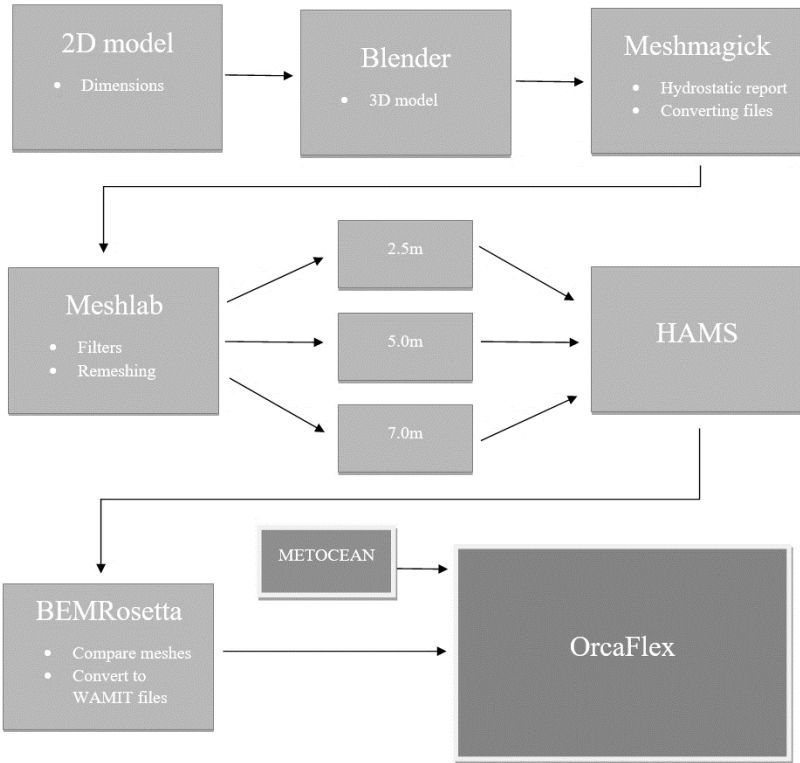- OrcaFlex: Dynamic analysis of offshore marine systems software (Orcina, 2022d).

Figure 21 - Flow chart ans the steps in developing input data for OrcaFlex

---

[5] https://www.blender.org/

A simple 2D drawing of ØyMerd was used to build a 3D model of the structure. The 2D model indicated the dimensions of the structure in terms of length and shape scaling. The 2D drawing is a simplification of the design of the aquaculture facility ØyMerd based on the known length measurements of the sides at the triangular platform. Further a 3D computer graphics software tool is used to 3D model the structure. A mesh is designed, which is the fundament for the further calculations of the hydrostatics and hydrodynamics properties.

To study the significance of the mesh for the hydrodynamics calculations, a mesh sensitivity test is performed. The mesh was divided into three different heights to be able to compare the hydrodynamic calculation coefficients. Furthermore, the result is converted to an input file which is suitable to import into the software OrcaFlex.

3.1 A model of ØyMerd

A 2D drawing of the aquaculture facility ØyMerd is studied in order to make a 3D model of the structure. The final model, which is going to be used to do the hydrodynamic calculations, is supposedly meant to be a simple geometric shaped simplification of the actual structure ØyMerd. The advantages of the structure design are that the floating structure is symmetrical, and the shape is simple geometry.

From digital illustrations of ØyMerd, which is publicly published, it is known that the structure is triangular with rounded corners. The platform is symmetrical and designed with three round wells. These wells are also symmetrical placed on the platform with equal circumference. The sides of the structure are 120 meters long, and the diameter of the wells in this project is assumed to be 55 meters, the total height is 10 meters (Gratanglaks, 2022). GeoGebra classic[6] is used as a graphic tool for visualizing the dimensioned and shape described of ØyMerd.

The 2D illustration of ØyMerd is drawn in the graphic tool where the dimensions are replicated. A coordinate system shows the scaling and ration between the wells and the outer line of the illustration. The approach of creating the 2D drawing is illustrated in Figure 23. The figure is based on a triangle with 120 meters sides and the assumption of wells with a diameter of 55 meters. Figure 22 shows a reference picture of the structure.
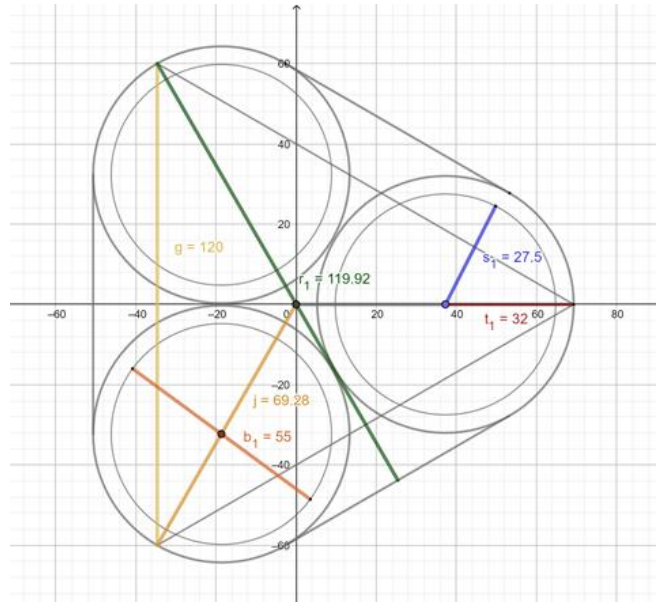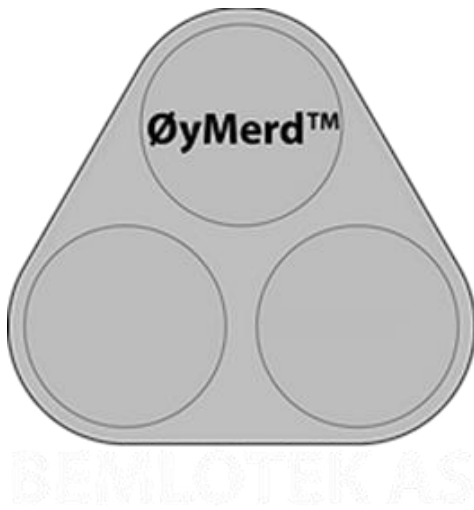
Figure 22 - Reference illustration of ØyMerd   *Figure 23 - Approach on creating 2D illustration*
(Bemlotek AS, 2022)

The final 3D model result should be a simple geometrically object with few details. The hull
is completely closed with no openings in the deck. The 2D illustration made in a graphic tool
shown in Figure 24 is imported into the 3D computer graphics software tool Blender. The
outer line ant the wells highlighted with thicker circles is used to poly build the vertexes,
edges and faces of a mesh.
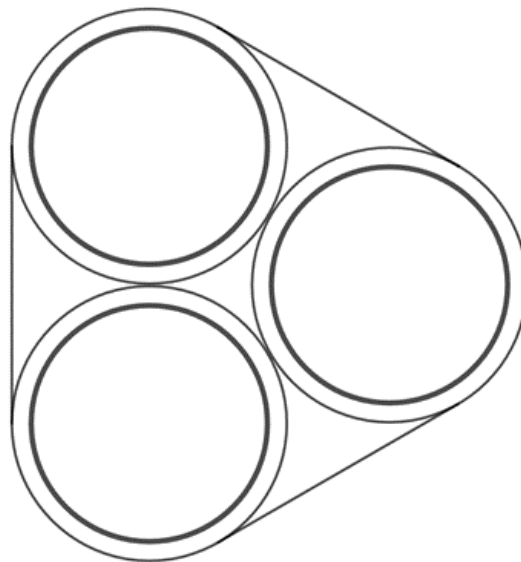
Figure 24 - 2D model of ØyMerd imported into Blender

When the 3D model is meshed a high number of minimum segments is avoided. A high number of vertices makes the model harder to work with because the file becomes bigger, this slows down the process of modeling. What the model needs is the opposite of many vertices, but not too few so the edges become too sharp. By excluding small elements and small details into the modelling, unnecessary detail work is avoided and are more fitted to the numeric solution in HAMS. The model still is supposed to be somehow smooth looking. The inside of the hull is hollow and there is no opening in the deck. The importance for the model is that the size, surfaces, orientation and volumes are correct in relation to the dimensions of the conceptual aquaculture facility.
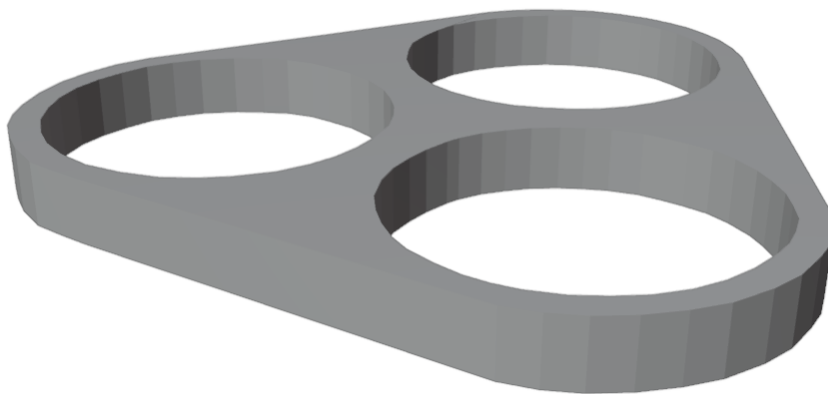
Figure 25 - Øymerd simplified 3D model

The object is scaled and rotated around the axes. The axis system origin in the center of the 3D object. The positive direction of x-axis is towards the "front", which is defined as one of the vertexes of the triangle shaped structure. The positive direction of the y-axis is towards the port side of Øymerd and the positive direction of z-axis is towards the top of the structure.

Because the object is illustrating a floating body, the reference position x, y, z (0 , 0 , 0) is edited to be located 2.5 m underneath the upper surface of the object. The reference position of the 3D object is then located in the waterline when we consider it as a floating body further in the calculations. The final 3D object is exported as a STL file format. A second object file is also saved from the 3D computer graphics software tool Blender. This obj. file is a triangulated ØyMerd mesh. The mesh needs to be triangulated to be visualized in the shaded graphic mode 3D view window in OrcaFlex.

3.2 Hydrostatic report

To calculate the wave loads and damping of the structure the hydrostatic is needed. The hydrostatics calculations are based on the ØyMerd 3D model. Also, the hydrostatic calculation is based on public information regarding the structures draft. It is known that the total height of the structure is 10 meters. The freeboard is 2.5 meters, and the draft is 7.5 meters. The mesh is imported from the Blender software. The reference origin is placed 7.5 meters above the bottom of the structure, this means that the origin is in the waterline.

Because the volume and mass displacement are unknown, the hydrostatic is calculated based on the knowledge of the structure's dimensions and draft. The geometry of the structure itself can be used to calculate wave loads and damping loads. However, to calculate the motions when floating the center of gravity, restoring forces and moments are needed. Also, to calculate the dynamics you need to know the rotation inertia which is related to the mass distribution of the structure. All can be estimated in Meshmagick as well as the displacements, stability and water plane stiffness etc.

Figure 26 shows the oxy plane. The oxy plane is 7.5 meters above the keel of the structure, which equals to the draft of ØyMerd.
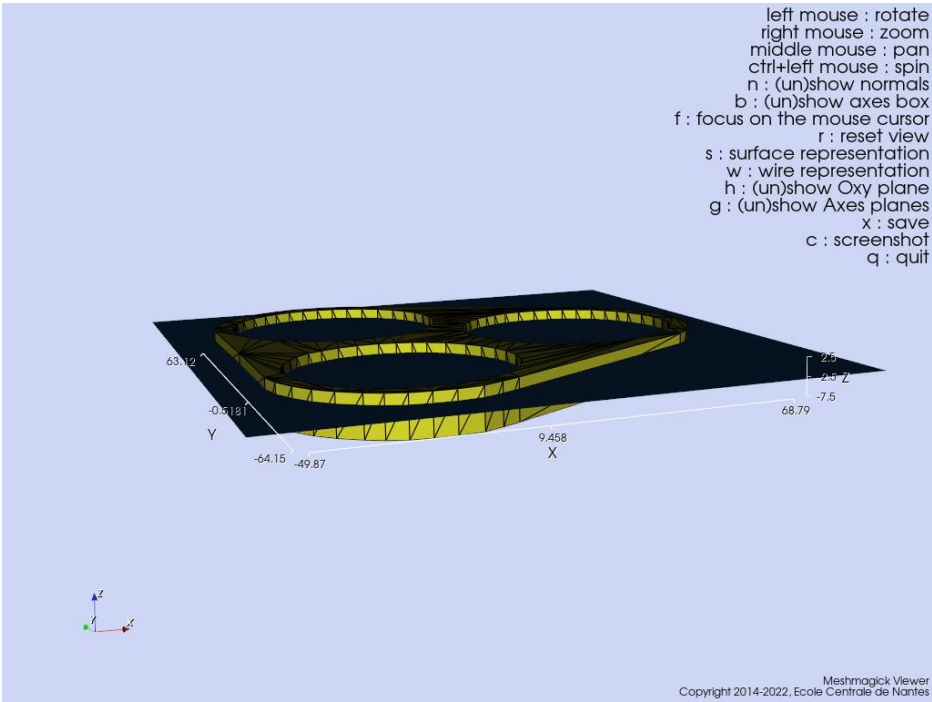
Figure 26 - Meshmagick viewer showing the oxy plane and axes box

The STL file format of the 3D model of the aquaculture structure is imported into Meshmagick. Figure 27 shows the mesh that is used to calculate the hydrostatic in Meshmagick. This is the same mesh that is presented in chapter 3.1. The boundary element method code provides options for hydrostatic computations as mentioned, where hydrostatic equilibrium for the given mass and center of gravity is solved for ØyMerd mesh. The command line utility as well as a python module are also used to edit the mesh to fit the calculations. It is particularly useful as a visualization tool.
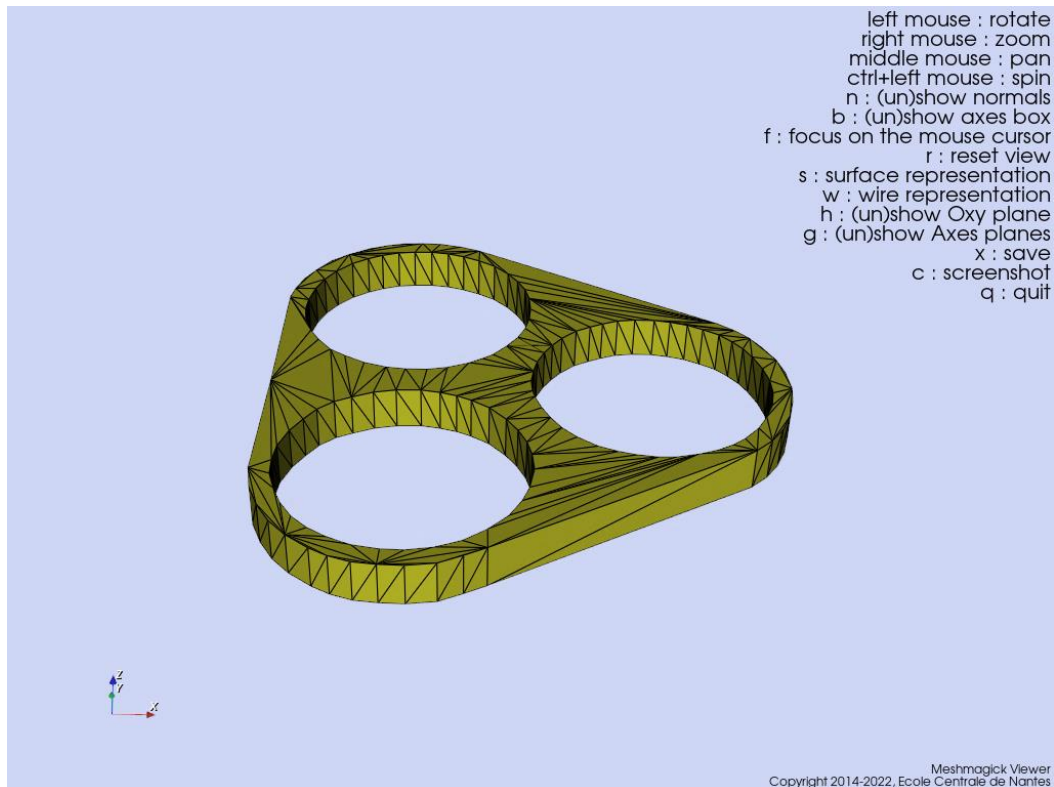
Figure 27 - Meshmagick view window

The mesh is scaled correctly with 0.0001 and is made sure that the dimensions are correct in the view window as in Figure 26. The interactive window is to be used to show the input mesh, and the correct scaling of the dimensions. It is of importance to set the translation magnitude accordingly to the original mesh. Further heal mesh is applied to remove unused vertices, degenerated faces, merge duplicate vertices, heal triangle description and normal orientations. The normal are flipped to be orientated outwards of the mesh. In the wells the normal are orientated towards the center of the wells. Heal normal checks and heal the normal consistency and verifying if they are outwards.
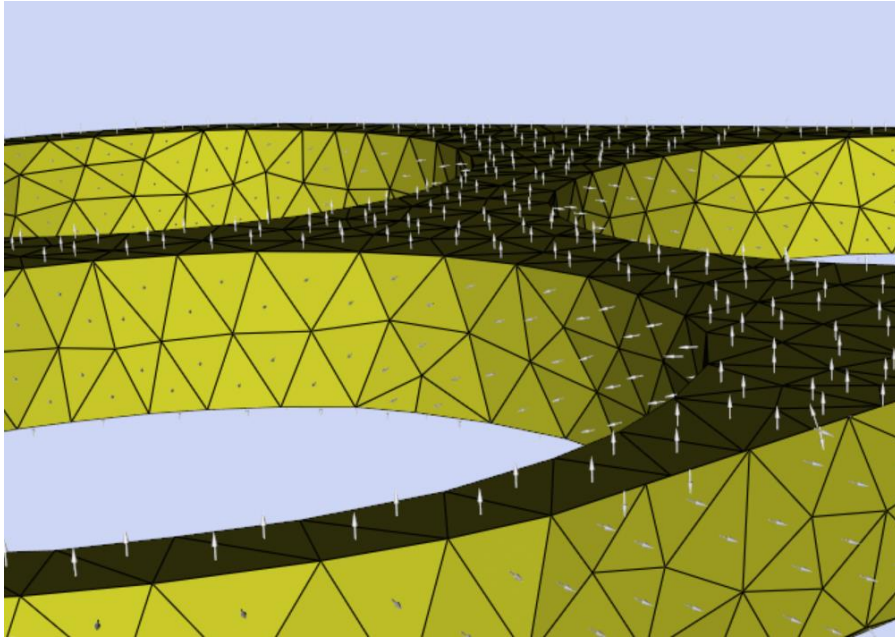
Figure 28 - Normal orientated outwards

By a simple splitting procedure all quadrangle faces are triangulate. Two triangles are generated and from both solutions the best aspect rations is kept. The mesh shown in Figure 27 is imported as a STL format, and is in a format that only deal with triangular cells so the triangulate quadrangles are modified.

For further calculations of the dynamic coefficient in HAMS solver, the body mass distribution and hydrostatic restoring forces can be obtained from Meshmagick. Meshmagick is used to distribute the mass of ØyMerd evenly in the closed volume. Before computing hydrostatic data, the center of gravity is estimated as well as specifying the density of salt water and gravity. The z position of the center of gravity is specified as -2.5 m. This is the center of the mesh ØyMerd shown in Figure 27. This position is -2.5 meters underneath the waterline which is the reference origin. This estimation is known, due to the even mas distribution. The density of salt water is specified as 1025 kg/m^3. Acceleration of gravity on the earth surface is defined as 9.81 m/s^2.

Hydrostatic data is calculated, and a hydrostatic report is thrown on the command line. Information as mass, body inertia matrix, hydrostatic restoring matrix, radii of gyration and center of buoyancy is used in further calculations in HAMS. The mesh is also converted to a WAMIT gdf. format in the Meshmagick.

3.3 Computing wave loads and motion

BEMRosetta is used to handling the ØyMerd mesh, extracting the submerge hull mesh, waterline mesh and set up the HAMS input files for computing wave loads. Hydrostatic data, mass distribution matrix and hydrostatic restoring matrix are calculated thru Meshmagick and is used for HAMS input.

The gdf. format converted in Meshmagick, of the mesh of ØyMerd, is imported into BEMRosetta for further analysing wave effect in the numerical computation software HAMS. By using mesh handling in BEMRosetta, hull mesh and water surface is extracted from the ØyMerd mesh. This is a method for removing irregular frequencies caused by the waterplane section of the parts of the floating body that intersects the free water surface. Assuming flow filling the inside of the submerge body mesh, the irregular frequencies correspond with the eigenfrequencies of the sloshing modes of the inner volume of the hull mesh (Orcina, 2022f). Ref. Article HAMS: A Frequency-Domain Preprocessor for Wave-Structure Integrations by Yingyi Liu (2019) *"In order to supress these frequencies, a kind of partially extended boundary integral equation can be developed, which assumes that the potential on the interior water plane are zero"*.
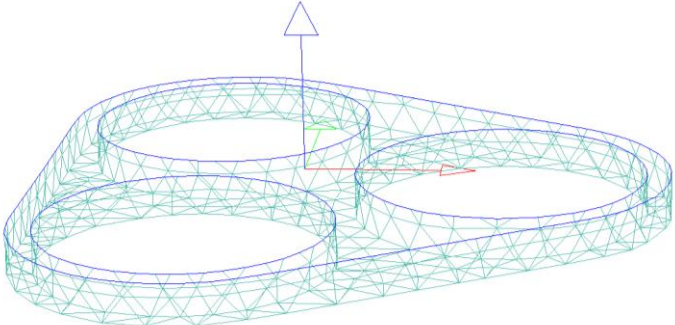
Figure 29 - Submerged hull extracted in BEMRosetta
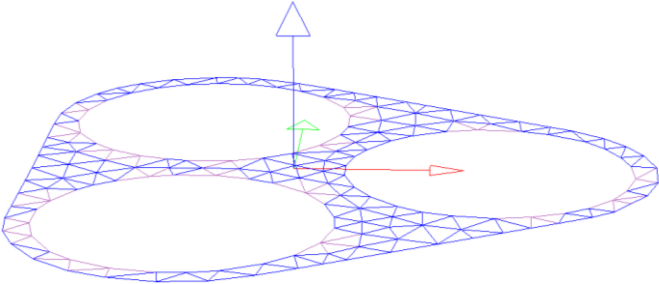
Figure 30 - Waterplane mesh extracted in BEMRosetta

The mesh, submerged hull mesh, waterplane mesh and the hydrostatic data from the hydrostatic report from Meshmagick calculation is feed into BEM solver and solved with HAMS. The general parameters like depth, wave frequencies and wave directions are edited and shown in Table 4. The body mass matrix and hydrostatic restoring matrix are shown in equation (34) and (35). The HAMS hydrostatic coefficients are saved as an output file and converted as a WAMIT .out format.

Table 4 - General parameters HAMS

Wave frequency

Number	Min [rad/s]	Max [rad/s]
120	0,1	3

Depth	Infinite	
rho	1025	[kg/m3]
g	9,81	[m/s2]

Wave direction

Number	Min [rad/s]	Max [rad/s]
9	0	180

3.3.1 Mesh sensitivity analysis

The ØyMerd mesh file from blender is imported into MeshLab to divide the hight of the mesh into 2.5m, 5.0m and 7.0m. Import the gdf formats of the three meshes divided into the different hight into BEMRosetta and calculate the wave loads and motion as described in chapter 3.3.
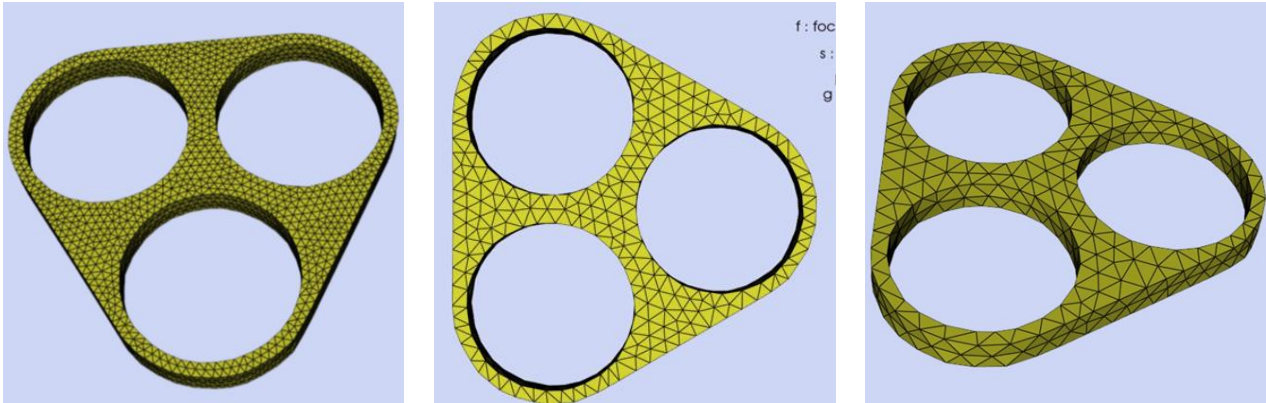
Figure 31 - Mesh ØyMerd divided into 2.5m, 5.0m and 7.0m mesh heights

3.4 OrcaFlex

OrcaFlex is used to model and simulate operation scenarios of ØyMerd. A model of ØyMerd is imported into the software, as well as hydrodynamic data. The modulations contain:

- ØyMerd: A model of the offshore aquaculture structure moored.
- Service vessel: Modulation of a standard OrcaFlex vessel type 1 (tanker).
- Service vessel docking: A model of the service vessel connected to ØyMerd in a side by side arrangement.
- ØyMerd crane operation: A model of the service vessel during a crane operation in relation to ØyMerd in waves.

A time domain analysis is run for all the model cases. Included in the static analysis is 6DOF, and the primary motion is set to 6DOF and treated as both low and wave frequency. This applies to both the vessel and ØyMerd object. The environmental parameters are a water depth of 200 meters, seabed is flat and no wind nor current is present. The wave modeled in the scenarios is an Airy wave, i.e a regular wave.

3.4.1 Hydrodynamic input

When modelling ØyMerd in OrcaFlex the software needs an input file of the hydrodynamic data. OrcaFlex can import data from WAMIT output text file with an .out extension. BEMRosetta was used to convert the hydrodynamic data from HAMS into the input file OrcaFlex can import data from.

The HAMS output files were converted to WAMIT format in BEMRosetta. The BEMRosetta converted WAMIT file text was edited to fit identical to a standard WAMIT .out file. More exactly the BEMRosetta generated .out format header of the text file was reformulated to WAMIT Version 6.314 header as shown in Figure 32. OrcaFlex has problems importing the response amplitude operators in the WAMIT file, so only the added-mass and damping coefficients and diffraction exiting forces and moments are included in the text file.

```
         -----------------------------------------------------------------------

                            WAMIT   Version 6.314

              Copyright (c) 1999-2007 WAMIT Incorporated
              Copyright (c) 1998 Massachusetts Institute of Technology

         -----------------------------------------------------------------------

              The X software performs computations of wave interactions with
              floating or submerged vessels.  X is a registered trademark of
              X Incorporated.  This copy of the X software is licensed to

                     Not actually wamit
                     BEMROSETTA
                     TROMSØ, Norway

              for end use at the above location.    Release date: 1 Jan 9999

         -----------------------------------------------------------------------
```

Figure 32 - WAMIT .out header

Further, the body parameters to the ØyMerd hydrostatic calculation are filled in the text file, and radii of gyrations are calculated whit the equations below:

$$I = mk^2 \tag{30}$$

$$k_x = \sqrt{\frac{I_x}{m}} \tag{31}$$

$$k_y = \sqrt{\frac{I_y}{m}} \tag{32}$$

$$k_z = \sqrt{\frac{I_x + I_y}{m}} \tag{33}$$

3.4.2 Vessel type settings

When OrcaFlex is opened a new vessel is inserted and the vessel-type form is opened. The vessel drawing is edited to visualize ØyMerd when modeling in wire frame view. The ØyMerd 3D mesh is imported into the shaded graphic for shaded 3D view visualization option in OrcaFlex.

The dataset from the WAMIT text file has its reference origin. Every load in the hydrodynamic data has its reference origin. This reference origin needs to cooperate with the

vessel type center of mass coordinates. The common point in both the vessel type and imported data set is the center of gravity. When importing the WAMIT input data, the center of gravity is only considered as a point to join the vessel type model and the data imported. Before importing edit the center of gravity position. A convenient position is the stern, centerline and waterline. Import the requested data. Ref. Orcina Importing hydrodynamic data: WAMIT (2022e):

"Almost all of the WAMIT data (with momentum-conservation QTFs being the sole exception) have their reference origin at WAMIT's vessel origin. OrcaFlex deduces the position of this WAMIT vessel origin, relative to OrcaFlex's vessel origin, from the difference between the centre of mass coordinates in the .out file (which are relative to the WAMIT vessel origin) and the centre of mass coordinates of the OrcaFlex vessel type (which are relative to the OrcaFlex vessel type origin). This is why the OrcaFlex vessel centre of mass must be set before import".
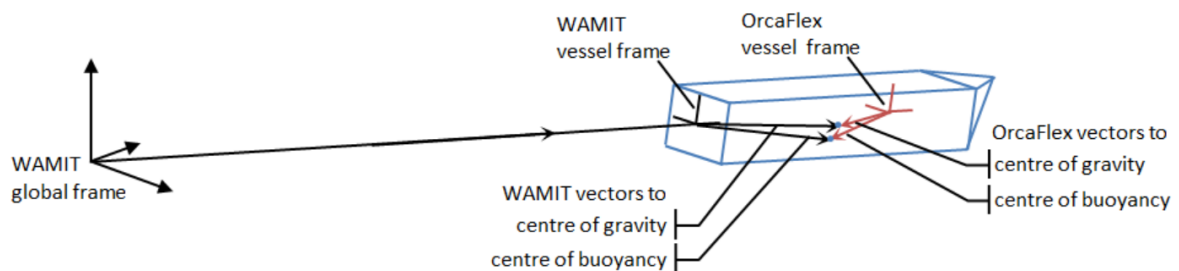
Figure 33 - Vessel axes and reference origins (Orcina, 2022e)

When the hydrodynamics are imported, the center of gravity and center of buoyancy are changed back to the position calculated in Meshmagick hydrostatic report. The center of gravity and center of buoyancy are then correctly located according to the local OrcaFlex vessel axes. To control the basic model a self-check is performed to confirm that the data was imported correctly:

   I.   Simulation time 300 seconds.
  II.   Wave height to zero.
 III.   Give ØyMerd an initial position above the equilibrium position of the structure.
 IV.   Run time domain analysis to control that the object returns into equilibrium position.
  V.   Add waves and analyze if the structure behaves normal.

Calculation method shown in Figure 34.

Figure 34 - Calculation method self-check hydrostatic data

3.4.3 ØyMerd moored

In this model ØyMerd is modelled by drawing the vessel type as ØyMerd, importing the shaded graphic file and importing the hydrodynamic data as described in chapter 3.4.1. The structure is then moored to the seabed by nine line objects. A time domain analysis is run several times with different environmental parameters.

ØyMerd is moored using three lines in each corner. The line type is modelled as a chain, and the connecting nodes are connected to the ØyMerd and anchored to the seabed. This system is often used as a temporary mooring but are in this model representing a permanent mooring. By this model in OrcaFlex the mooring is representing a permanent mooring for position keeping, and the dynamic of the structure ØyMerd connected to the chains are analyzed.
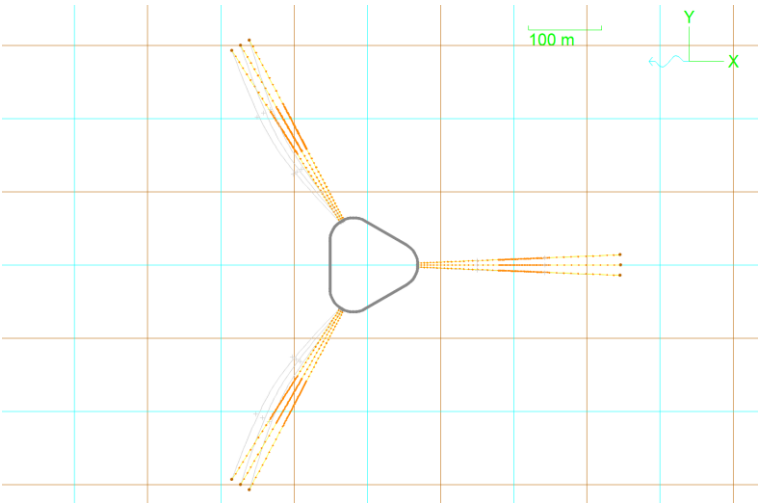
Figure 35 – 3D view of ØyMerd moored by 9 lines in OrcaFlex

The nine mooring lines are composed of chain sections. These are drawn yellow with three sections with 20, 40 and 10 segments numbers. The end A of the chain is connected to ØyMerd and following the dynamics of the structure, while end B is anchored to the seabed. Total length of a mooring line is 380 meters. The mass per unit length is 0.219 te/m, meaning the total mass is 83.22 ton. The position of the attachments is calculated in GeoGebra classic coordinate system. In each corner there is attach three lines where the outer lines are angled 5 degrees to the middle mooring line. The three-attachment point are then scaled with 5 for the anchor points to the seabed.
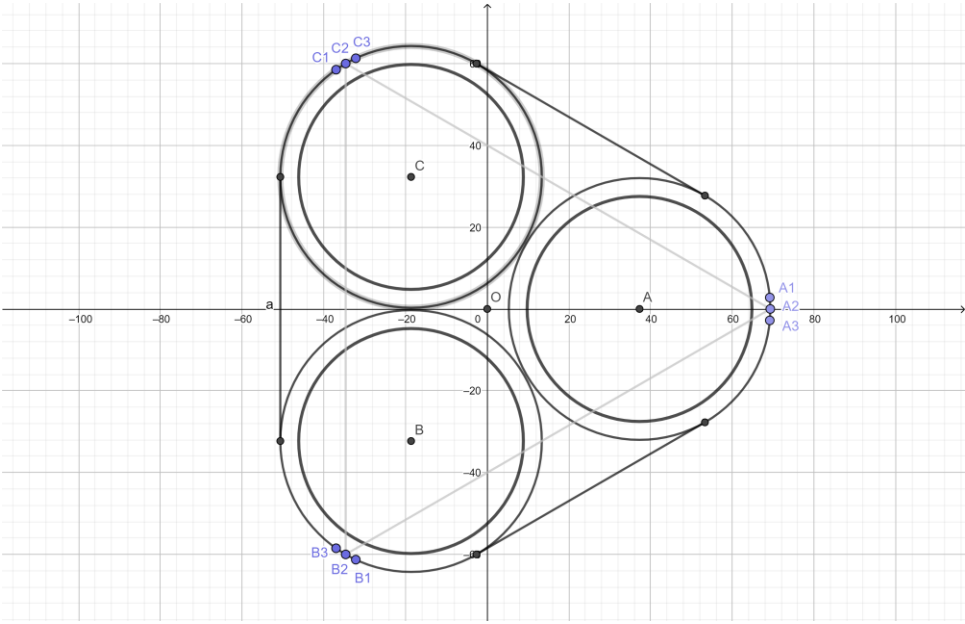
Figure 36 - Mooring line connection points

Table 5 - Mooring attachment points to ØyMerd and seabed

ØyMerd	x	y	z	Seabed	x	y	z
A1	69,16	2,79	-7,5	A1.1	345,8	13,95	0
A2	69,28	0	-7,5	A2.1	346,4	0	0
A3	69,16	-2,79	-7,5	A3.1	345,8	-13,95	0
B1	-32,16	-61,29	-7,5	B1.1	-160,8	-306,45	0
B2	-34,64	-60	-7,5	B2.1	-173,2	-300	0
B3	-36,99	-58,5	-7,5	B2.1	-184,95	-292,5	0
C1	-36,99	58,5	-7,5	C1.1	-184,95	292,5	0
C2	-34,64	60	-7,5	C2.1	-173,2	300	0
C3	-32,16	61,29	-7,5	C3.1	-160,8	306,45	0
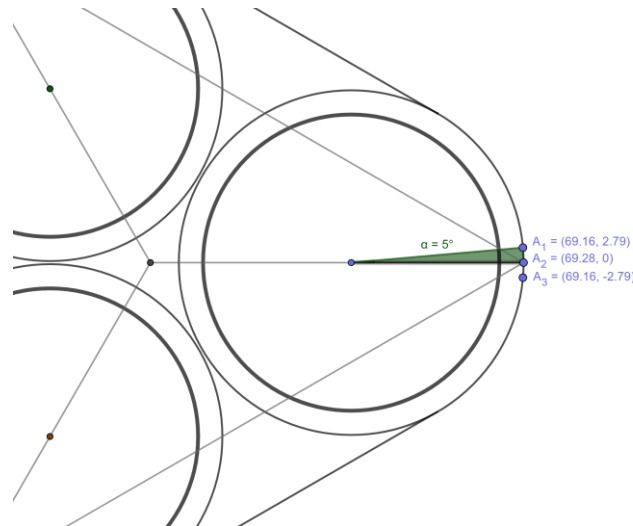
Figure 37 - Attachment points for line and angle

The ØyMerd motion is calculated in all six degrees of freedom. Because some effects depend on all of the primary motion both low frequency and wave frequency, therefore a mixture of both is specified. Primary motion is set to 6DOF, and included effects are wave load 1st order, added mass and damping, and other damping. For the solver to run the chain statics method step 1 is chosen as spline and step 2 full statics.

Environmental parameters are edited. Water depth is 200 meters, seabed is flat, and no wind or current is present. A regular wave (Airy wave) is chosen with a wave height of 2 meters, which equals to an amplitude of 1 meter. The wave is incoming straight ahead of the structure from the global x-direction as shown in Figure 35. Simulation time is set to 360 seconds. Simulation is run 13 times with the frequency of 0,1 to 1,0 [rad/s].

Table 6 - Wave frequency and period

$$Frequency = \frac{1}{Period}$$

Frequency	0,1	0,2	0,3	0,4	0,5	0,6	0,7	0,8	0,9	1
Period	10	5	3,33	2,5	2	1,67	1,43	1,25	1,11	0,83

To find ØyMerd natural period a modal analysis on the whole system is performed. The model is reset and the ØyMerd data form is opened. The included in static analysis option is set to 6DOF and static is run. Open the modal analysis form from the result menu. Select the whole system in the object box and calculate mode shape is selected. Then press the calculate

option, and make sure the animation period is set to fixed 5 seconds. The natural period of the ØyMerd is then presented for all the degrees of freedom.

3.4.4 Service vessel

In this model a service vessel is simulated by using the OrcaFlex standar vessel type. The simulation is than run the same as described in chapter 3.4.3.

For the models, a vessel type 1 vessel is used. This vessel type is a standard OrcaFlex vessel option. The vessel length is 103 meters, breadth 15.95 meters, draught 6.66 meters, transverse GM is 1.84 meters, longitudinal GM is 114 meters, and a block coefficient of 0.804. The mass is 9017.95 ton. Other properties data like stiffness, added mass, damping and displacement, and load RAOs are all from an NMIWave diffraction analysis of a 103 meter long tanker (Orcina, 2022).
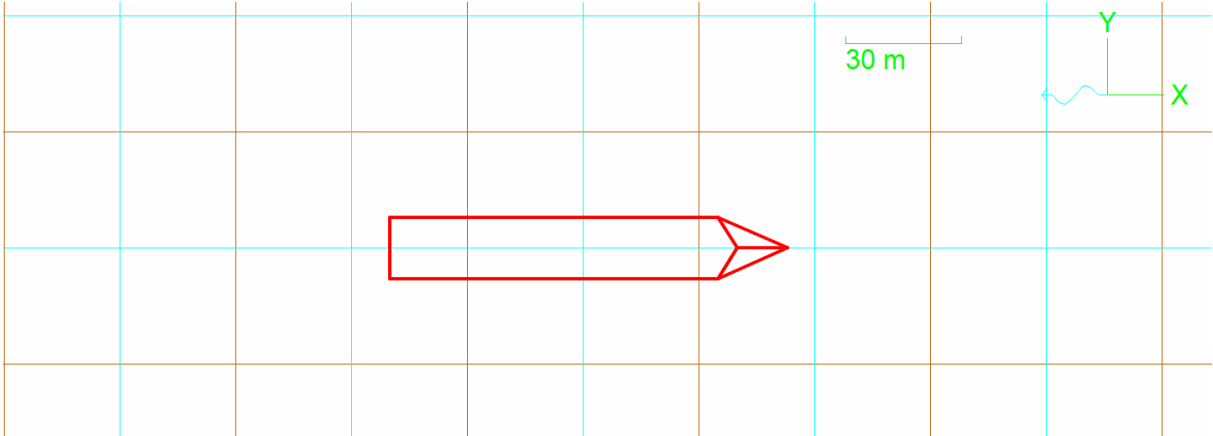
Figure 38 – 3D view of vessel in OrcaFlex

The vessel motion is calculated in all six degrees of freedom, and both low and wave frequency is included in the statics. The environmental parameters are set to air wave type, seabed flat and water depth 200 meters. The vessel is experiencing a regular wave ahead in global x-direction. The wave height and period are edited, and 20 simulations is run with wave amplitude 1 and wave frequency 0.07 to 1.0 [rad/s]. The simulation time is set to 360 seconds.

3.4.5 Service vessel docking

The service vessel and ØyMerd are connected with a wire object to analyze the dynamic when interacting.

The vessel object has been modelled by using the default vessel type described in chapter 3.4.4, and ØyMerd is moored as described in chapter 3.4.3. The mooring line between the service vessel and ØyMerd "quayside" have been modelled as a constant tension winch object. The vessel is moored with a stern breast and spring, as well as a bow breast and spring shown in Figure 39. The length of the wires are 10 meters.
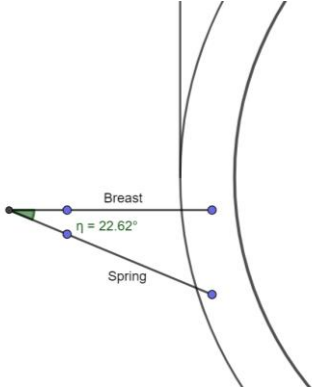
Figure 39 - Blue dots attaching points docking

For the calculations, the service vessel and ØyMerd included in the static calculation, and also primary motion is set to calculate 6DOF. Included effects are wave load 1st order, added mass and damping, and other damping. The objects are experiencing an Airy wave with a wave amplitude of 1 meter and wave frequency 0,1 to 1,0 rad/s. The wave is incoming in global x-direction.
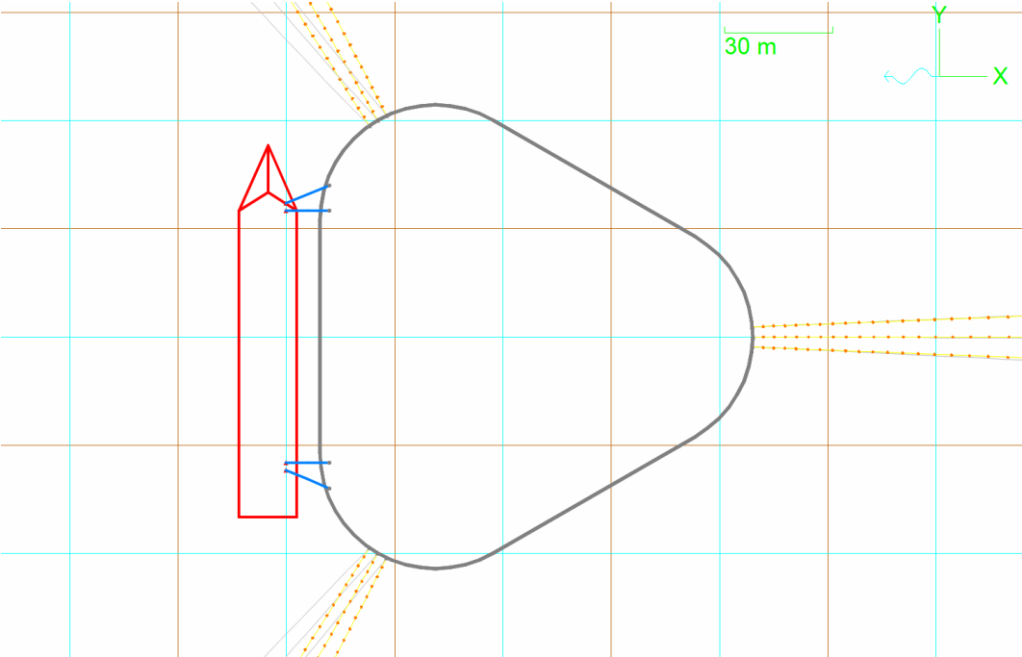
Figure 40 - Service vessel docking

3.4.6 Crane operation

The model has the ØyMerd structure moored, the service vessel docking and the crane object. The crane is modeled on the service vessel deck and are facing towards one of the wells of the offshore aquaculture facility structure.

The model has been run for two crane motion analysis:

I.   The crane motion in wave height of 2 meters and wave period of 10 seconds.
II. The crane motion comparison for three wave heights and three different wave periods.
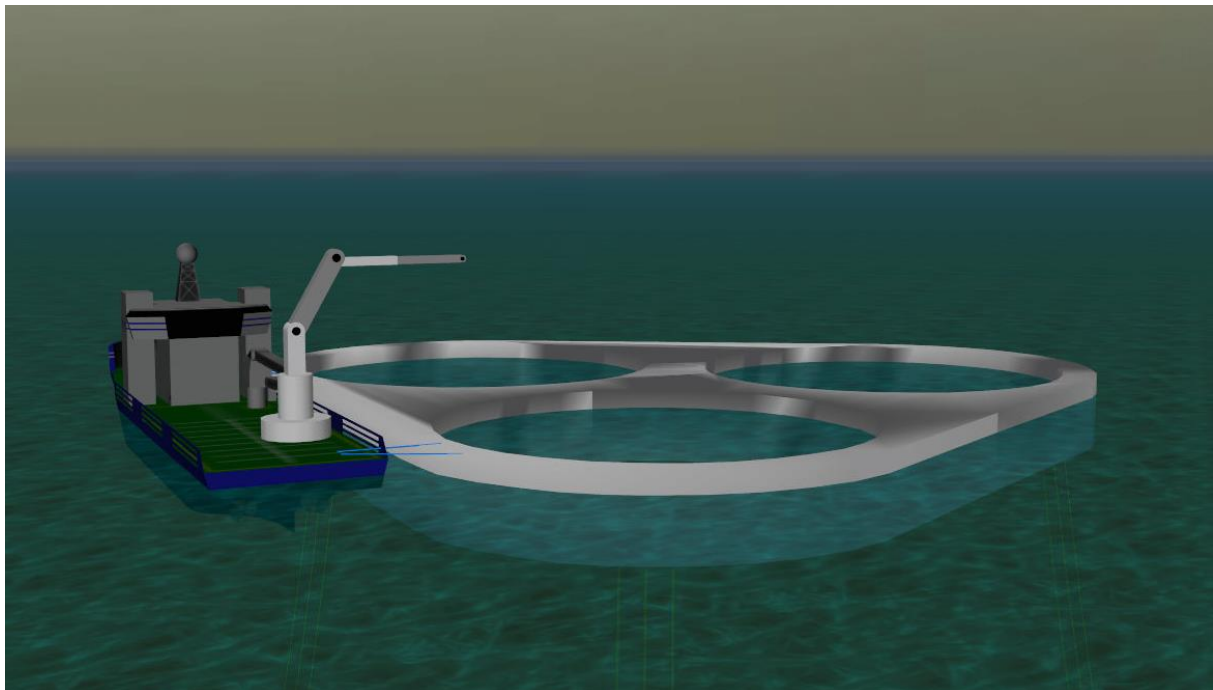
Figure 41 - Service vessel crane operation shaded 3D view OrcaFlex

To create a simple crane, 13 shape objects are modelled. The shape objects are connected to the vessel movement. The total height of the crane is 20 meters when fully extensive and can extend 15 meters horizontally. There is no impact from the crane weight on the vessel stability.
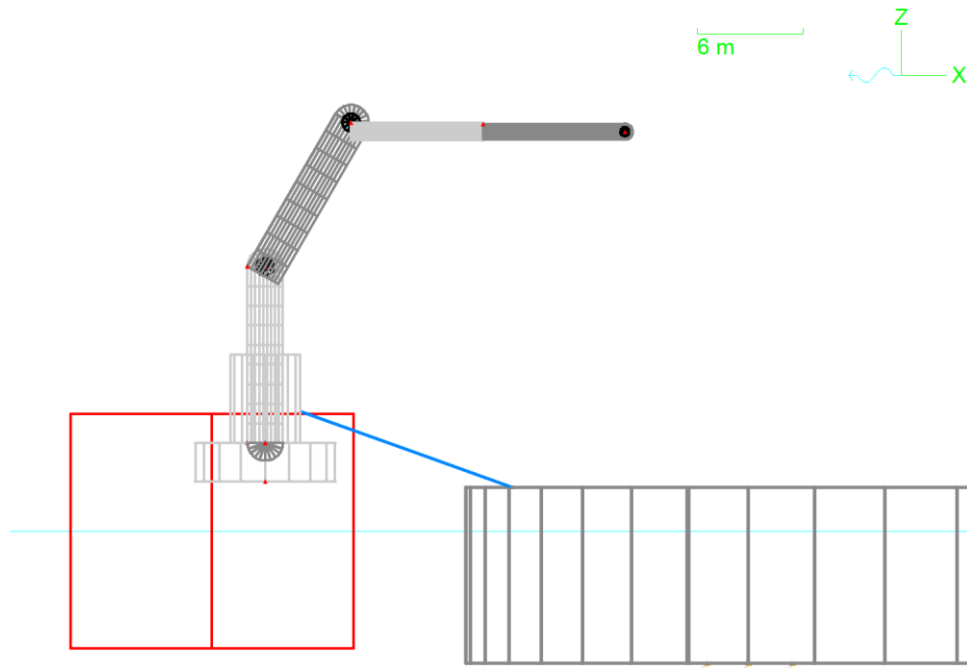
Figure 42 - Crane model on service vessel deck

Both vessel and ØyMerd are included in the static calculation. Included in the dynamic calculation are 1st order wave loads, added mass and damping, and other damping. Because the vessel is subjected to waves and wave frequency excitation the primary motion is treated as both low and wave frequency. Wave parameters are set to wave height of 2 meters and wave period of 10 second. The wave type is Airy wave, wind and current are excluded in the model. The service vessel is orientated with the bow heading in the global y-direction, and the wave is incoming on the starboard side. ØyMerd is orientated with the local x-direction in the direction of the incoming wave as shown in Figure 43.

For the comparison of the wave tip motion in different wave height and wave periods the calculation has been run 9 times for the wave data. The wave is incoming from global x-direction:

Table 7 - Wave parameters in crane operation simulations

Wave height (m)	Airy wave, wave period (s)		
1	10	5	3
2	10	5	3
3	10	5	3
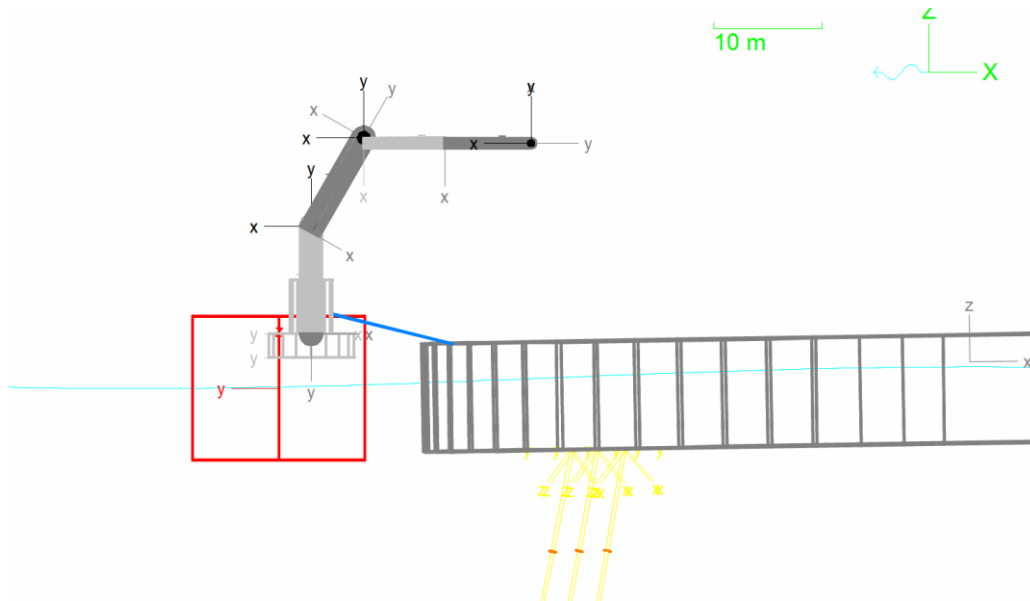
Figure 43 - Crane model local axes

3.5 Weather window analysis

To quantify the level of access for vessel operation in Vestfjorden in North-Norway, wave data from Norwegian Meteorological Institute is analysed. The wave data is operational data which has been developed over time. The dataset used is called NORA3. This is a reanalysis or hindcast is analysis of old envionmental data. The wave data which are analysed are used to quantify:

1. Wave height and wave period distribution during year 2018-2019.
2. Annual mean exceedance when the wave height is above a certain level.
3. The seasonality of the wave regimes.
4. The number of weather windows for various vessel operation access occurring for one year.
5. The waiting periods in between the weather windows during a month with expected heavy environmental conditions.

The site used for the weather data is located in Vestfjorden outside "Hamarøya", more specific the coordinate of the location is N 16° 8ʹ10.72ʺ and E 15° 13ʹ22.22ʺ.

Figure 44 - Aquaculture facility site for weather window analysis (Norgeskart, 2022)

The processed data is resulting in the significant wave height and wave period from 01. January 2018 to 01. January 2019 for each hour. The data set contains 8762 data points. Once the wave data has been retrieved from the Norwegian Meteorological Institute thredds server the analysis was carried out using weather window models based on Excel. The Excel spreadsheets used the wave data as a database for varius graphs and tables which is produced to be presented in this thesis.

3.5.1 Vessel operations

The weather window analysis for different vessel operations is based on the vessel type wave height limit, wave period limit and operation time presented in chapter 2.7.2 and 2.8.1. The analysis is carried out for three scenarios:

Table 8 - Cases for weather window analysis for vessel operations.

	Vessel type	**Vessel operation**	**OP$_{WF}$ [Hs]**	**Wave period limit [Tp]**	**Duration**
I.	Catamaran	Crew transfer	2,0 m	12 s	1 hour
II.	Workboat	Thermal, hydro and freshwater de-lice	2,0 m	16 s	7, 11 and 13 hours
III.	Workboat	Mooring maintenance	2,0 m	16 s	-

4 Results

A model of the offshore aquaculture facility ØyMerd has been modeled and the hydrostatic and hydrodynamics have been calculated. In OrcaFlex the response and dynamic analyze is performed for the structure moored, and in interaction with a vessel object. Each object is analyzed but also combined in models to study vessel crane operation and docking in relation to the ØyMerd structure in exposed environment. Environmental conditions for a location are collected and a weather window analysis for the data is conducted.

4.1 Hydrostatic results

Table 9 - ØyMerd hydrostatic report from Meshmagick

Hydrostatic report

Gravity acceleration	m/s^2	9,81		
Density of water	kg/m^3	1025,00		
Waterplane area	m^2	3939,90		
Wetted surface area	m^2	10724,40		
Displacement volume	m^3	29603,50		
Displacement mass	tons	30343,59		
Centre of buoyancy	m	0,342	-0.397	-3,745
Centre of gravity	m	0,342	-0.397	-2,5
Draft	m	7,50		
Length overall submerged	m	118,66		
Breadth overall submerged	m	127,27		
Forward perpendicular	m	68,63		
Transversal metacentric radius	m	138,60		
Longitudinal metacentric radius	m	137,20		
Transversal metacentric height	m	137,36		
Longitudinal metacentric height	m	135,95		

Inertias from standard approximations [Rxx= 0.3; Ryy = Rzz = 0.25 Lpp]

RXX	m	38,18
RYY	m	29,618
RZZ	m	29,618
IXX		4,42E+10
IYY		2,66E+10
IZZ		2,66E+10

From Meshmagick the hydrostatic are calculated. The displacement volume is 29603.5 m^3 and the displacement mass is 30343.6 tons. The mesh of the structure is symmetrical, so the buoyancy point is -3.745 meters below the waterline, and the center of gravity is -2.5 meters below the waterline. From the hydrostatic report we have the body mass matrix and hydrostatic restoring matrix in equation (34) and (35).

Body Mass Matrix

$$
\begin{matrix}
3.0343585e7 & 0 & 0 & 0 & 0 & 0 \\
0 & 3.0343585e7 & 0 & 0 & 0 & 0 \\
0 & 0 & 3.0343585e7 & 0 & 0 & 0 \\
0 & 0 & 0 & 3.233e10 & 0 & 0 \\
0 & 0 & 0 & 0 & 3.2e10 & 0 \\
0 & 0 & 0 & 0 & 0 & 6.282e10
\end{matrix}
\qquad (34)
$$

Hydrostatic Restoring Matrix

$$
\begin{matrix}
0 & 0 & 0 & 0 & 0 & 0 \\
0 & 0 & 0 & 0 & 0 & 0 \\
0 & 0 & 3.9617e7 & 1.6034e5 & -2.5655e5 & 0 \\
0 & 0 & 1.6034e5 & 4.0468e10 & 0 & 0 \\
0 & 0 & -2.5655e5 & 0 & 4.0468e10 & 0 \\
0 & 0 & 0 & 0 & 0 & 0
\end{matrix}
\qquad (35)
$$

4.2 Hydrodynamic coefficients/mesh sensitivity analysis

A comparison of the hydrodynamic coefficients of the mesh height 2.5, 5.0 and 7.0 meters are shown in Figure 45 and Figure 46. The pink graph represents the 2.5 mesh, yellow graph 5.0 mesh and blue graph 7.0 mesh.
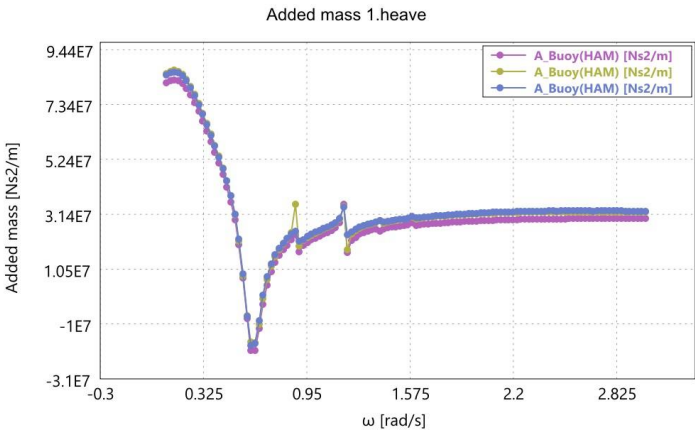
Figure 45 - Added mass 1. heave mesh sensitivity analysis
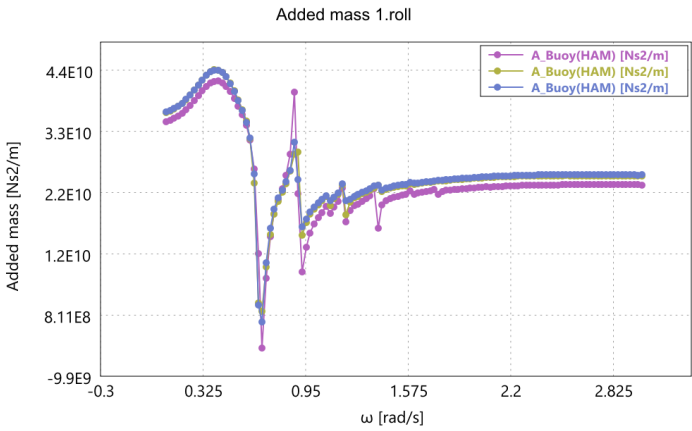
Figure 46 - Added mass 1. roll mesh sensitivity analysis

Figure 45 and Figure 46 shows the added mass in heave for the three different mesh heights. The added mass coefficient of the floating ØyMerd mesh is shown as a function of the angular wave frequency of heave and roll motion. Irregular frequencies occur during the frequency around 0.88 and 1.17 rad/s.

Radiation damping 1.heave
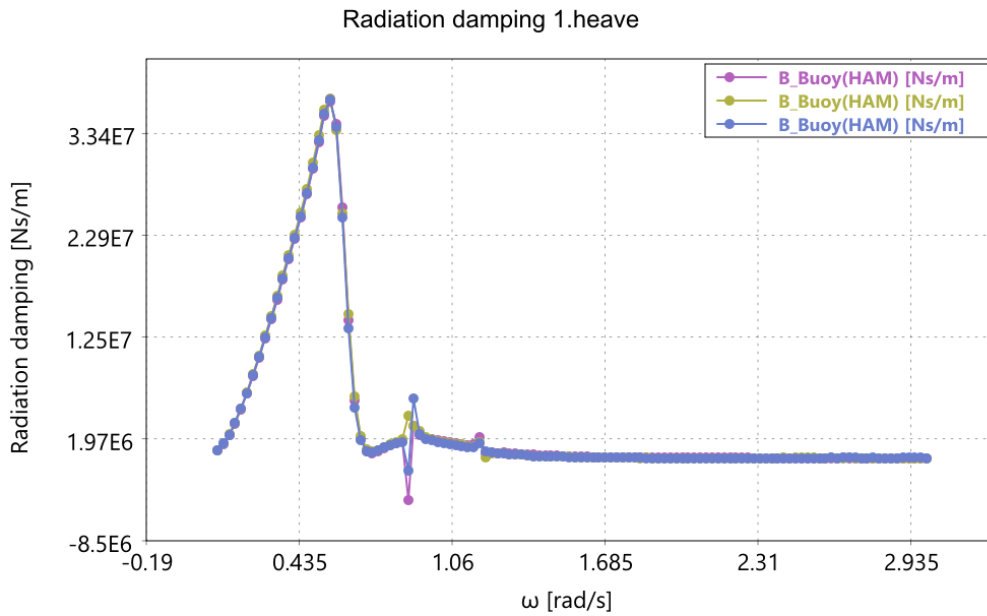
Figure 47 - Radiation damping 1. heave mesh sensitivity analysis

Radiation damping 1.roll
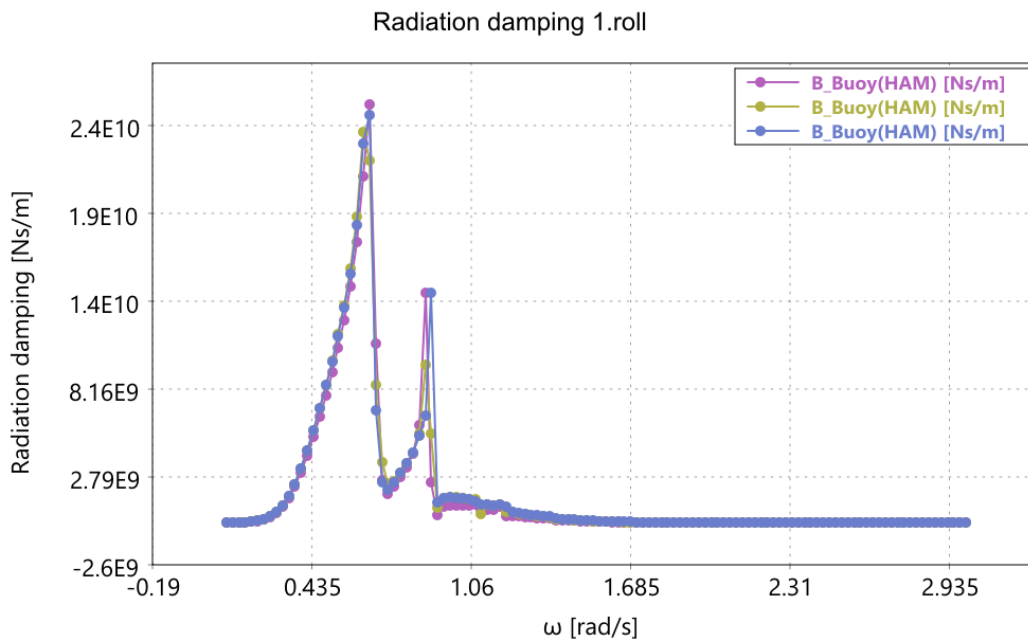
Figure 48 - Radiation damping 1. roll mesh sensitivity analysis

Figure 47 and Figure 48 shows the radiation damping coefficients of the floating body ØyMerd as a function of the angular wave frequency of heave and roll motion. Irregular frequency occurs around the frequency 0.88 and 1.17 rad/s.

4.3 Structure and Vessel dynamics

The model of ØyMerd with imported hydrodynamic data is tested during a self-check of the system. The initial position of the structure is 5 meters above waterline and Figure 49 shows the position z of the structures when simulation is run.
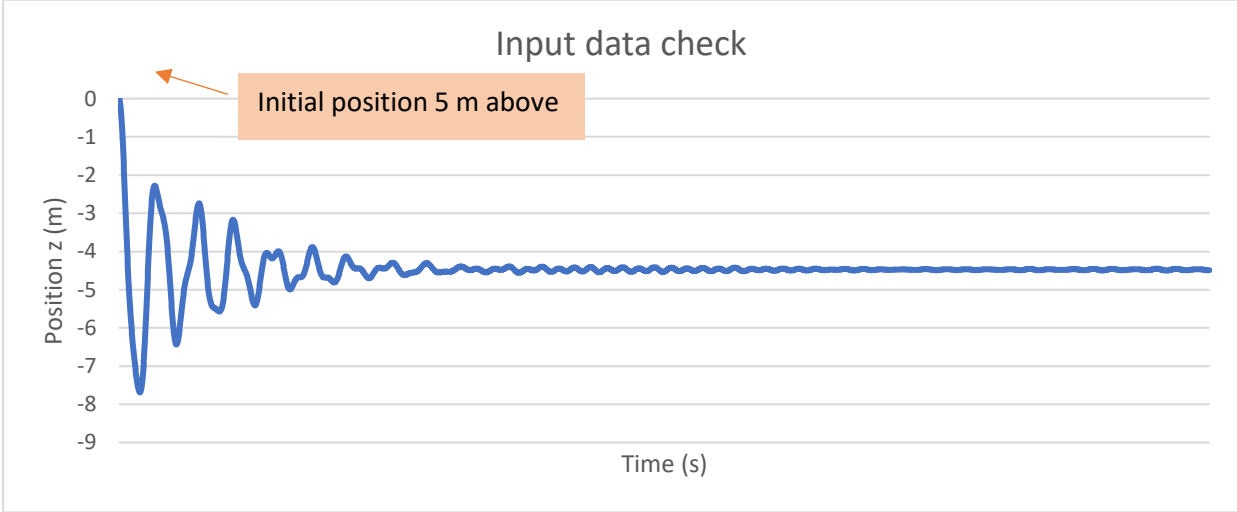
Figure 49 - Input data check on ØyMerd, return to equilibrium

Figure 50 show the iteration count for the simulation of ØyMerd moored for simulation duration of 360 seconds.
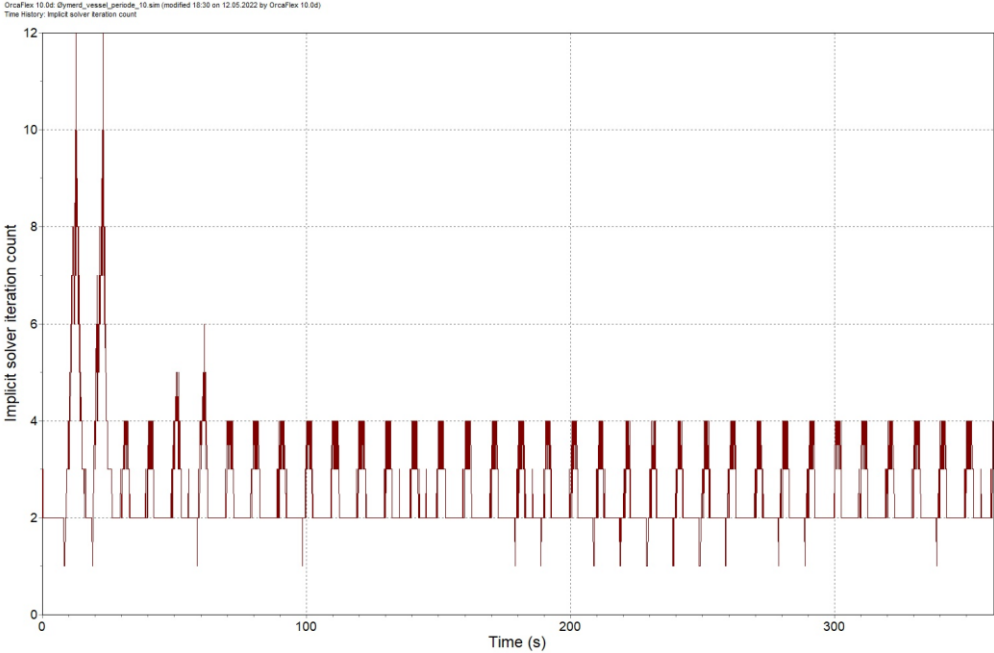
Figure 50 - Implicit solver iteration count for ØyMerd moored OrcaFlex

Results from the dynamics of service vessel and ØyMerd in wave amplitude 1 meter and a variation of wave frequency (rad/s). Some waves have a height greater than the theoretical breaking height. These regular waves are higher than 1/7 of the wavelength, and therefor nonphysical waves. The dynamics of the vessel and structure is relative to the static position p and the static orientation of the object. The position of p is in the center-waterline of ØyMerd, and the very center of the service vessel.
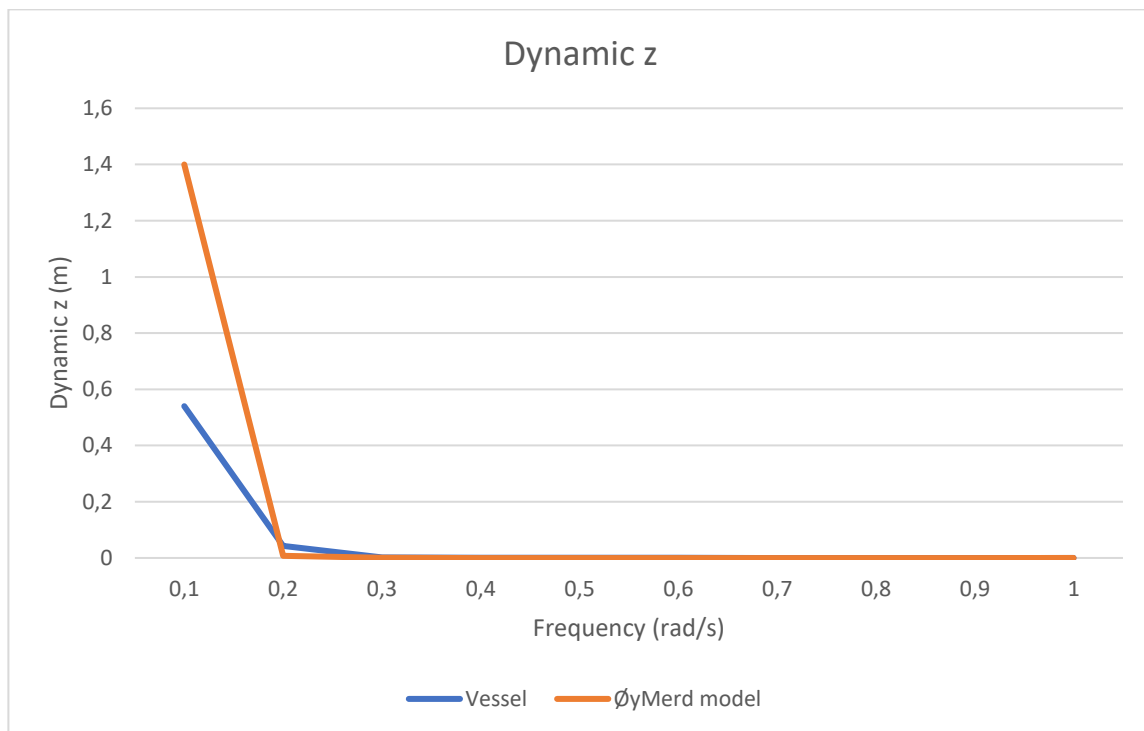
Figure 51 - Dynamic z, vessel and ØyMerd model

The dynamic calculation in OrcaFlex shows that the dynamic z for ØyMerd object is vanishing from the wave frequency 0,2 and higher as shown in Figure 51.

Figure 52, Figure 53, Figure 54 and Figure 55 compares the superimposed motion results for heave and pitch for the vessel and ØyMerd. This are the position and orientation of the vessels and structure due to superimposed motion relative to the primary position of the objects. This are wave-generated part of the motions. Figure 52 shows a comparison of the heave motion of the vessel and ØyMerd in Airy wave with the same wave amplitude of 1 meter and 10 seconds wave period. The peak deflection in heave of ØyMerd is 1.4 meters. The vessel has a deflection of 0.5 meters.
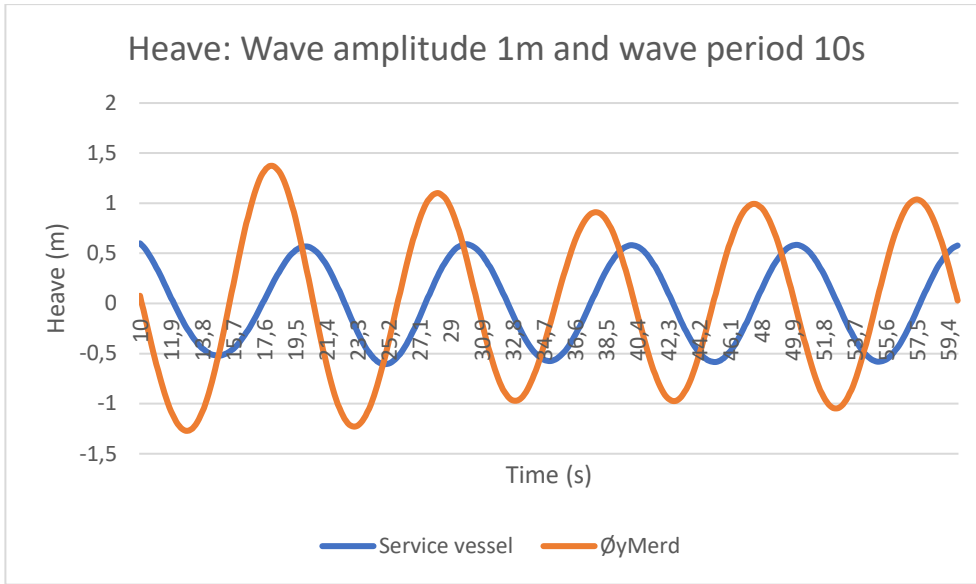
Figure 52 - Comparison vessel and ØyMerd heave motion. Wave amplitude 1 meter and wave period 10 seconds.
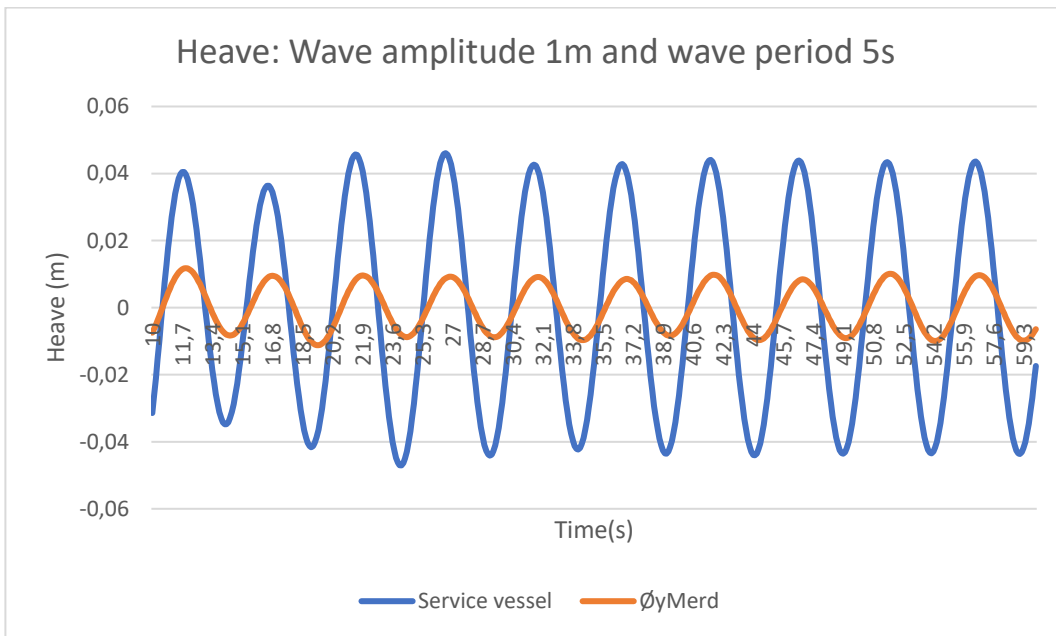
Figure 53 - Comparison of vessel and ØyMerd heave motion. Wave amplitude 1 meter and wave period 5 seconds.

Figure 52 and Figure 53 shows the heave superimposed translational displacement component in the primary vessel axes direction, relative to its primary motion position.
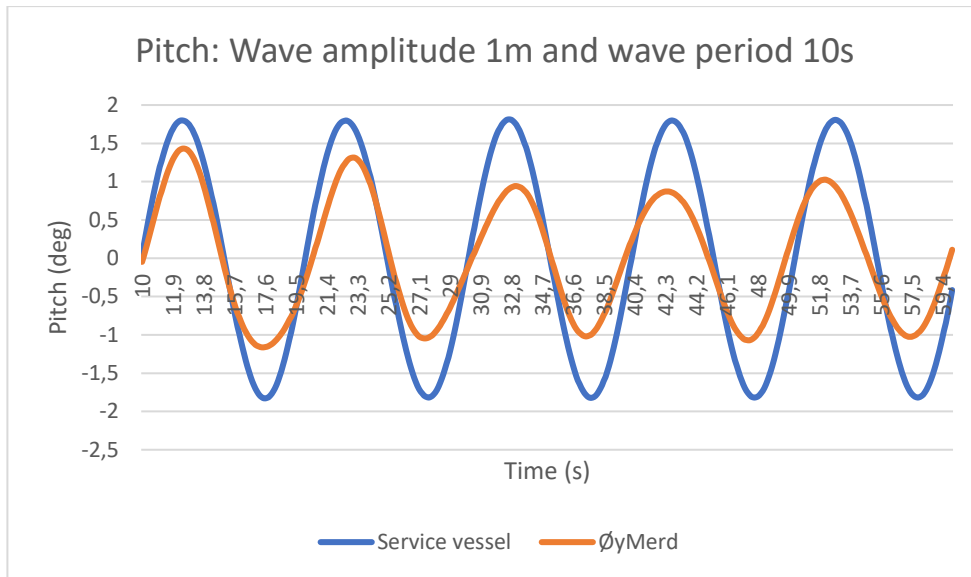
Figure 54 - Comparison of vessel and ØyMerd pitch motion. Wave amplitude 1 meter and wave period 10 seconds.
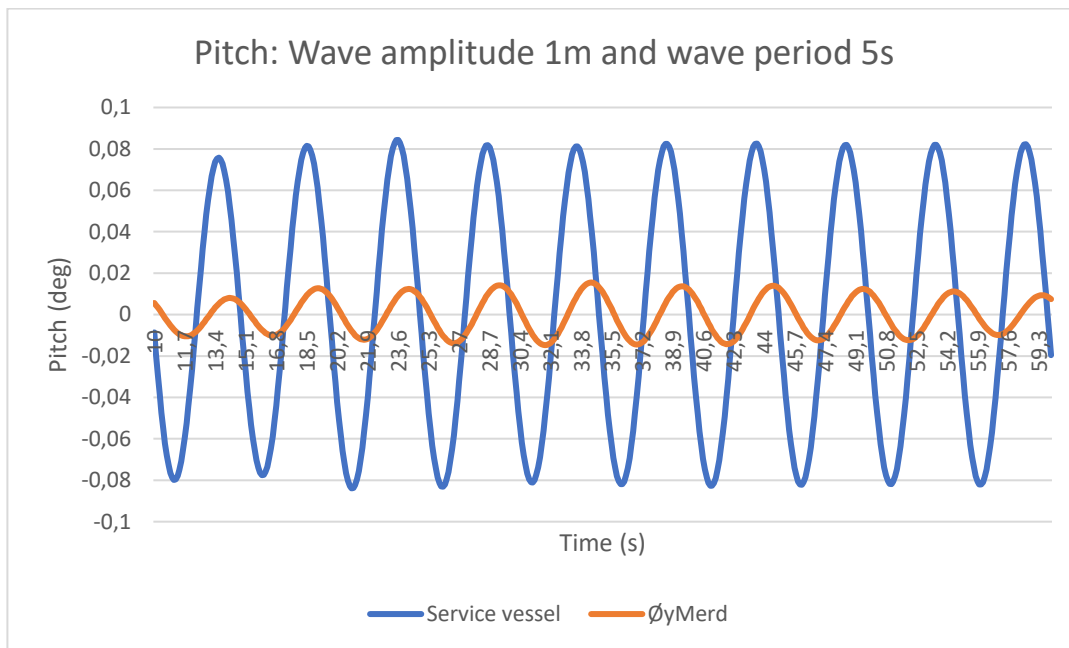
Figure 55 - Comparison of vessel and ØyMerd pitch motion. Wave amplitude 1 meter and wave period 5 seconds.

Figure 54 and Figure 55 shows the pitch superimposed rotational angle relative to the primary vessel axes direction due to the superimposed motion.

The distribution of forces is illustrated in Figure 56 and Figure 57. The sum of all the local and global applied loads are a combination of added mass and damping loads, wave 1st order loads, hydrostatic stiffness force and connection force from the mooring lines. The hydrostatic stiffness force makes up 31% of the forces present. Wave 1st order force makes up 36%.

FORCES ØYMERD

- Connections Force
- Hydrostatic Stiffness Force
- Wave (1st order) Force
- Added Mass & Damping Force
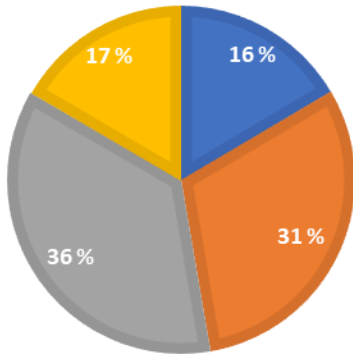
Figure 56 - Forces, model of ØyMerd in 2 meters wave height and 10 second wave period.

FORCES VESSEL

- Hydrostatic Stiffness Force
- Wave (1st order) Force
- Added Mass & Damping Force
- Other Damping Force
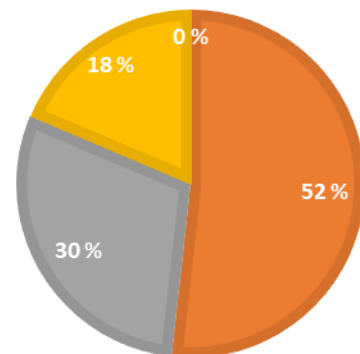
Figure 57 - Forces, model of Vessel in 2 meters wave height and 10 second wave period.

.

Forces included in the dynamic analysis is hydrostatic stiffness, wave (1st order), added mass and damping, connection force and other damping. In Figure 56 and Figure 57 the distribution of the sum of the loads are illustrated. The connection load includes the structural inertia and added inertia loads on the connected mooring line connected to ØyMerd. The results shows that other damping is not present during the calculation.
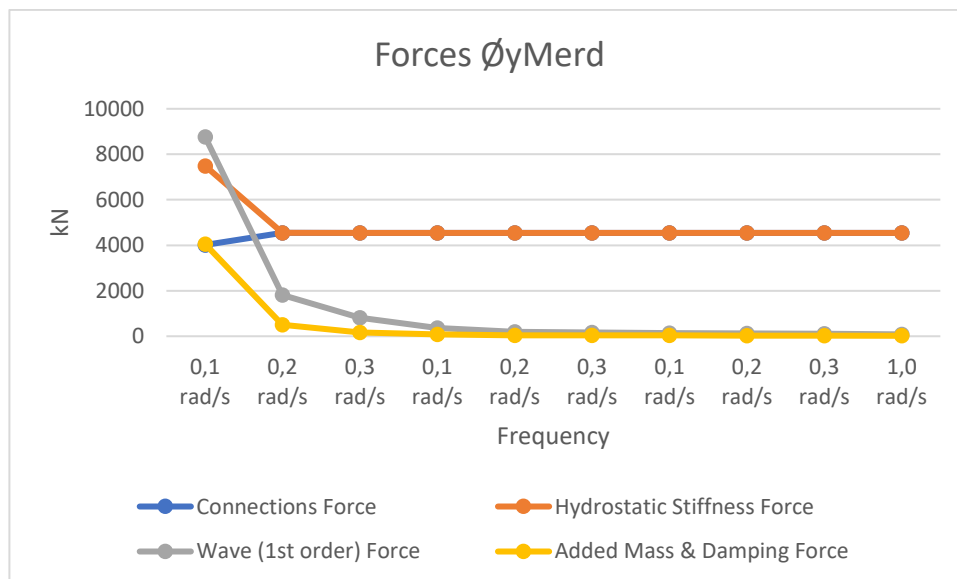
Figure 58 - Average forces ØyMerd. Wave amplitude 1m in relation to wave period.
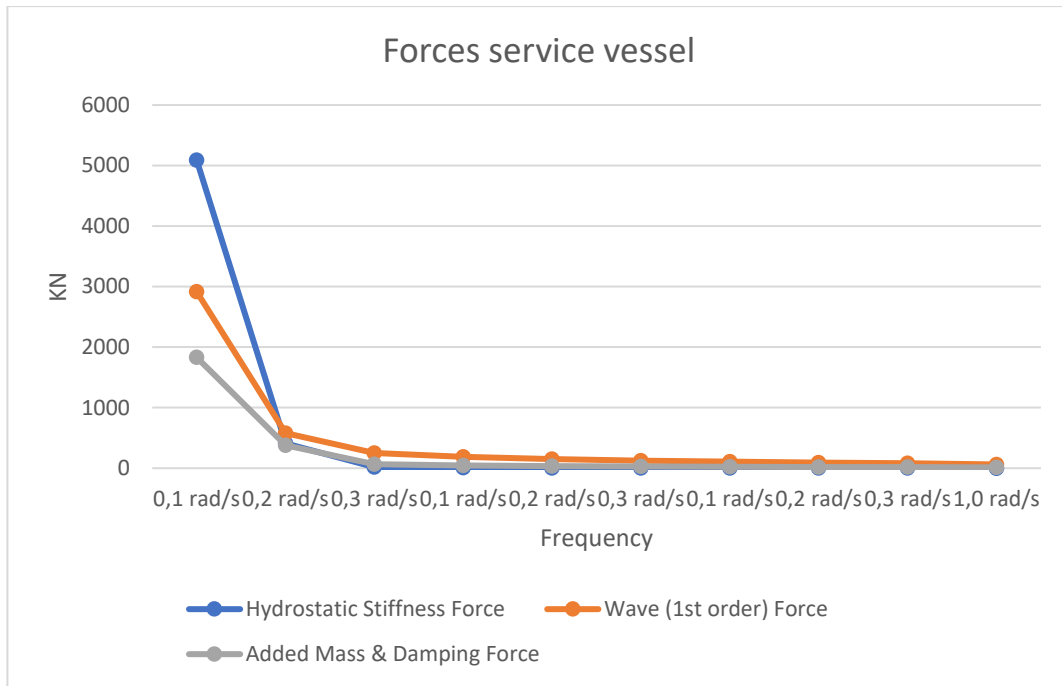
Figure 59 - Average forces service vessel in wave amplitude 1m in relation to frequency.

Table 10 shows the natural periods on the whole system of ØyMerd. Mode 1 is a natural sway period of the vessel, mode 2 is the natural surge period and mode 3 is the natural yaw period.

Table 10 - ØyMerd modal analysis

	Mode 1	Mode 2	Mode 3
Period	214,3078	213,7512	144,485
Frequency	0,00467	0,00468	0,00692
x (m)	0,0002	1,00	0,00
y (m)	1,00	-0,0002	-0,0008
z (m)	0,00	0,007	0,00
Rx (deg)	0,0014	0,00	-0,0047
Ry (deg)	0,00	-0,0015	0,00
Rz (deg)	0,0017	0,00	0,84

4.4 Service vessel docking

The dynamic analysis results of service vessel in a side by side arrangement with ØyMerd is presented in this chapter. The service vessel is docking with 10 meters breast and spring wire objects to ØyMerd. The system is experiencing Airy wave with and wave height of 2 meters and 10 seconds wave period. The wave is incoming from global x-direction.
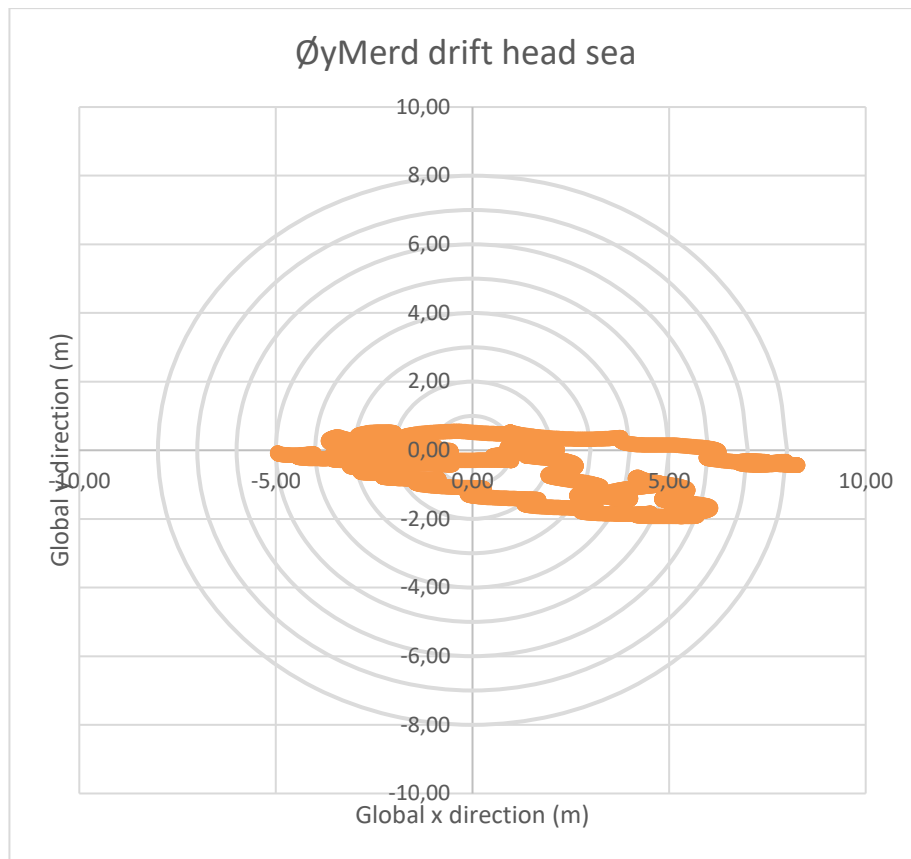
Figure 60 - ØyMerd drift head sea 1 meter wave amplitude and wave period 10 seconds
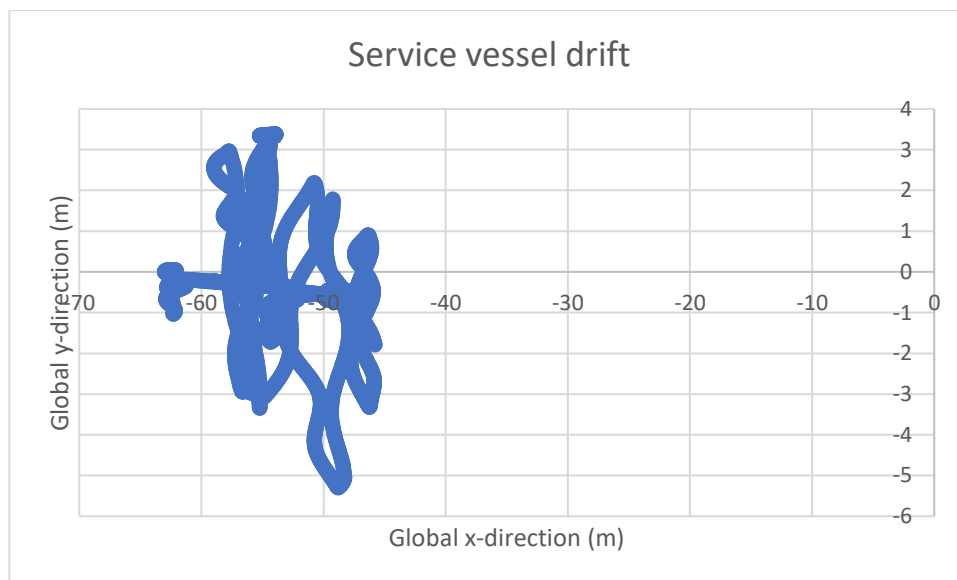
Figure 61 - Service vessel docking to ØyMerd in 1 meter wave amplitude and wave period 10 seconds

The illustrations show the drift of the system consisting of the vessel attached to ØyMerd. The displacement in position of the structures is illustrated as an overview of the position in global y- and x-direction.

In the dynamic analysis the objects are experiencing an Airy wave with a wave amplitude of 1 meter and wave frequency of 0,1 rad/s to 1,0 rad/s. The wave is incoming in global x-direction. The following graphs shows the comparison of the surge, sway, heave, roll, pitch and yaw motion of the vessel docking to ØyMerd and ØyMerd moored.
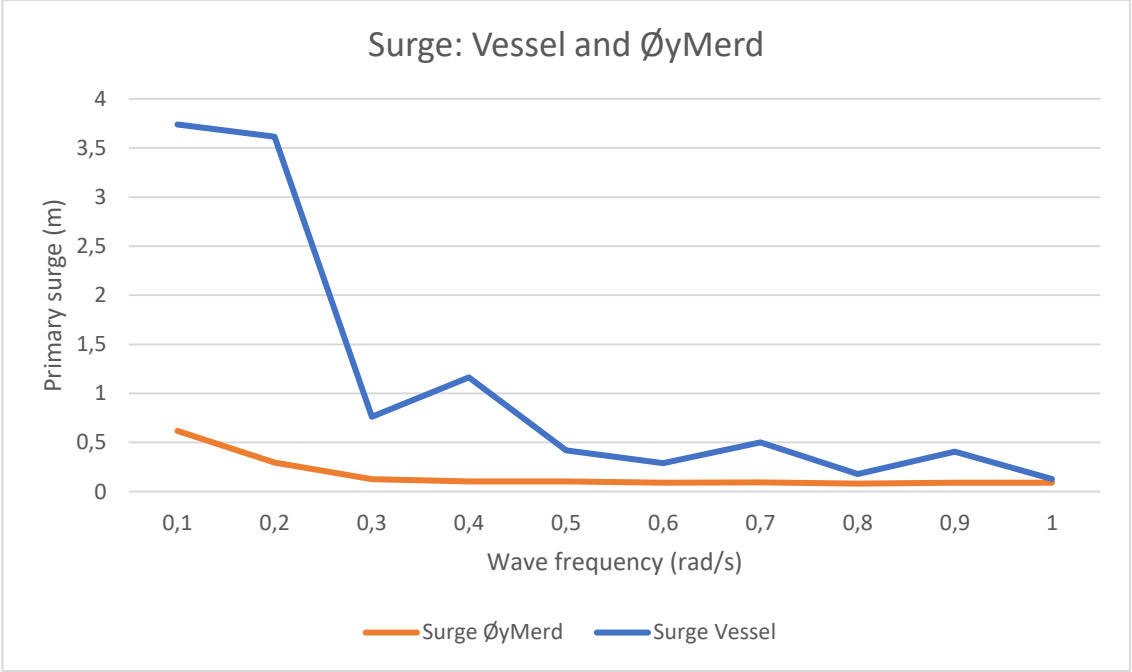
Figure 62 – Comparison of primary surge for Vessel docking and ØyMerd in wave amplitude 1 meter.
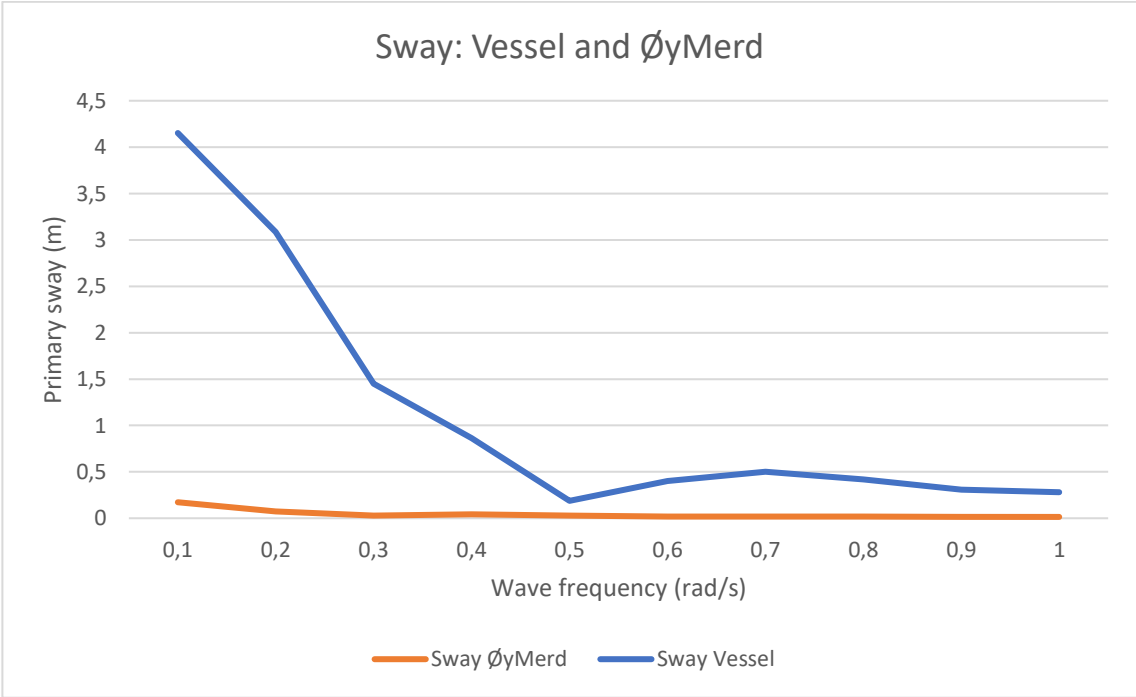
Figure 63 – Comparison of primary sway for vessel docking and ØyMerd in wave amplitude 1 meter.
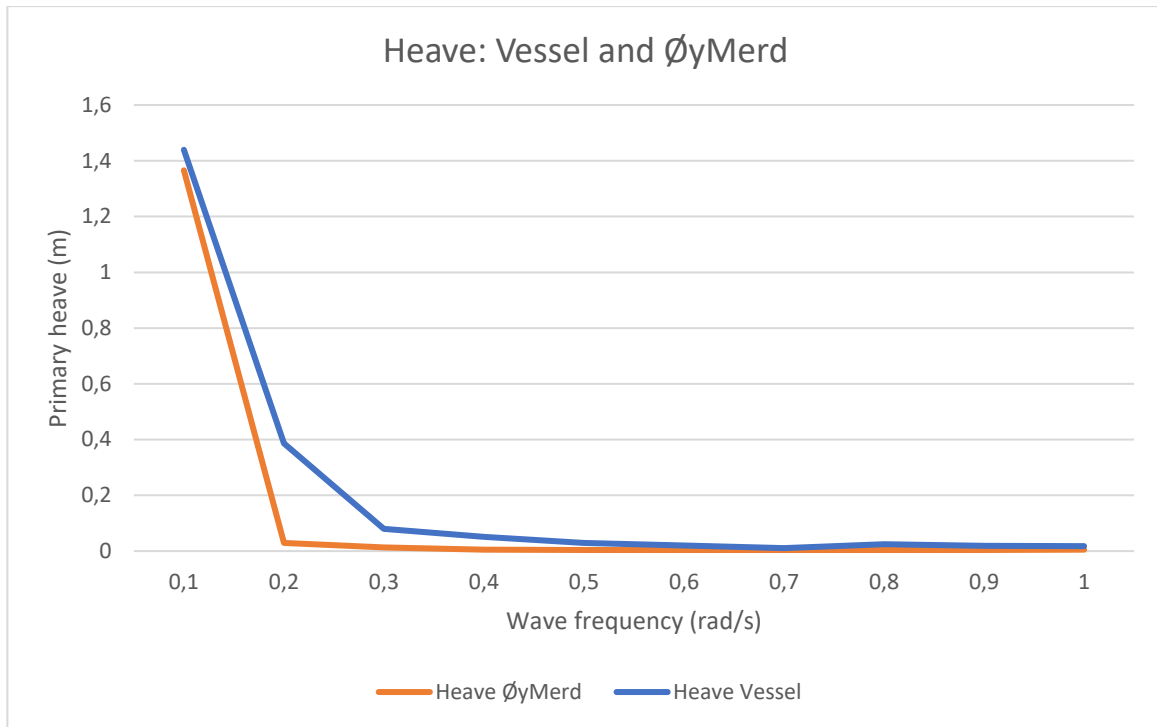
Figure 64 – Comparison of primary heave for vessel docking and ØyMerd in wave amplitude 1 meter.
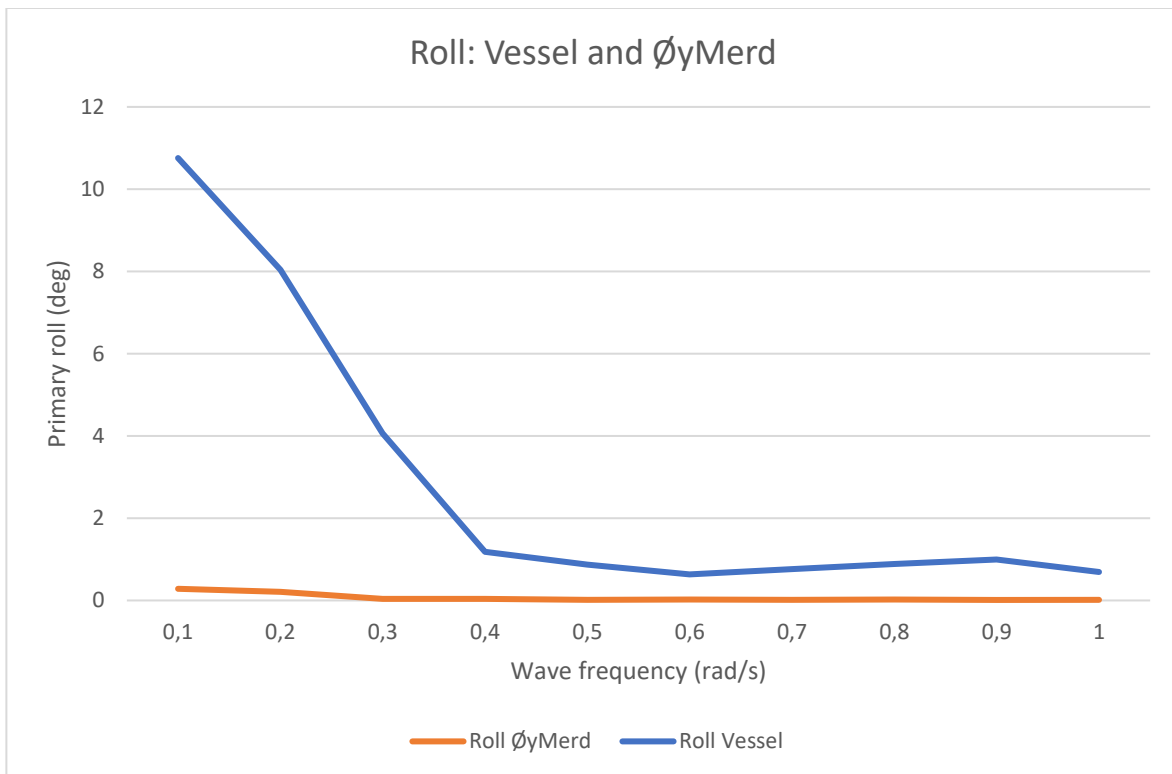
Figure 65 – Comparison of primary roll for vessel docking and ØyMerd in wave amplitude 1 meter.
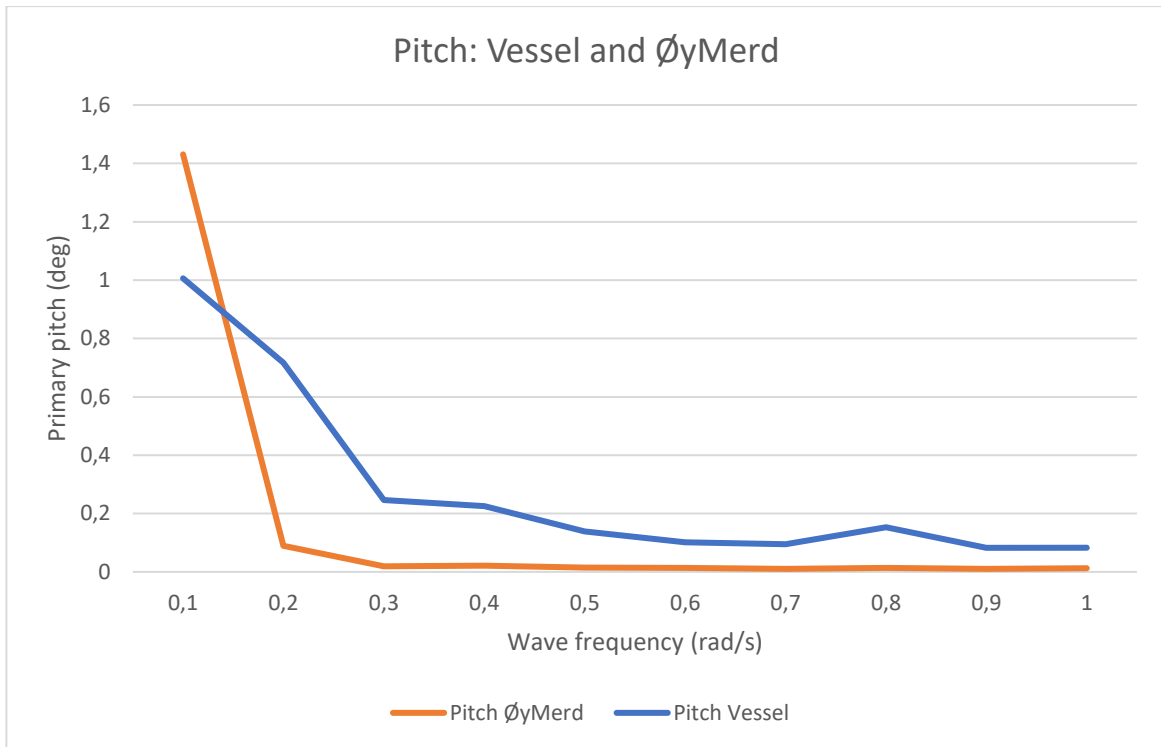
Figure 66 – Comparison of primary pitch for vessel docking and ØyMerd in wave amplitude 1 meter.
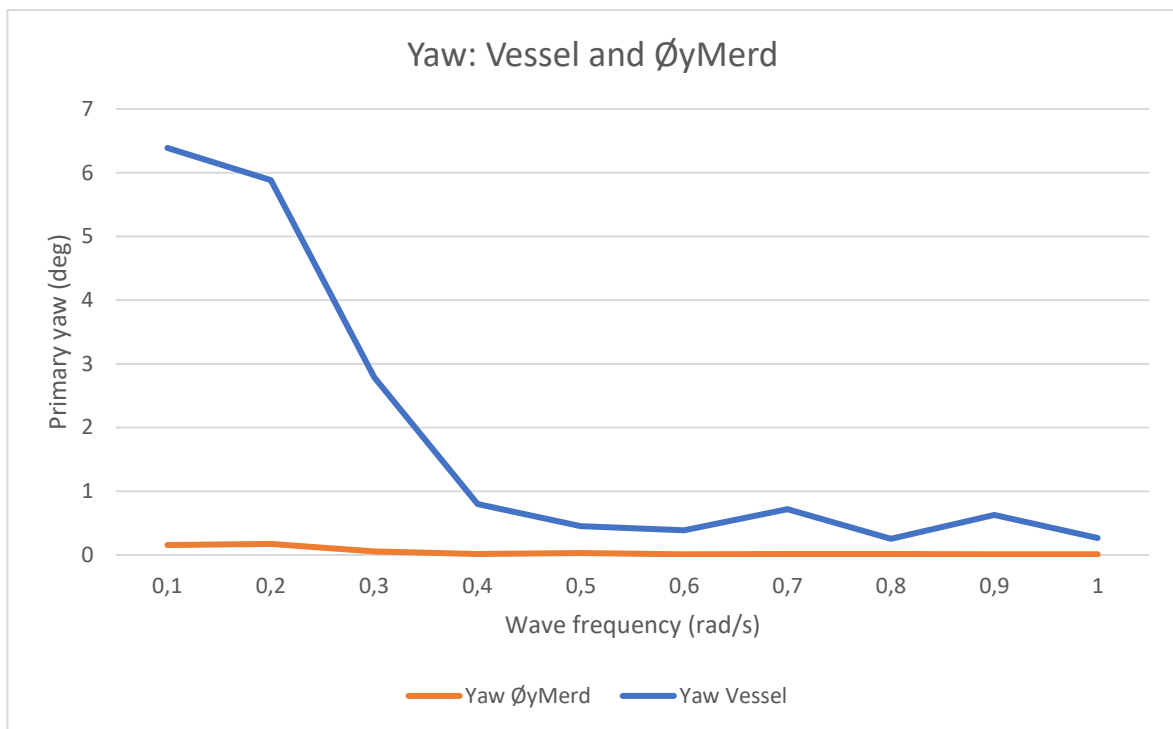
Figure 67 – Comparison of primary yaw of vessel docking and ØyMerd in wave amplitude 1 meter.

4.5 Service vessel crane operation

The simulation of the crane operation shows how the crane moves in the airy wave type with a wave height of 2 meters, and wave period of 5 seconds. The crane moves in the global z and x direction. The Figure 68 shows the maximum and minimum position of the crane tip.
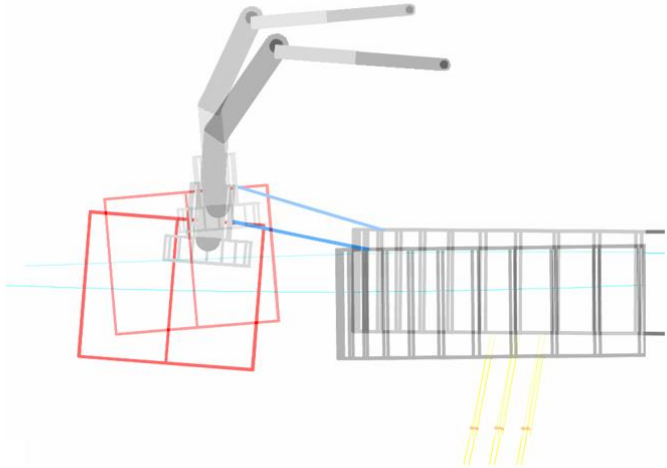
Figure 68 - Crane motion in wave height 2 meters and wave period 10 seconds
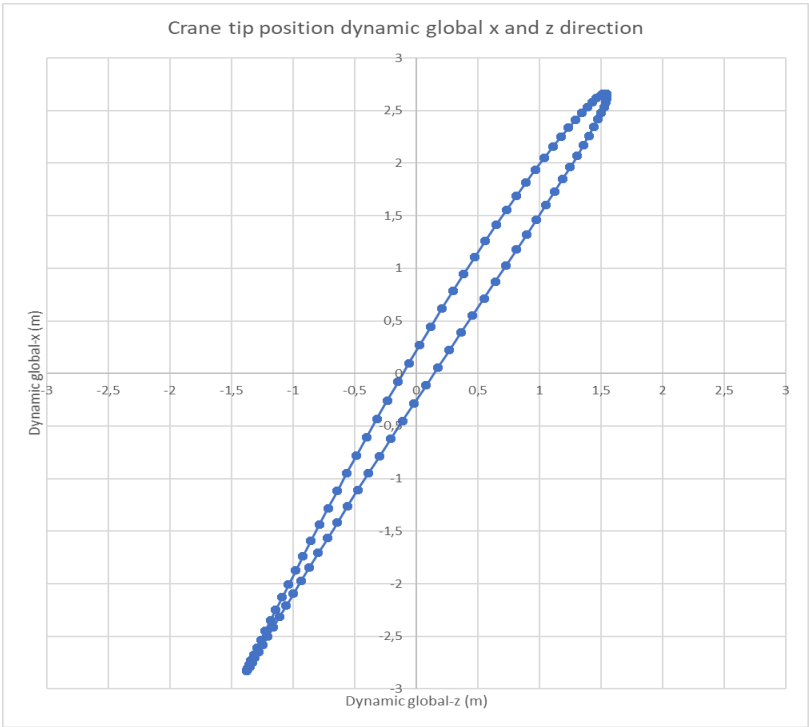
Figure 69 - Crane tip position, dynamic in x and y direction

Figure 69 shows the crane tip position every tenth seconds of the 4-minute simulation in global z and x direction. The vessel bow is heading towards the global y-direction and are experiencing incoming wave from starboard side. The simulation results shows that the

movement in global y-direction are less than 0.02 meters and can be disregarded. The crane tip movement in global z and x direction corms a circular movement. The maximum deviation value from initial position is 2.7 meters and minimum -2.8 in z-direction. In x-direction the crane tip displaces laterally with ± 1.5 meters.
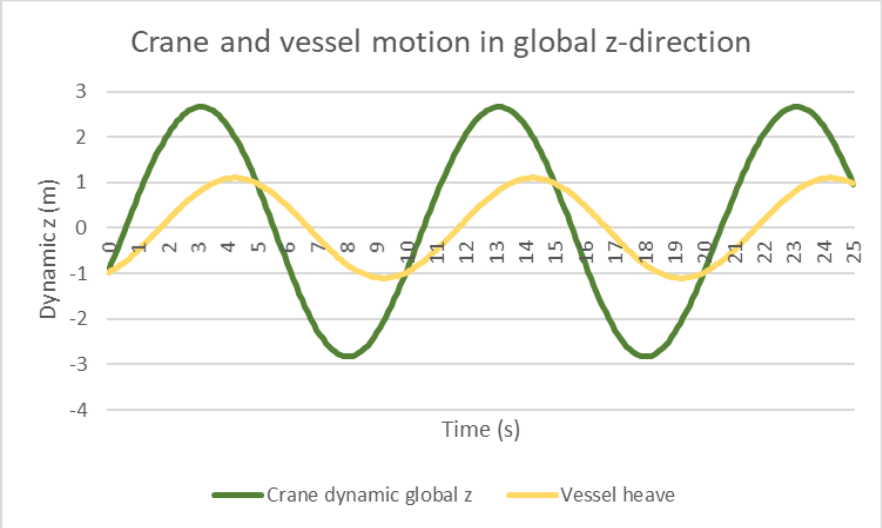
Figure 70 - Comparison of crane tip and vessel heave in global z-direction

Figure 70 shows the comparison of the service vessel and crane tip motion in global z-direction. Green graph shows the crane tip deflection with a peak of 2.7 meters in positive z-direction. Vessel heave deflection in positive global z-direction is 1 meter.
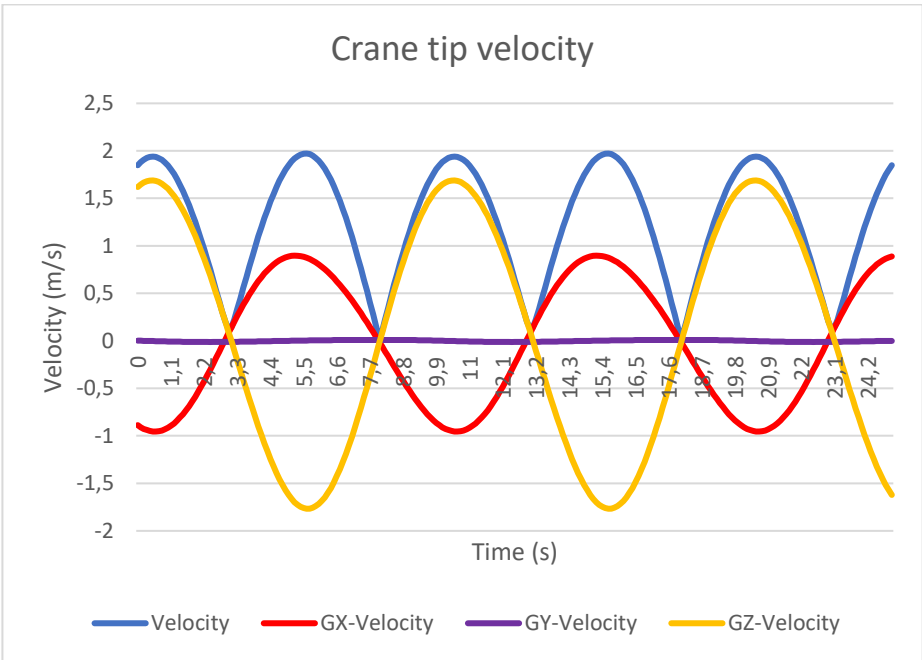
Figure 71 - Crane tip velocity, global x-velocity, global y-velocity and global z-velocity. Wave period 10 s and wave height 2 meters.

Figure 71 shows the magnitude and components, with respect to global axes, of the velocity and acceleration of the crane tip origin. The crane tip velocity in global y-direction is equal to 0 m/s. Global z-velocity peak is 1.6 m/s.

4.5.1 Comparison of crane tip motions

Figure 72 and Figure 73 shows the deflection for the crane tip for different wave heights in relation to different wave periods. The results are grouped according to the wave periods of 10, 5 and 3 seconds.
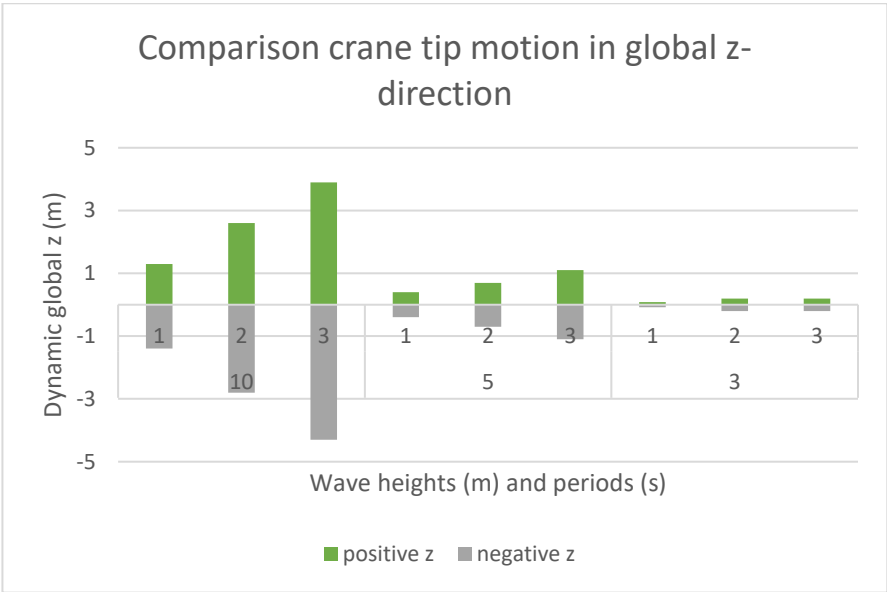
Figure 72 - Crane tip motion in global z-direction. Comparison of wave heights 1,2 and 3 meters, and wave periods 10, 5 and 3 seconds.
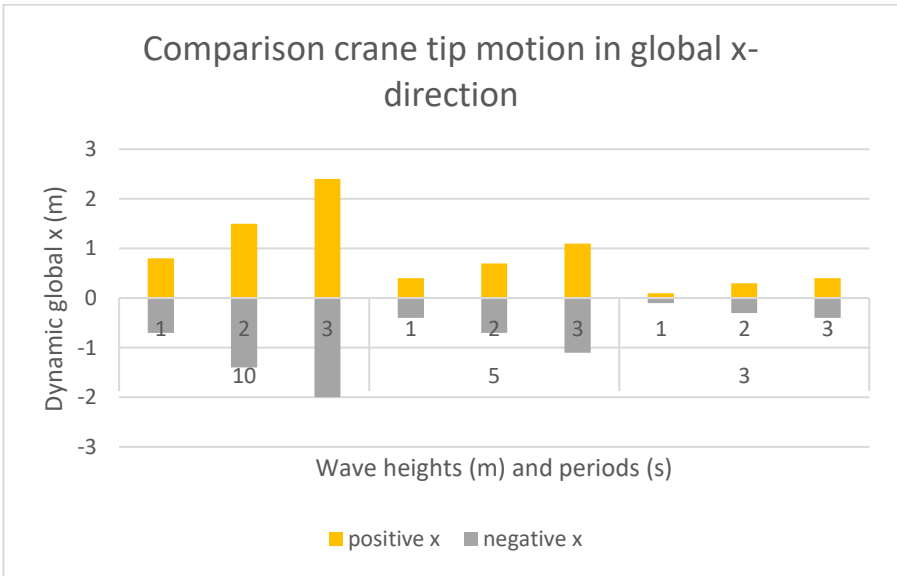
Figure 73 - Crane tip motion in global x-direction. Comparison of wave heights 1,2 and 3 meters, and wave periods 10,5 and 3 seconds.

4.6 Weather-window

This analysis is focused on vessel operation access of an offshore aquaculture facility. Therefore, the wave height and period are analyzed to map the level of access in Vestfjorden. Wave height and period also applies to other offshore installations like wind farms and platforms. However, the length of weather window varies due to the operation time needed. The results also assumes that the windspeed and daylight is excluded, even though wind parameters could cause operation limits. The significant wave height and wave period is the only parameters which is assessed in these results.

4.6.1 Wave data distribution year 2018-2019

Graph showing the wave height and wave period during one year from January 2018 to January 2019. The distribution for each month is shown in Figure 74 and Figure 75.
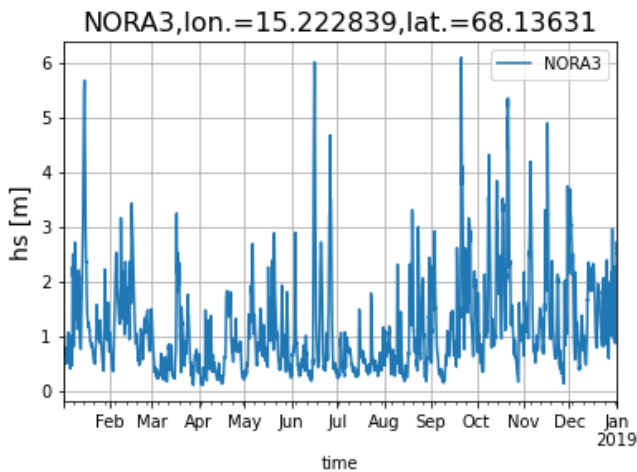
Figure 74 - Significant wave height year 2018 to 2019
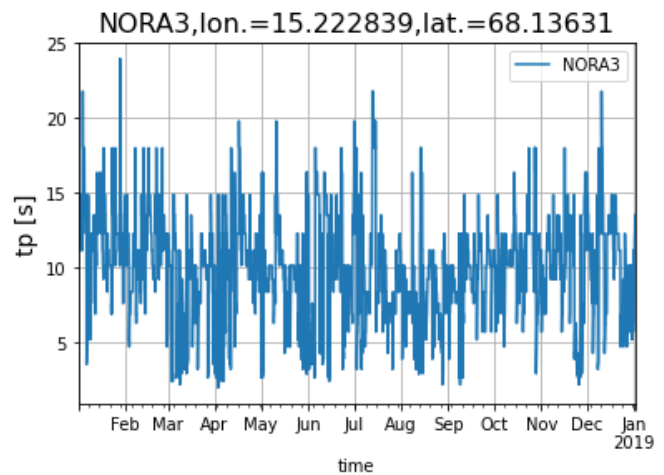
Figure 75 - Wave period year 2018 to 2019

It can be observed that the wave height is coherent lower than 3 meters in the spring/summer months, April to the middle of June. The wave height is 3 meters or higher more frequently in the autumn and winter season from September- February. The graph in Figure 74 shows that the significant wave height is under 2 meters in April-May and July-August. The wave period is distributed over a length of 2.0 seconds to 23.9 seconds.

Table 11 - Avarage Hs and Tp 2018-2019

Average 2018-2019		
Significant wave height	1,1	[m]
Significant wave period	10,1	[s]

Figure 76 and Figure 77 shows the graph for significant swell height and period from January 2018 to January 2019.
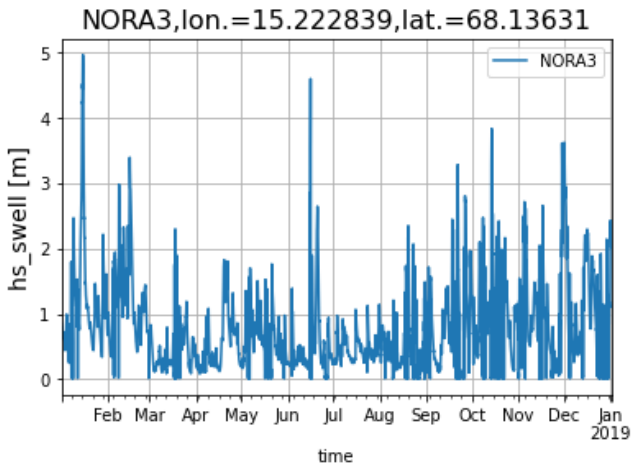
Figure 76 - Swell 2018-2019
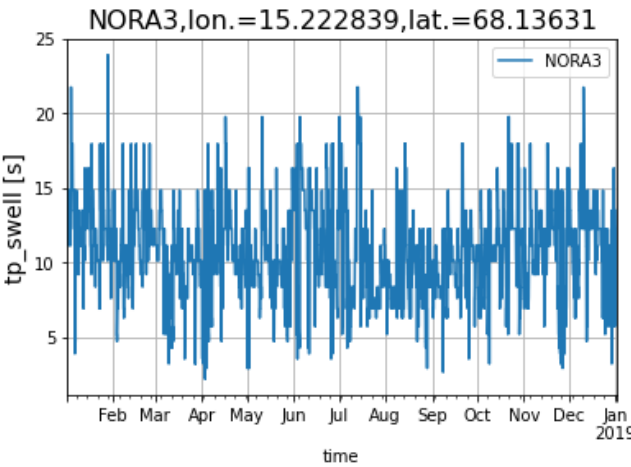
Figure 77 - Swell period 2018-2019

Swell height is peaking in month January and middle of June. During the autumn moths it is frequency a swell height more than 2 meters. The swell period is distributed over a length of 2.2 seconds and 23.9 seconds.

Table 12 - Average Hs swell and Tp swell 2018-2019

Average 2018-2019		
Significant swell height	0,8	[m]
Significant swell period	10,8	[s]

4.6.2 Annual mean exceedance

The exceedance graph is shown in Figure 78. The graph shows the percentage of the year when the waive height is above a certain level. The minimum waive height is 0.1 meters, and the maximum wave height is 6.1 meters. It is observed that 13% of the waves heights is above 2.0 meters. Less than 10% of the waves have a wave height between 2.5-6 meters.
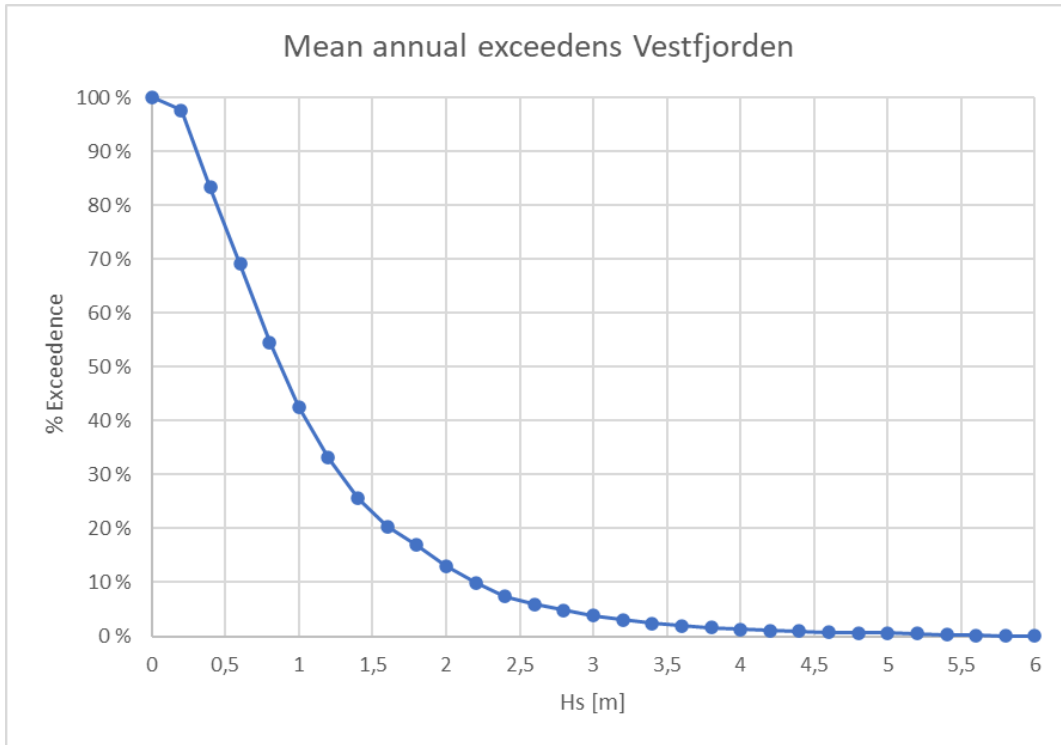
Figure 78 - Mean annual exceedens Vestfjorden

4.6.3 The seasonality of the wave regimes

Figure 79 shows the seasonal average significant wave height. October moth has the highest average wave height of 1.58 meters, and July has the lowest average of 0.55 meters. The six months with highest average wave height are the winter months.
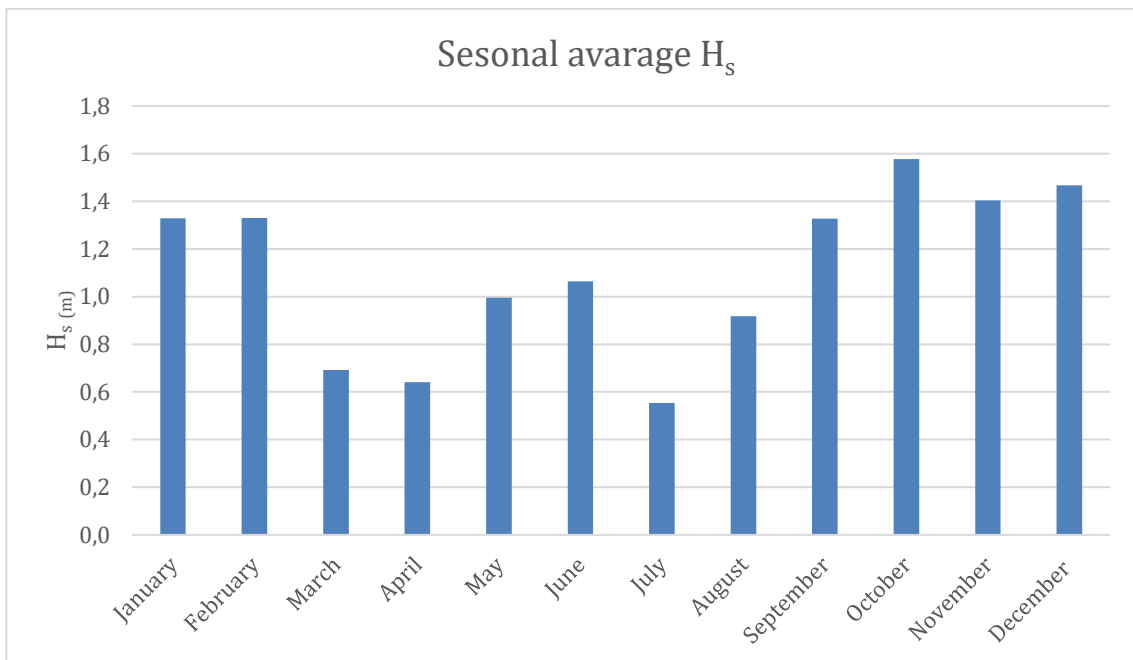
Figure 79 - Seasonal average significant wave height

Figure 80 shows the monthly hours with wave height below limits of 1.0, 1.5, 2.0, 2.5 and 3.0 meters. The spring moths March and April, and the summer month July has most hours with Hs below the wave limits.
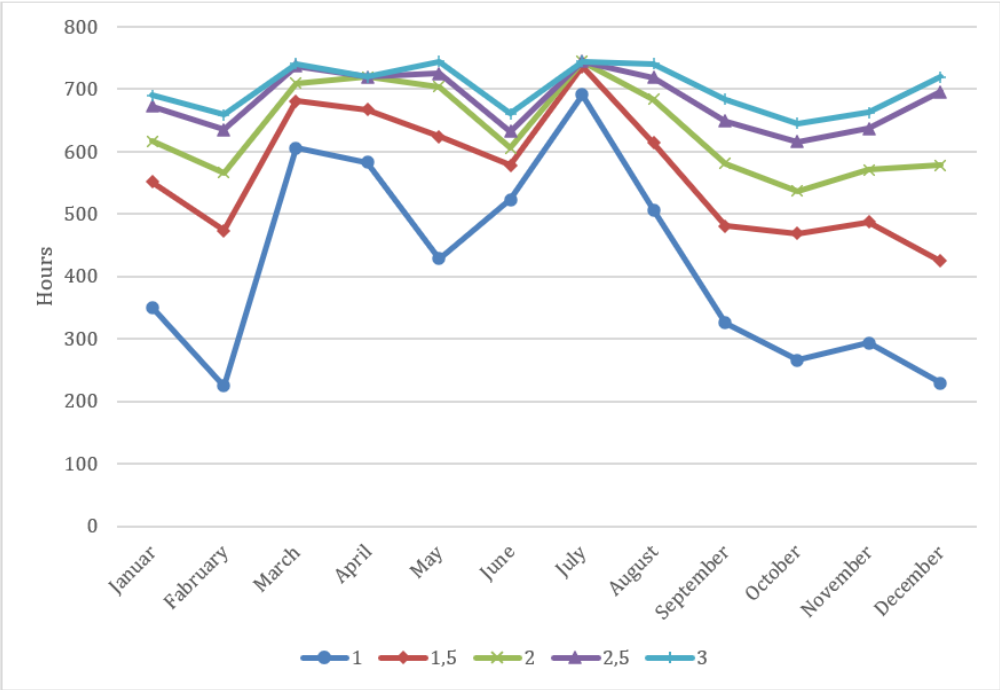
Figure 80 - Monthly hours with wave height below limit of Hs 1.0, 1.5, 2.0, 2.5 and 3.0 meters

4.6.4 Weather windows for vessel operations

Operation duration, max wave height and period criteria is parameters used in a weather windows analysis. The wave data used in the analysis is significant wave height and period during year 2018-2019 with time step of 1 hour.

Crew transfer catamaran

Crew transfer weather windows number in Vestfjorden during the specific year is 157.

Table 13 - Weather windows crew transfer with catamaran

Weather window Hs		
Criteria		
Wave height max criteria	**2**	**m**
Wave period max criteria	**12**	**s**
Duration of window	**1**	**hours**
Number available weather windows	157	

De-lice methods workboat

Figure 81 provides an overview of the number of weather windows for the different de-lice methods when use of a "workboat". Fresh water de-lice method is the operation which has lowest number of weather windows during year 2018-2019.
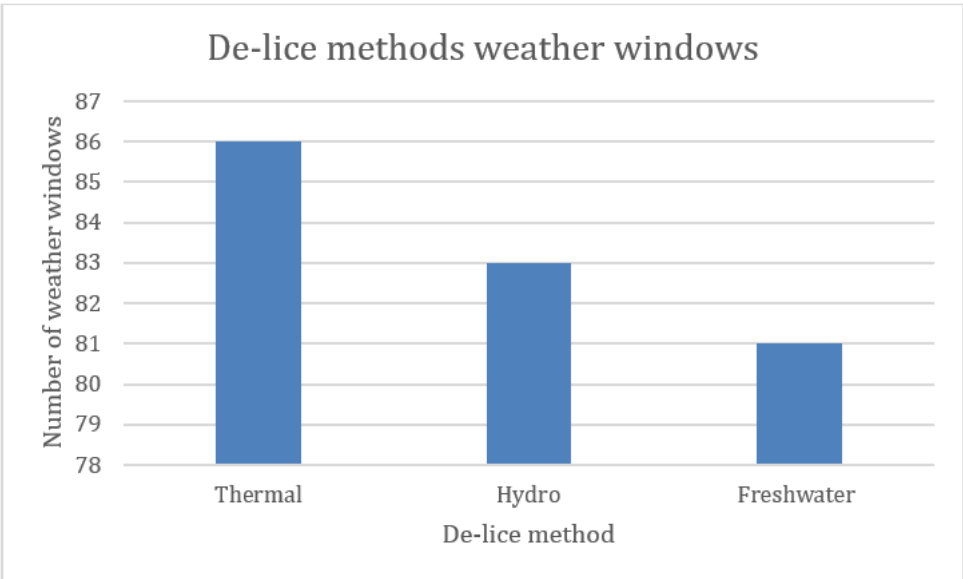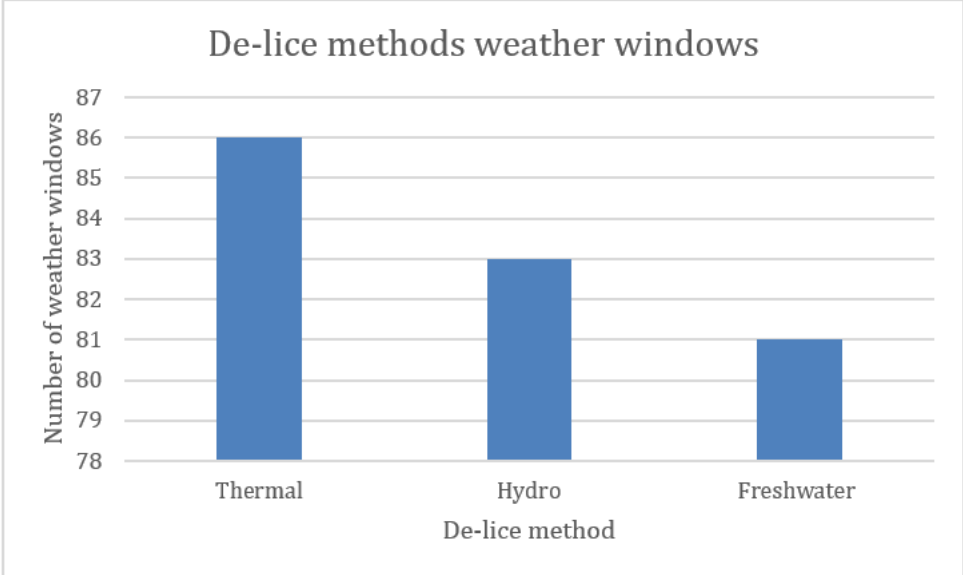
Figure 81 - Weather windows de-lice methods year 2018-2019

Workboat mooring maintenance operation

Figure 82 shows the number of weather windows with a curtain length for one year.
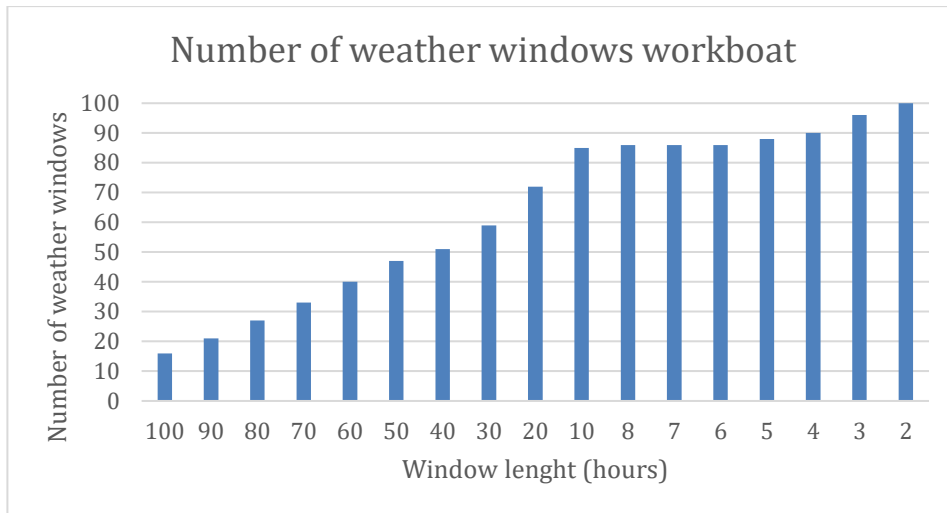
Figure 82- Number of weather windows for workboat during year 2018-2019

During November moth there is approximately 200 hours of waiting time for the workboat with an operation limit of 2 meters wave height and 16 s wave period. Figure 83 and Figure 84 shows the Hs and Tp peak shaving for November moth in Vestfjorden.
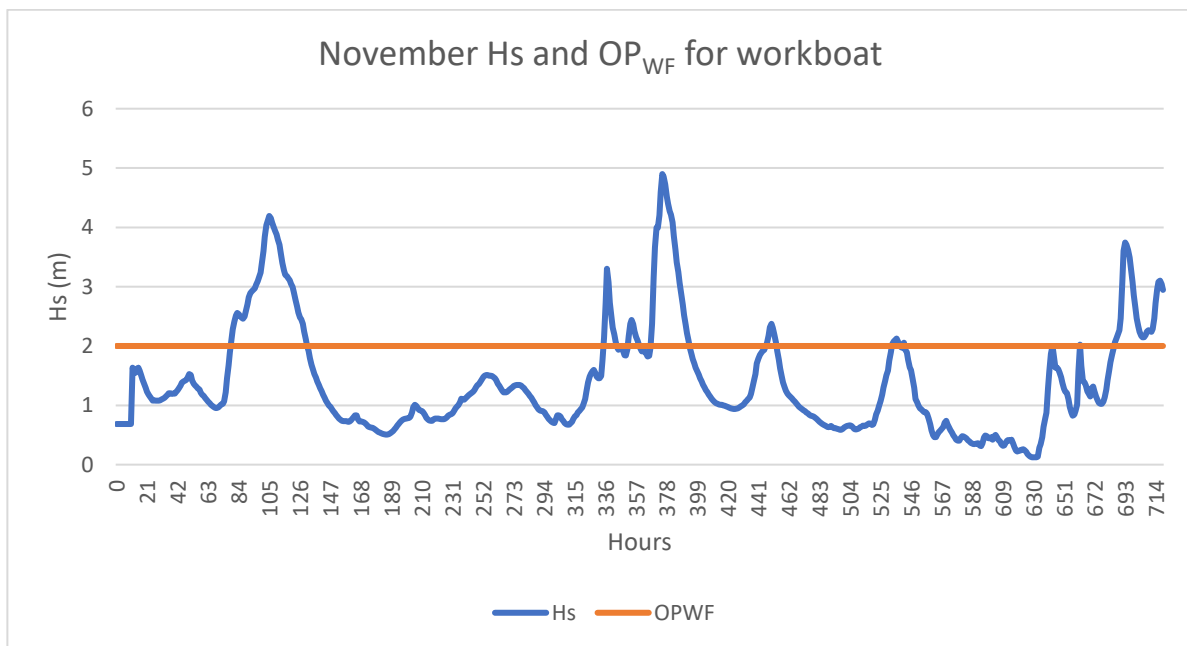
Figure 83 – November 2018 Hs and OP$_{WF}$ for workboat
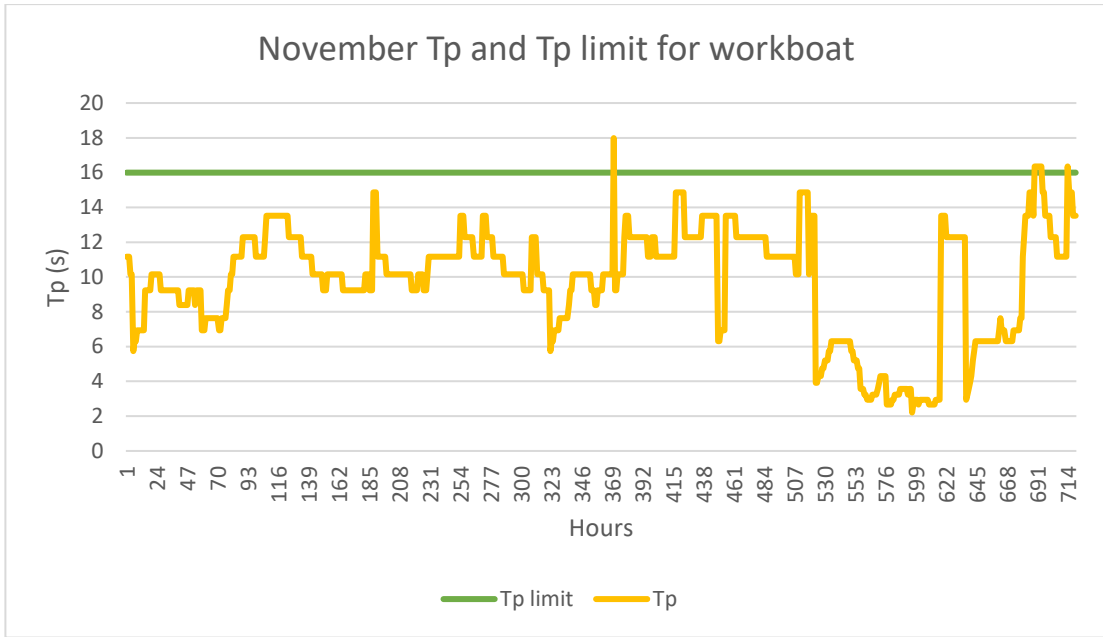
Figure 84 – November 2018 Tp and Tp limit

5 Discussion

Aquaculture facilities are increasingly being established offshore and may be occupy larger ocean areas in the future. The maritime space and offshore developments can offer significant benefits that applies to the economy, optimization of operations and production, as well as minimizing the impact on the coastal areas. New locations of production leads to new environmental and operational challenges. Different aspects need to be considered when determine the design and location of an offshore aquaculture facility. The new structures are rigid and designed for offshore environmental conditions. In determining location, the seabed characteristics, hydrodynamic conditions, logistics, environment and social acceptance needs to be considered.

Structure model and dynamic analysis

The traditional design of structures is changing due to new environmental challenges. SalMar has developed the Ocean Farming[7] which is an innovating design to be in deeper water. Nordlaks has the concepts Havfarm[8] which also is a platform intended for open water with offshore industry technology. The conceptual offshore aquaculture facility ØyMerd[9] has been modeled in this thesis. In order to calculate the hydrostatic and hydrodynamics of the structure, the structure has been modulated as a 3D object. The model is simplified as a simple geometric triangle shape with three wells. Some assumptions have been made in this study method due to well sizes and even mass distribution. Free-standing object on deck are neglected, such as operating buildings, railing and other equipment.

The hydrostatic report presented in chapter 4.1 provides the foundation for further hydrodynamic data from the HAMS solver. One of the key findings is the metacenter height (GM). The GM is almost 140 meters. A positive GM means that the system is stable, and the stability would be significant high because of the restoring force (GZ) achieved when floating in waves. Due to the width of the structure and gravity center 2.5 meters underneath the waterline, a high metacenter is not unrealistic. However, such significant stability means "tight" compensation of movements. This means that for example in roll motion, the structure finds the wave back to the initial position with a powerful restoring force. The structure can

---

[7] https://www.salmar.no/en/offshore-fish-farming-a-new-era/

[8] https://www.nordlaks.no/utvikling/om-havfarm-prosjektet

[9] https://www.gratanglaks.no/oymerd

be characterized with stiff movements due to the GM, but the hydrostatic calculations also shows that the structure has some inertia. This inertia will balance the correction from the restoring force, which leads to inertia in the movements.

Furthermore, by studying the submerge hull of the structure, one will see that the structure is far from comparable to a conventional ship hull. When a ship heels, the residual stability increases as long as the waterline area increases. The waterline area for a conventional ship decreases when the water reaches the first open deck. For ØyMerd, the free board is 2.5 meters above the water line. This means that the waterline area does not have that much to increase with, relative to the large areal already achieved with its length and width. Therefor, compared to a cruise ship for example, ØyMerd does not have the great residual stability.

When meshing the object used for input in the HAMS solver, three mesh heights where analyzed. The mesh sensitivity shows that the graphs for the hydrodynamic coefficients presented in chapter 4.2 is approximately the same for the mesh heights 2.5, 5.0 and 7.0. The mesh with the 2.5 height was chosen for the further hydrodynamic calculation in HAMS. It is preferred to choose a mesh with the smallest division possible in order to get the most accuracy calculations. For this analysis, the smallest mesh height did not delay the calculation and modulation time. Due to the hydrodynamic coefficient result, it can be discussed if the two irregular frequencies showing originates from some disturbance in the mesh. When the solver calculates the hydrodynamics, the input meshes are the object mesh, underwater hull mesh and waterplane mesh. The reason for the two irregular frequencies might come from the solver, when calculating the waves for the wave frequencies around 0.8 rad/s and 1.1 rad/s.

To investigate whether the hydrodynamic data calculated in HAMS was imported successfully into OrcaFlex, a method was developed to self-check the model of ØyMerd. The results shows that the damping force is present. When running the simulation, the structure deviates from the inertial position, but due to hydrodynamic forces returns to equilibrium. In theory the structure, excluding the hydrodynamic forces, would oscillate for eternity. Figure 49 shows that the structure returns to equilibrium.

The implicit time scheme was preferred because the implicit time scheme was fast when running a simulation in OrcaFlex. The implicit time scheme was used with a time step larger than the explicit time scheme could. Because the model of ØyMerd did not have high frequency responses that needed to be captured. However, if that were the case for this model

the explicit time scheme would have been more beneficial. To ensure the study method, in case of what time scheme that is more efficient, a time step sensitivity study could be performed to confirm the accuracy of the results. The implicit time scheme uses an iterative method to calculate the dynamic equilibrium of the model of ØyMerd at set intervals of time steps. The default time step was 0,1 seconds for the dynamic analyses. For every time step the calculation was allowed a number of attempts to find equilibrium for the object, this is shown in Figure 50. The figure shows that the iteration count is beneath 4 times for the primary time of simulation. The counts are slightly higher in the build-up phase of the simulation, with max iteration of 12 times. This means that the solver is struggling, most likely with high frequency events. This could be due to mooring lines colliding. If a high count of iteration ware frequently appearing during the simulation a shorter time step are necessary. Also, Figure 50 shows a full line graph which means that the simulation is completed. If the solver fails part way thru, the graph would have been partially filed in. The graph shows the simulation run time is optimized because the iterations are low and the graph don't show any bad behavior.

An offshore aquaculture facility compared to a vessel is large and rigid. As shown in Figure 51 the dynamic response in dynamic z direction increases with decreasing wave frequency, and decreases rapidly for heigh frequency excitations. The minor response for heigh-frequency excitations would indicate that the overall structure system is highly damped for ØyMerd. This is an effect of the inertia of the construction. For a rigid structure with these great dimensions, the resistance for high wave frequencies is expected. This can be considered as a strength of large rigid offshore platforms and structures, and is addressed from the offshore industry for oil platforms. The structure withstands low wave periods, and the danger is long period waves and swells. ØyMerd is 120 meters, for long wave periods close to the total length of the structure, the wave impact load increase to the structure itself. This in relation to the high stability due to the width and GM leads to greater demands to the strength of the construction. The danger of fatigue is due to large loads over a longer period of time. One can argue that rigid structures can cause problems due to fatigue in the steel construction. Especially for ØyMerd, consisting of concrete and steel, such fatigue can be a challenge especially in the transition between the steel and concrete. For a beam layer of a ship hull, one will be able to describe such loads in the solid mechanics as hogging and sagging. A long object will deform into bending when loading is applied. If the hull experiences a wave crest closer to midship, the beam curves upwards called hogging stress.

While when a hull is in the trough of two waves the stress causes a sogging where the beam bends downwards.

Figure 52 shows the heave motion in a wave height of 2 meters and wave period of 10 seconds. The heave motion of ØyMerd is more than twice the exceeds than the vessel heave motion. This also means that the larges buoyancy force is being applied as the structure is moving upwards. For wave period of 5 seconds the heave motion decreases rapidly. This means that the positive buoyance force is being present as the structure is moving upwards. When the wavelength is decreasing the force will not be as large since there will be air gaps at points along the structure. It makes sense that the natural period in heave corresponds with longer wavelengths.

However, due to the stiffness of the offshore structure, the rotations motion is lower due to the great restoring force. Figure 54 shows the pitch rotation in degrees comparison of the vessel and ØyMerd moored. The rotation motion of ØyMerd is lower compared to the vessel. This is due to the inertia of the structure. However, due to the asymmetry between the "bow" and aft of the structure when rises in heave motion, the buoyancy and mass leads to the structure pitching. Therefore, the heave and pitch peaks are corresponding to the same wave frequency. This indicates the coupling of the heave and pitch motion when comparing the heave and pitch graph in Figure 52 and Figure 54.

Vessel operation, and vessel – structure interaction

To lower the operation cost and downtime of operations, it is beneficial to have a vessel able to perform a variety of operations in relation to an offshore aquaculture facility. This would be achieved by having a multi-purpose service vessel with the possibilities for crane operations, crew transfer and other maintenance operations. This can reduce the need of other special designed vessels and lowering operational cost in relation to the facility. Offshore locations could be in long reach from one operation area to another operation area. Therefor waiting time on different specialized service vessels could cause a longer period of downtime. However, the aquaculture industry relies on well boats for transfer fish, medical treatment and de-lice treatment. The well boats could often be on a schedule, to make sure the fish are transported from a location to another, or into a slaughterhouse for the food production. Therefor the well boats are considered as a necessary for the fleet repertoire for the offshore aquaculture industry.

Some vessel operations also show to be subjected to higher risk than other operations. Krane operations and mooring maintenance work could cause hazardous events if the service vessel is not specialized in design or operates in exposed weather conditions. All depends on the location and the design of the offshore aquaculture facility and mooring system required in case of mooring maintenance operations. Due to a rather new industry and design of offshore aquaculture facilities, it is shown not to be much research on accidents related to personnel, environment, fish health and material values. The modulation of the vessel and structure dynamics is a method that commonly are used in the early stages of a design process, to identify hazards and potential risk during operations. The method is subjected to some uncertainties but are still deliver some indications of the motion expected in certain environmental conditions. This would also make it possible to indicate the frequency and consequences of possible hazardous events by use of expert judgement.

When the vessel is docking to ØyMerd it is following the drift of the structure. Long wave periods increase the loads due to physical interaction and tension in the connecting lines. The dynamic analysis of the vessel, in a side by side arrangement with the structure, shows how surge, sway, heave, roll, pitch and yaw motion is exaggerated. The vessel experiences great impact due to the structure response of ØyMerd. It is worth mentioning that the wire objects used to model the connection lines when docking are indestructible. However, this points out the differences in response between the two constructions. The effect of the waves decreases rapidly around the wave frequency of 0.2 rad/s for the ØyMerd structure. While, when comparing the response of the vessel when docking to ØyMerd during a wave period of 10 seconds, the motion deviated from the ship's original characteristics in the same sea conditions. Considering the size, mass and response of ØyMerd, this effect on the vessel is not surprising itself. However, it points out the challenges of vessel operations in wave frequencies close to the natural frequency of the structure itself.

It is especially important to avoid operations when the sea state condition is close to one of ØyMerd or vessel natural frequency when transferring personnel or during crane operations. Although the structure ØyMerd is stable in waves, large movements relative between the vessel and structure can cause danger during operations. During crane operations the relative motion between the structures can lead to snap loads. Although some vessels have heave dampening systems for cranes, operations could not be carried out during sea conditions which can cause resonance. Another aspect of large crane motions is the danger to fish health.

The aquaculture management regulations provide explicit regulations to provide improper handling of fish.

Weather window analysis

The weather window analysis is focused on vessel operation access of an offshore aquaculture facility. Therefore, the wave height and period are analyzed due to the level of access in Vestfjorden. Wave height and period also applies to other offshore installations like wind farms and platforms. However, the length of weather window varies due to the operation time needed. The results also assumes that the windspeed and daylight is excluded, even though wind parameters and daylight could cause operation limits.

The significant wave height and wave period data is retrieved from the Norwegian meteorological institute. The data is based on a 3 kilometres Norwegian Reanalysis (NORA3) model. The significant wave height and wave period is model data and not observations. Therefore, it is important to be aware of the limitations inherent in the dataset. The deviation can be quite large in areas with complicated bottom topography, but also near the coast of Norway due to the complicated terrain which affects wind systems. However, the NORA3 model gives an indication of the accessibility of the location chosen in relation to waves parameters.

The location can not be defined as an offshore area. However, the Vestfjorden are known for harsh weather and sea state. As the Table 11 shows, the average wave period is 10.1 seconds, and from the Figure 78 we can see that 13% of the waves during the year is above 2 meters. These are parameters that are not necessarily limiting to the vessel itself and vessel operations. However, for the dynamic of a large structure, we have seen that such wave parameters can lead to large forces and response. This makes it more challenging for vessel – structure operations. Some operations in relation to aquaculture facilities, like de-licing operations, are time consuming. The vessels need to be docking for 13 hours for some de-lice methods. Freshwater de-lice method had the lowest number of available weather windows during year 2018-2019. The workboat used in this thesis had a significant wave height limit of 2 meters, and wave period limit of 16 seconds for crane operations. The total number of available weather windows where 81 for the workboat freshwater de-lice method. According to the Figure 80 it is likely that the density of weather windows is lowest during late autumn and winter months. This means that for freshwater de-lice, the length of waiting periods could be longer and more often in these months.

Weather windows are used in the planning phase of operations. The analysis is therefore dependent on reliable prediction of weather conditions. Especially in the polar areas, this will be challenging in danger of polar low pressured weather systems in winter times. In the event of such incidents, longer waiting periods between operations will have to be taken into account. It can also be pointed out that during periods of the harshest sea conditions, there are periods of polar nights, and duration of daylights are shorter in the northern parts of Norway. This would potentially also affects the operation limits.

6 Conclusion

New types of offshore facility structures are rather unexplored compared to offshore wind. Both in relation to operation efficiency and dynamic behavior. Particular issues related to design guidelines and standards, where today there is a large variation in the structure design that are being developed.

The structure ØyMerd and the vessel have differences in dynamic response and behavior. The dynamics of the large rigid offshore aquaculture facility decreases when the wave effect abates. The response for high-frequency excitations could indicate that the overall construction system is highly damped as an effect of the inertia of the structure. Compared to the vessel this also might leads to smaller rotation motion.

Vessel operations in relation to new types of offshore aquaculture facilities could potentially face higher risks due to the exposed areas the facilities are designed to adapt to. It is important to avoid operations when the sea condition is close to either the aquaculture facility or the vessel natural frequency. Even though a structure like ØyMerd is stable in waves, sea conditions can lead to great response. Large movements relatively between the structure and vessel cause higher risk and are potentially dangerous during crane operation or other operations like crew transfer. This is also why weather window analysis are applied during a planning phase of operations, and operation limits are addressed.

By modeling vessel and structure dynamics, one can obtain an indication of what type of challenges may arise due to both environmental and operational parameters. This makes it possible to imply the frequency and consequences of possible hazardous events. For future work, structure monitoring and design guidelines will be important topics developments within this field. For ØyMerd it will be important to look at the effect of the wave interaction and disturbance. This is particularly interesting regarding vessel operations. On the sheltered side of the structure, there will be an effect of the wave refraction. This shielding effect could be beneficial for vessel operations, and for the accessibility of the structure. The industry today depends on well boats for certain operations, and offshore locations could lead to challenges. The shielding effect could affect the operating criteria and the number of weather windows.

7 References

Akvakulturdriftsforskriften. (2008). *Forskrift om drift av akvakulturanlegg (Akvakulturdriftsforskriften)*. Nærings- og fiskeridepartementet. https://lovdata.no/dokument/SF/forskrift/2008-06-17-822?q=forskrift%20om%20drift%20akvakult

Barrass, B., & Derrett, C. D. R. (2011). *Ship Stability for Masters and Mates* (6th ed.). Elsevier. https://books.google.no/books?hl=no&lr=&id=4E4FZ988AtYC&oi=fnd&pg=PP1&dq=ship+stability&ots=2KnUibVIeE&sig=02dAdxbooFGfq1bk23g-kfDbeWM&redir_esc=y#v=onepage&q=ship%20stability&f=false

Bemlotek AS. (2022). *OyMerdTM*. Bemlotek. https://www.bemlotek.no/projects

Berge, A. (2022, May 5). *Her sjøsettes verdens største brønnbåt*. iLaks. https://ilaks.no/her-sjosettes-verdens-storste-bronnbat/

Browne, V. C. (2013). *Assessment of Low-Frequency Roll Motions on the Semisubmersible Drilling Rig COSL Pioneer*. Institutt for marin teknikk. https://ntnuopen.ntnu.no/ntnu-xmlui/handle/11250/238498

Buran Holan, A., Roth, B., S.W. Breiland, M., Kolarevic, J., J. Hansen, Ø., Iversen, A., Hermansen, Ø., Gjerde, B., Hatlen, B., Mortensen, A., Lein, I., Johansen, L.-H., Noble, C., Gismervik, K., & Espmark, M. (2017). *Beste praksis for medikamentfri lusekontroll (MEDFRI)*. Nofima. https://www.fhf.no/prosjekter/prosjektbasen/901296/

Cermaq. (2022, May 8). *Verdikjeden vår*. Cermaq Norway. https://www.cermaq.no/vår-produksjon/verdikjeden

Chung, J., & Hulbert, G. M. (1993). A Time Integration Algorithm for Structural Dynamics With Improved Numerical Dissipation: The Generalized-α Method. *Journal of Applied Mechanics*, *60*(2), 371–375. https://doi.org/10.1115/1.2900803

DNV. (2011). *DNV-OS-H101: Marine Operations, General*. DNV. https://rules.dnv.com/docs/pdf/DNVPM/codes/docs/2011-10/Os-H101.pdf

Edvardsen, T., & Almås, K. A. (2017). Norsk havøkonomi mot 2050 – en videreføring av OECD's rapport The Ocean Economy in 2030. In *44*. SINTEF Ocean. https://sintef.brage.unit.no/sintef-xmlui/handle/11250/2456384

Faltinsen, O. M. (1990). *Sea Loads on Ships and Offshore Structures*. Cambridge University Press.

Fiskeri-og kystdepartementet. (2005). *Ot.prp. Nr. 61 (2004-2005)* [Proposisjon]. regjeringen.no. https://www.regjeringen.no/no/dokumenter/otprp-nr-61-2004-2005-/id398345/

Gentry, R. R., Lester, S. E., Kappel, C. V., White, C., Bell, T. W., Stevens, J., & Gaines, S. D. (2017). Offshore aquaculture: Spatial planning principles for sustainable development. *Ecology and Evolution*, *7*(2), 733–743. https://doi.org/10.1002/ece3.2637

Gratanglaks. (2022, May 4). *Kopi av ØyMerd*. Gratanglaks. https://www.gratanglaks.no/kopi-av-oymerd

Haakenstad, H., Breivik, Ø., Furevik, B. R., Reistad, M., Bohlinger, P., & Aarnes, O. J. (2021). NORA3: A Nonhydrostatic High-Resolution Hindcast of the North Sea, the Norwegian Sea, and the Barents Sea. *Journal of Applied Meteorology and Climatology*, *60*(10), 1443–1464. https://doi.org/10.1175/JAMC-D-21-0029.1

Havemann, S., & W.Fellner, D. (2022). *Generative mesh modeling* (p. 11). Institute of Computer Graphics, University of Technology. https://www.researchgate.net/profile/Dieter-Fellner-4/publication/228690469_Generative_mesh_modeling/links/09e4150bd340e6ee19000 000/Generative-mesh-modeling.pdf

Holte, E. A., Sønvisen, S. A., & Holmen, I. M. (2016). *Havteknologi—Potensialet for utvikling av tverrgående teknologier og teknologisk utstyr til bruk i marin, maritim og offshore sektorer—MT2015 A-182*. SINTEF Ocean. https://sintef.brage.unit.no/sintef-xmlui/handle/11250/2607655

Jaime Matthijs, P. (2020). *Validation of aero-hydro-servo-elastic load and motion simulations in BHawC/OrcaFlex for the Hywind Scotland floating offshore wind farm*. NTNU. https://ntnuopen.ntnu.no/ntnu-xmlui/handle/11250/2780185

Journée, JMJ., & Massie, W. (2005). *Offshore hydromechanics* (2000th ed.). CITG Section Hydraulic Engineering. https://ocw.tudelft.nl/wp-content/uploads/OffshoreHydromechanics_Journee_Massie.pdf

Leira, B. J. (2017). Multi-Purpose Offshore-Platforms: Past, Present and Future Research and Developments. *Volume 9: Offshore Geotechnics; Torgeir Moan Honoring Symposium*, V009T12A015. https://doi.org/10.1115/OMAE2017-62691

Lekang, O.-I. (2013). *Aquaculture Engineering* (1st ed.). John Wiley & Sons, Ltd. https://doi.org/10.1002/9781118496077

Lin, Y.-H., & Trethewey, M. W. (1990). Finite element analysis of elastic beams subjected to moving dynamic loads. *Journal of Sound and Vibration*, *136*(2), 323–342. https://doi.org/10.1016/0022-460X(90)90860-3

Liu, Y. (2019). HAMS: A Frequency-Domain Preprocessor for Wave-Structure Interactions—Theory, Development, and Application. *Journal of Marine Science and Engineering*, *7*(3), 81. https://doi.org/10.3390/jmse7030081

Liu, Y. (2021, September 9). *Introduction of the Open-Source Boundary Element Method Solver HAMS to the Ocean Renewable Energy Community*. The 14th European Wave and Tidal Energy Conference (EWTEC2021), Plymouth, UK. https://www.researchgate.net/publication/355585903_Introduction_of_the_Open-Source_Boundary_Element_Method_Solver_HAMS_to_the_Ocean_Renewable_Energy_Community

Løken, A. E., Sødahl, N., & Hagen, Ø. (1999, May 3). *Efficient Integrated Analysis Methods for Deepwater Platforms*. Offshore Technology Conference. https://doi.org/10.4043/10809-MS

Lund Pettersen, V. (2022, May 4). *Oppdrettsanlegg opptar større havområder enn før*. Havforskningsinstituttet. https://www.hi.no/hi/nyheter/2022/april/oppdrettsanlegg-opptar-storre-havomrader-enn-for

Martic, I., Degiuli, N., Farkas, A., & Basic, J. (2017, June 25). *Mesh Sensitivity Analysis for the Numerical Simulation of a Damaged Ship Model*. The 27th International Ocean and Polar Engineering Conference. https://onepetro.org/ISOPEIOPEC/proceedings/ISOPE17/All-ISOPE17/ISOPE-I-17-624/39094

Meshmagick User's Guide. (2022, May 14). *Meshmagick User's Guide (3.2)—Meshmagick User's Guide 3.2 documentation*. https://lheea.github.io/meshmagick/

Nedrejord, R. (2021, May 28). *Får fire utviklingstillatelser for utvikling av Øymerd: – Hadde håpet på et bedre resultat | IntraFish.no*. IntraFish.No | De Siste Nyhetene Om Oppdrettsnæringen. https://www.intrafish.no/pressemeldinger/far-fire-utviklingstillatelser-for-utvikling-av-oymerd-hadde-hapet-pa-et-bedre-resultat/2-1-1017588

Noer, G., Saetra, Ø., Lien, T., & Gusdal, Y. (2011). A climatological study of polar lows in the Nordic Seas. *Quarterly Journal of the Royal Meteorological Society*, *137*(660), 1762–1772. https://doi.org/10.1002/qj.846

Norgeskart. (2022, May 8). *Norgeskart*.
https://norgeskart.no/#!?project=norgeskart&layers=1002&zoom=3&lat=7197864.00
&lon=396722.00

NYTEK-forskriften. (2011). *Forskrift om krav til teknisk standard for flytende
akvakulturanlegg (NYTEK-forskriften)*. Nærings- og fiskeridepartementet.
https://lovdata.no/dokument/SF/forskrift/2011-08-16-849#KAPITTEL_8

O'Connor, M., Bourke, D., Curtin, T., Lewis, T., & Dalton, G. (2012, October 17). *Weather
windows analysis incorporating wave height, wave period, wind speed and tidal
current with relevance to deployment and maintenance of marine renewables*. 4th
International Conference on Ocean Energy (ICOE 2012), Dublin.
https://www.researchgate.net/publication/326711082_Weather_windows_analysis_inc
orporating_wave_height_wave_period_wind_speed_and_tidal_current_with_relevanc
e_to_deployment_and_maintenance_of_marine_renewables

OECD. (2016). *The Ocean Economy in 2030*. Organisation for Economic Co-operation and
Development. https://www.oecd-ilibrary.org/economics/the-ocean-economy-in-
2030_9789264251724-en

Olafsen, T., Winther, U., Olsen, Y., & Skjermo, J. (2012). *Verdiskaping basert på produktive
hav i 2050* [Rapport]. regjeringen.no.
https://www.regjeringen.no/no/dokumenter/verdiskaping-basert-pa-produktive-hav-i-
/id697596/

Olsen, C. W. (2015). *Including the Effect of Shielding in Prediction of Weather Window for
Offshore Lifting Operations*. NTNU. https://ntnuopen.ntnu.no/ntnu-
xmlui/handle/11250/2350714

Orcina. (2022a, April 4). *Line theory: Overview*. Line Theory.
https://www.orcina.com/webhelp/OrcaFlex/Content/html/Linetheory,Overview.htm

Orcina. (2022b, May 6). *Vessel types*.
https://www.orcina.com/webhelp/OrcaFlex/Content/html/Vesseltypes.htm

Orcina. (2022c, May 8). *Dynamic analysis: Time domain solution*.
https://www.orcina.com/webhelp/OrcaFlex/Content/html/Dynamicanalysis,Timedoma
insolution.htm#Implicit

Orcina. (2022d, May 14). *OrcaFlex—Dynamic analysis software for offshore marine systems*.
Orcina. https://www.orcina.com/orcaflex/

Orcina. (2022e, May 15). *Importing hydrodynamic data: WAMIT*.

https://www.orcina.com/webhelp/OrcaFlex/Content/html/Importinghydrodynamicdata
,WAMIT.htm

Orcina. (2022f, May 15). *Theory: Irregular frequencies*.

https://www.orcina.com/webhelp/OrcaWave/Content/html/Theory,Irregularfrequencie
s.htm

Pawar, S., & Brizzolara, S. (2019). Relevance of transition turbulent model for hydrodynamic

characteristics of low Reynolds number propeller. *Applied Ocean Research*, *87*, 165–
178. https://doi.org/10.1016/j.apor.2019.02.018

ScaleAQ. (2022, May 8). *Thermolicer—ScaleAQ - We are aquaculture*. ScaleAQ.

https://scaleaq.no/produkt/thermolicer/

Smir. (2022, May 8). *Skånsom avlusing av fisk i lukket vannsøyle | Hydrolicer | Smir*. smir.

https://smir.no/produkter/hydrolicer/

Tordella, D., Scarsoglio, S., & Belan, M. (2006). A synthetic perturbative hypothesis for

multiscale analysis of convective wake instability. *Physics of Fluids*, *18*, 054105.
https://doi.org/10.1063/1.2201114

van Bussel, G. (2002). *Offshore wind energy, the reliability dilemma*. 1–4.

https://www.researchgate.net/publication/228797645_Offshore_wind_energy_the_reli
ability_dilemma

Zabala, I., Peña Sanchez, Y., Kelly, T., Henriques, J., Penalba, M., Faedo, N., Ringwood, J.,

& Ilzarbe, J. (2021, September 5). *BEMRosetta: An open-source hydrodynamic
coefficients converter and viewer integrated with Nemoh and FOAMM*. Proceedings
of the 14th European Wave and Tidal Energy Conference 5-9th Sept 2021, Plymouth,
UK. https://www.researchgate.net/publication/354543926_BEMRosetta_An_open-
source_hydrodynamic_coefficients_converter_and_viewer_integrated_with_Nemoh_a
nd_FOAMM

Appendix 1 – Hydrostatic report

```
HYDROSTATIC REPORT (Meshmagick version 3.2)

[1]     Corrections made on initial mesh:
        Z CORRECTION (M)------------------------------>   0.000
        HEEL CORRECTION (DEG)------------------------->   0.000
        TRIM CORRECTION (DEG)------------------------->  -0.000

        GRAVITY ACCELERATION (M/S**2)---------------->    9.81
        DENSITY OF WATER (KG/M**3)------------------->    1025.0

        WATERPLANE AREA (M**2)----------------------->    3939.9
        WATERPLANE CENTER (M)------------------------>    0.348     -0.393      0.000
        WETTED SURFACE AREA (M**2)------------------->    10724.4
        DISPLACEMENT VOLUME (M**3)------------------->    29603.498
        DISPLACEMENT MASS (TONS)--------------------->    30343.585
        BUOYANCY CENTER (M)-------------------------->    0.342     -0.397     -3.745
        CENTER OF GRAVITY (M)------------------------>    0.342     -0.397     -2.500

        DRAFT (M)------------------------------------>    7.500
        LENGTH OVERALL SUBMERGED (M)----------------->    118.66
        BREADTH OVERALL SUBMERGED (M)---------------->    127.27
        LENGTH AT WATERLINE LWL (M)------------------>    118.47
        FORWARD PERPENDICULAR FP (M)----------------->    68.63
        [2] LENGTH BETWEEN PERPENDICULARS LPP (M)---->    118.47

        TRANSVERSAL METACENTRIC RADIUS (M)----------->    138.603
        LONGITUDINAL METACENTRIC RADIUS (M)---------->    137.195
        TRANSVERSAL METACENTRIC HEIGHT GMT (M)------->    137.357
        LONGITUDINAL METACENTRIC HEIGHT GML (M)------>    135.949

        HYDROSTATIC STIFFNESS COEFFICIENTS (at COG horiz. Pos.):
        K33 (N/M)------------------------------------>    3.9617E+07
        K34 (N)-------------------------------------->    1.6034E+05
        K35 (N)-------------------------------------->   -2.5655E+05
        K44 (N.M)------------------------------------>    4.0887E+10
        K45 (N.M)------------------------------------>    8.5925E+06
        K55 (N.M)------------------------------------>    4.0468E+10

[2]     INERTIAS from standard approximations: [Rxx = 0.3 B; Ryy = Rzz = 0.25 Lpp]
        RXX (M)-------------------------------------->    38.180
        RYY (M)-------------------------------------->    29.618
        RZZ (M)-------------------------------------->    29.618
        IXX------------------------------------------>    4.423E+10
        IYY------------------------------------------>    2.662E+10
        IZZ------------------------------------------>    2.662E+10

        INERTIAS from homogeneous immersed hull approximation:
        RXX------------------------------------------>    32.642
        RYY------------------------------------------>    32.475
        RZZ------------------------------------------>    45.500
        IXX------------------------------------------>    3.233E+10
        IYY------------------------------------------>    3.200E+10
        IZZ------------------------------------------>    6.282E+10
```

Appendix 2 – Python script wave data

```
#Code taken from met_waves repository: https://github.com/KonstantinChri/MET_waves
#Python environment and dependencies were installed with miniconda.
#Spyder IDE - The Scientific Python Development Environment | Spyder-IDE.org | Python 3.7.9 64-bit | Qt 5.12.10 | PyQt5 5.12.3 | Windows 10
#Modified for the required variables.
#Each line of code was run separately.
########################################################################

import met_waves

met_waves.plot_timeseries(start_time='2018-01-01T12:00', end_time='2019-01-01T12:00', lon=15.25,
                lat=68.13, product='NORA3', variable='hs', write_csv=True, ts_obs=None)

met_waves.plot_timeseries(start_time='2018-01-01T12:00', end_time='2019-01-01T12:00', lon=15.25, lat=68.13, product='NORA3', variable='tp', write_csv=True, ts_obs=None)

met_waves.plot_timeseries(start_time='2018-01-01T12:00', end_time='2019-01-01T12:00', lon=15.25,
                lat=68.13, product='NORA3', variable='hs_swell', write_csv=True, ts_obs=None)

met_waves.plot_timeseries(start_time='2018-01-01T12:00', end_time='2019-01-01T12:00', lon=15.25,
                lat=68.13, product='NORA3', variable='tp_swell', write_csv=True, ts_obs=None)
```